V.I. Il`icev Pacific Oceanological Institute
Far East Branch, Academy of Sciences of Russia
Vladivostok, Russian Federation

Acoustic Studies on the North East Sakhalin Shelf
Volume 2: Analysis, Conclusions and Recommendations

15 August to 20 September, 2003

Sakhalin, Russian Federation

M.V. Kruglof
A.N. Rutenko

Prepared for
Exxon Neftegas Limited
&
Sakhalin Energy Investment Company,
Yuzhno-Sakhalinsk, Sakhalin,
Russian Federation

30 April 2004

Table of Contents

LIST OF FIGURES ..... **III**

LIST OF TABLES ..... **VI**

EXECUTIVE SUMMARY ..... **VII**

1 INTRODUCTION **1**

1.1 Acoustic recording and processing equipment 2

1.2 Low Frequency and High Frequency transducers and hydrological sonde 6

1.3 Terminology and algorithms used in the report 7

1.4 Units 7

2 IMPACT OF WEATHER CONDITIONS ON THE AMBIENT ACOUSTIC FIELD OF THE NE SAKHALIN SHELF **8**

2.1 Measurements of acoustic noise generated by meteorological sources in 2003 9

3 THEORETICAL & EXPERIMENTAL ANALYSIS OF SOUND PROPAGATION AT PA-B & CHAYVO **18**

3.1 Impact of the hydrodynamic field on sound propagation in the Chayvo area 18

3.2 Analysis of sound propagation and TL from PA-B to the inshore feeding area 22

3.2 Analysis of sound propagation and TL from PA-B to the inshore feeding area 23

3.2 Analysis of sound propagation and TL from PA-B to the inshore feeding area 24

3.2 Analysis of sound propagation and TL from PA-B to the inshore feeding area 25

3.3 Analysis of sound propagation and TL from Orlan to the offshore feeding area 34

4 ANALYSIS OF SOUND PROPAGATING FROM THE CHAYVO WELL SITE **38**

4.1 Experimental analysis of acoustic level vs. drilling operations at Chayvo 40

4.1.1 Acoustic monitoring (Orlan monitor station) - 20 August 2003 40

4.1.2 Acoustic monitoring (Chayvo-1, Chayvo-2 & Orlan) - 6 September 2003 40

4.1.3 Acoustic monitoring (Chayvo-1, Chayvo-2 & Orlan) - 7 to 10 September 2003 41

4.1.4 Acoustic monitoring (Chayvo-1 & Chayvo-3) - 18 to 19 September 2003 42

4.2 Results of the analysis of acoustic level vs. drilling operations at Chayvo 57

4.2 Results of the analysis of acoustic level vs. drilling operations at Chayvo 58

4.2 Results of the analysis of acoustic level vs. drilling operations at Chayvo 59

5 ANALYSIS OF ACOUSTIC PULSES FROM MARINE LIFE, ANTHROPOGENIC AND NATURAL SEISMICITY **60**

5.1 Impulses generated by the seismic survey at Lunskoye 60

5.2 Impulses of possible biogenic origin recorded in 2003 65

5.3 Natural seismicity of the Sakhalin area 66

6 RESULTS AND CONCLUSIONS **75**

7 FUTURE PLANS.....80
8 ACKNOWLEDGEMENTS.....82
9 AUTHORS 82
10 BIBLIOGRAPHY.....83
APPENDIX A - DESCRIPTION OF DATA USED FOR THE TL STUDIES 85

LIST OF FIGURES

Figure 1.1. **AUAR prepared for deployment.**

Figure 1.2. **Map showing the AUAR locations and kernel probability contours showing the density distributions of western gray whales from the 2001 to 2003 aerial surveys.**

Figure 2.1. **Sonogram *G(f,t)* of data recorded at the control station on 16 August 2003 during the approach of a storm.**

Figure 2.2. **Map showing the locations where AUARs were deployed during the 2003 acoustic program.**

Figure 2.3. **Sonograms *G(f,t)* of noise synchronously recorded at the control point, Odoptu-N, PA-B-1, Piltun and Orlan on 16 August, 2003.**

Figure 2.4. **Spectra *G(f)* of noise synchronously recorded 120 km apart at the control point (a) and Orlan monitor station (b) on 16 August 2003.**

Figure 2.5. **Sonograms *G(f,t)* and spectra *G(f)* of acoustic noise recorded at the control station on 3 September 2003.**

Figure 2.6. **Sonograms *G(f,t)* recorded at locations Chayvo-1, Chayvo-2 and Lunskoye on 10 September 2003, during a change in weather conditions from calm to storm.**

Figure 3.1. **Hydrological data acquired near the proposed PA-B location over August and September 2003.**

Figure 3.2. **Map showing the locations of the autonomous CW-320 transducer, the transducer at the proposed location of the Orlan platform (P-Orlan) and the Chayvo-1, Chayvo-2 and Orlan AUARs deployed on 6-11 September 2003.**

Figure 3.3. **Variations in the Intensity I(t) of the 320 Hz acoustic field synchronously measured at Chayvo-1 and Chayvo-2 when an autonomous transducer was deployed at point CW-320.**

Figure 3.4. **Variations in the Intensity I(t) of the 320 Hz acoustic field synchronously measured at Chayvo-1, Chayvo-2 and Orlan when an autonomous transducer was deployed at point CW-320.**

Figure 3.5. **Map showing the locations of the proposed PA-B platform and the Odoptu-N, PA-B-1 and PA-B-2 monitor stations 16-19 September 2003.**

Figure 3.6. **(a) Bathymetric profile from PA-B to PA-B-1 showing the source, receiver and hydrologic data locations (b) Frequency dependent TL data from the proposed PA-B location to PA-B-1, PA-B-2 and Odoptu-N acquired on 16 September 2003.**

Figure 3.7. **Hydrologic data acquired at (a) PA-B on 18 September 2003 (b) PA-B, PA-B-1 and PA-B-2 on 16 August 2003.**

Figure 3.8. **(a) Bathymetric profile from PA-B to PA-B-1 showing the source and receiver locations and parameters used in the modeling (b)**

Theoretical and experimental frequency dependent TL from PA-B to PA-B-1, PA-B-2 and Odoptu-N.

Figure 3.9. **Theoretical (line) and experimental (diamond) values of frequency dependent Relative Transmission Loss (RTL) between PA-B-2 and PA-B-1 for acoustic signals transmitted from PA-B.**

Figure 3.10. **Spectra *G(f)* of tonal signals transmitted from the proposed PA-B location and received at the Orlan monitor station on 16 August 2003.**

Figure 3.11. **Frequency dependent TL between PA-B and the PA-B-1, Odoptu-N, Piltun and Orlan monitor stations for acoustic signals transmitted from PA-B on 16 August 2003.**

Figure 3.12. **Hydrologic data acquired at Orlan, Chayvo-2 and Chayvo-1 on 5 September 2003.**

Figure 3.13(a). **Bathymetric profile from Chayvo-1, through Chayvo-2 to Orlan showing the locations of the monitor stations (b) Experimental frequency dependent TL between the proposed Orlan platform location and Chayvo-1 (7.9 km), Chayvo-2 (2.5 km) and Orlan (14.2 km).**

Figure 3.14(a). **Map showing the profile from the Chayvo well site to Orlan (b) Bathymetric profile from the Chayvo well site to Orlan showing the model parameters (c) Theoretical range dependent TL profiles for 30 Hz, 50 Hz and 200 Hz (d) Theoretical frequency dependent TL profiles for Chayvo-1, Chayvo-2 and Orlan.**

Figure 4.1. **AUAR recording schedule and Chayvo drilling operations log for the evaluation period.**

Figure 4.2(a). **Sonogram *G(f,t)* [0-1 kHz] recorded at Orlan on 20 August 2003, while the Chayvo rig was drilling a deviated well.**

Figure 4.2(b). **Sonogram *G(f,t)* [0-10 kHz] recorded at Orlan on 20 August 2003, while the Chayvo rig was drilling a deviated well.**

Figure 4.3(a). **Sonograms *G(f,t)* [0-1 kHz] recorded at Chayvo-1, Chayvo-2 and Orlan on 6 September 2003, while the Chayvo rig was conducting tripping operations.**

Figure 4.3(b). **Sonograms *G(f,t)* [0-10 kHz] recorded at Chayvo-1, Chayvo-2 and Orlan on 6 September 2003, while the Chayvo rig was conducting tripping operations. Figure 4.4(a) - Sonograms *G(f,t)* [0-1 kHz] recorded at Chayvo-1, Chayvo-2 and Orlan on 7 September 2003, while the Chayvo rig was running casing and conducting topside operations.**

Figure 4.4(b). **Sonograms *G(f,t)* [0-10 kHz] recorded at Chayvo-1, Chayvo-2 and Orlan on 7 September 2003, while the Chayvo rig was running casing and conducting topside operations.**

Figure 4.5(a). **Sonograms *G(f,t)* [0-1 kHz] recorded at Chayvo-1, Chayvo-2 and Orlan on 8 September 2003, while the Chayvo rig was running casing and conducting topside operations.**

Figure 4.5(b). **Sonograms *G(f,t)* [0-10 kHz] recorded at Chayvo-1, Chayvo-2 and Orlan on 8 September 2003, while the Chayvo rig was running casing and conducting topside operations.**

Figure 4.6(a). **Sonograms *G(f,t)* [0-1 kHz] recorded at Chayvo-1 and Chayvo-2 on 9 September 2003, while the Chayvo rig was conducting casing and topside operations.**

Figure 4.6(b). **Sonograms *G(f,t)* [0-10 kHz] recorded at Chayvo-1 and Chayvo-2 on 9 September 2003, while the Chayvo rig was conducting casing and topside operations.**

Figure 4.7(a). **Sonograms *G(f,t)* [0-1 kHz] recorded at Chayvo-1 and Chayvo-2 on 10 September 2003, while the Chayvo rig was conducting casing operations.**

Figure 4.7(b). **Sonograms *G(f,t)* [0-10 kHz] recorded at Chayvo-1 and Chayvo-2 on 10 September 2003, while the Chayvo rig was conducting casing operations.**

Figure 4.8(a). **Sonograms *G(f,t)* [0-1 kHz] recorded at Chayvo-1 and Chayvo-3 on 18-19 September 2003, while the Chayvo rig was drilling a deviated well.**

Figure 4.8(b). **Sonograms *G(f,t)* [0-10 kHz] recorded at Chayvo-1 and Chayvo-2 on 18-19 September 2003, while the Chayvo rig was drilling a deviated well.**

Figure 4.9(a). **Chayvo-1 spectral density, recorded on 18-19 September 2003, while the Chayvo rig was drilling a deviated well.**

Figure 4.9(b). **Chayvo-3 spectral density, recorded on 18-19 September 2003, while the Chayvo rig was drilling a deviated well.**

Figure 5.1. **Sonogram *G(f,t)* recorded at Lunskoye on 9 September 2003, showing the signals generated by a seismic survey in the Lunskoye license area.**

Figure 5.2. **Impulses recorded at the Lunskoye monitor station on 10 September 2003.**

Figure 5.3. **Repetitive seismic impulses (and impulses of biogenic origin) recorded at the Lunskoye monitor station on 9 September 2003.**

Figure 5.4. **Comparison of seismic impulses and impulses of biogenic origin recorded at the Lunskoye monitor station on 10 September 2003.**

Figure 5.5. **Plot of the received level [peak, rms and cosine filtered rms (~250 m filter length)] of impulses from the Lunskoye seismic survey received at the Lunskoye monitor station on 9 September 2003.**

Figure 5.6. **Biogenic impulses recorded at the control station on 17 August 2003.**

Figure 5.7. **The plots from Figure 5.5 at a larger scale.**

Figure 5.8. **Detailed analysis of a biogenic impulse recorded at the Lunskoye monitor station on 9 September 2003.**

Figure 5.9. **Further biogenic impulses recorded at the control station on 17 August 2003.**

Figure 5.10. **Further biogenic impulses recorded on the HF channel (30 kHz sample rate) of the control station - 17 August 2003.**

Figure 5.11. **Impulses generated by natural seismicity - Lake Mikizha, Kamchatka - 3 March 2004.**

Figure 5.12. **Impulses generated by natural seismicity - recorded on three channels to determine orientation - Lake Mikizha, Kamchatka - 9 March 2004.**

LIST OF TABLES

Table 3.1. **TL and absorbtion loss over the PA-B to Orlan profile.**

Executive Summary

In 2003, the Pacific Oceanological Institute (POI) developed and deployed six Autonomous Underwater Acoustic Recorders (AUARs) to conduct acoustic measurements on the NE Sakhalin shelf as part of the gray whale research program. The goal of the program was to investigate whether the development of the oil and gas resources off the NE Sakhalin coast could impact the sensitive Korean-Okhotsk gray whale (*Eschrichtius robustus*) population[1].

The 2003 acoustic program measured anthropogenic and ambient noise levels and made Transmission Loss (TL) measurements along profiles from some proposed facilities to the western gray whale home ranges. These TL measurements will be used to calibrate acoustic models that, in conjunction with the spectrum of noise sources, will be used to predict the level of noise received in the gray whale feeding areas, allowing the appropriate mitigation measures to be applied.

A number of ambient noise measurements were taken in conditions ranging from a cyclone to calm seas. These measurements correlated well with relationships between noise and sea-state proposed in the literature. Acoustic signals generated by marine mammals and natural seismicity were regularly recorded on the NE Sakhalin shelf. The TL experiments showed that:

- Intensity variations due to spatial and temporal fluctuations in the velocity field can be significant, hydrologic measurements will allow these fluctuations to be modeled.
- TL experiments between the proposed PA-B and Orlan platform locations and the gray whale feeding areas allowed TL spectra to be developed. These TL spectra showed that propagation at frequencies lower than ~30Hz was through the earth, that the TL was at a minimum between 100-200 Hz and that the TL increased sharply in shallower water (a significant effect for propagation from offshore to the inshore feeding area).

Acoustic monitoring found no correlation between drilling operations at the Chayvo well site and the level of the acoustic field monitored offshore. The rms level of impulses from the seismic survey at Lunskoye and recorded at the southern edge of the offshore feeding area were 25 dB below those known to cause disturbance to feeding gray whales.

[1] The Korean Okhotsk (western) gray whale population is listed as endangered in the Russian Red Book and critically endangered by the International Union for the Conservation of Nature (IUCN).

1 Introduction

The shallow water (6 - 15 m) part of the NE Sakhalin shelf starting south of the mouth of Piltun Bay and extending northwards up the Sakhalin coast is one of the most important summer feeding areas for the Korean-Okhotsk (western) gray whales. For this reason acoustic studies have been conducted in the area since 1999. In 2001 another gray whale feeding area was discovered offshore in deeper water (30-50 m) approximately 20 km to the South East of the mouth of Chayvo Bay[2].

The acoustic program conducted on the NE shelf of Sakhalin Island in 2003 had three main objectives:

1. The first was to study the temporal and spatial variations in the amplitude and frequency characteristics of ambient and anthropogenic acoustic noise at a series of monitoring stations located throughout the development area. These monitoring stations were positioned to be at the outside edge of the gray whale feeding area nearest a proposed facility. The goal of this annual acoustic monitoring program is to estimate any increase in the cumulative noise in the gray whale feeding areas due to the oil development and producing activity.
2. The second objective was to study sound propagation and variation in frequency dependent transmission loss (TL) from proposed oil facilities (PA-B, Orlan) to the nearest gray whale feeding area. These TL profiles would allow an estimation of the increase in acoustic level that would be expected if a facility with a defined noise signature was placed at the proposed location. Broadband noises generated by the vessel *Nevelskoy*, a low frequency (LF) (24-33 Hz) resonance transducer and a high frequency (HF)(1-10 kHz) transducer, both with known acoustic characteristics, were used in these studies.
3. The third objective was to measure the amplitude and spectral characteristics of any acoustic noise generated at the Chayvo drill site and propagating into the ocean. These measurements were taken during a number of different drilling activities at the Chayvo drill site.

[2] Gray whales were seen feeding in the offshore feeding area throughout the 2002-2003 field seasons.

The report for the 2003 acoustic program has been divided into two separate sections. The first report describes the equipment used for the 2003 program, its testing and calibration as well as the operational strategy and methodology for the 2003 field program [Borisov et al., 2004]. The report also contains sonograms for all the data displayed in 24-hour segments.

This report is dedicated to analysis of the data, conclusions and recommendations for future work. The analysis includes a quantitative spectral analysis of the variation in ambient acoustic level with weather conditions and TL analysis. The TL analyses were conducted from the proposed PA-B platform location to the inshore gray whale feeding area and from the Chayvo drill site to the offshore feeding area. The report also contains acoustic data recorded near the Chayvo drill site to evaluate if there is any correlation between the noise recorded and drilling operations at Chayvo. Finally, a temporal analysis is made of acoustic pulses measured on the Sakhalin shelf (generated by sea animals, industrial activity or geological events). These are compared with acoustic pulses measured during seismic at Lunskoye and geological signals measured in 2004 at Lake Mikizha on Kamchatka.

1.1 Acoustic recording and processing equipment

Individually deployed Autonomous Underwater Acoustic Recorders (AUARs) were developed at POI FEB RAS[3] (POI) to accurately measure acoustic signals in the frequency band from 1 Hz to 15 kHz (Figure 1.1).

The AUAR[4] is made of welded titanium alloy and is rated to depths of up to 100 m. Two external sensors (hydrophones, accelerometers or hydrologic measuring equipment) can be input to the AUAR electronics. Inside the AUAR there are two batteries secured in a titanium frame and a tray containing the AUAR electronics and power handling circuitry. The two sealed batteries can provide continuous operation of the AUAR for over 15 days. Spherical hydrophones of type G61H (Г61Н) with integrated pre-amplifiers designed specifically for the hydrophones were used for the AUARs.

The AUARs digital recorder is based on the Prometheus single board computer, which has an integrated 16 bit analog to digital converter (ADC). In order to optimize the dynamic

[3] POI FEB RAS - The Pacific Oceanological Institute, Far East Branch of the Russian Academy of Sciences.
[4] AUAR dimensions are length 0.8 m, diameter 0.38 m, weight in air ~105 kg.

range of the 16 bit ADC the signal amplitudes should be equal across the entire frequency range. However, ambient noise generally has an amplitude maximum at low frequencies and drops off with higher frequencies. The ADC does not have the dynamic range to record frequencies from 1 Hz to 15 kHz. The AUAR therefore has two analog channels: a Low Frequency (LF) channel with no correction and a High Frequency (HF) channel with the low frequency component (<1.5 kHz) removed by a low cut filter. This allows the gain coefficient for frequencies above 1 kHz to be increased without overloading the ADC.

Figure 1.1 - AUAR prepared for deployment.

The primary AUAR data storage is a compact laptop 56 GB hard drive. To prevent electromagnetic and acoustic noise generated by the rotating hard drive from contaminating the data a 489 MB flash memory drive is used as a buffer. While data is being recorded on the flash drive the hard drive is in standby mode with its motor off. When the flash memory drive is full, the recording cycle is halted while the flash memory drive writes to the hard drive; the data therefore contains controlled gaps. The size of these gaps depends on the size of the flash memory drive and the recording parameters[5].

[5] For a 489 MB flash memory drive the gap was approximately 9 minutes every 3.5 hours (LF channel).

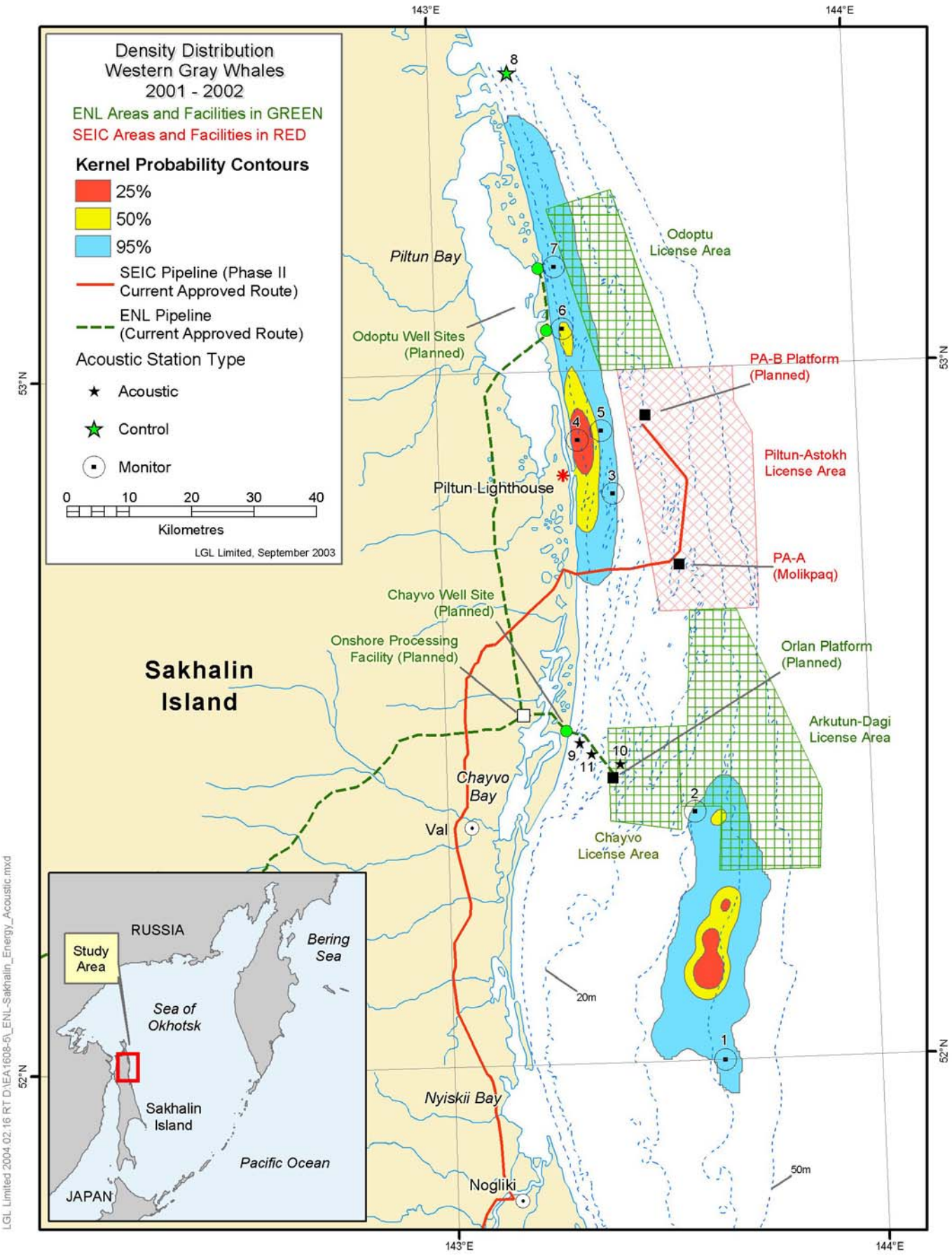

Figure 1.2 - Map showing the AUAR locations and kernel probability contours showing the density distributions of western gray whales from the 2001 to 2003 aerial surveys.

A floating buoy connected to a 24 kg anchor by a 50 m rope marks the location of the AUAR on deployment. This anchor is linked to the AUAR by a 65 m long rope weighted down with lead weights. If necessary the vessel can grapple for the 65 m rope between the anchor and the AUAR since the GPS coordinates of both are logged during deployment. The AUAR can therefore still be recovered in the event that the surface buoy is lost; one AUAR was recovered in this manner during the 2003 field season.

Practical experience has shown that at shallow deployment depths (10-30 m), movement of the surface buoy due to wave action can be mechanically conducted down the rope to the hydrophone, where this mechanical movement can be recorded as acoustic noise. The AUAR is deployed so as to reduce this noise by isolating the hydrophone from the surface buoy with an anchor, thus reducing the mechanical coupling between the surface buoy and the hydrophone. The hydrophone is also deployed 15 m from the AUAR to prevent distortion of the acoustic field by scattering or masking by the AUAR container at high frequencies. The hydrophone is deployed inside a pyramid shaped wire frame and attached by rubber bands to the frame, isolating it to the best extent possible from the sea floor.

In 2003 it was decided that the entire acoustic program would be operated from the vessel *Nevelskoy*. The *Nevelskoy* was also the operational platform for all for the vessel-based biology programs (Photo ID, benthic, MMO). During the 2003 field season AUARs were deployed and synchronous acoustic measurements recorded at stations ranging from north of Odoptu to the southern edge of the offshore feeding area (Figure 1.2), an area that extended 120 km up the NE Sakhalin shelf. Before the AUAR is deployed its computer is programmed for the desired recording schedule. Computers on the *Nevelskoy* were used as the main data storage units. The acoustic data on the AUAR hard drive was copied to CD's and a removable hard drive before the files on the AUAR drive were deleted prior to redeployment.

To compute TL from acoustic measurements made by different AUARs, the data has to be calibrated to an absolute pressure standard. The hydrophones were manufactured with nominal sensitivities and the gains were set in the field. Field cross-calibrations conducted in 2003 confirmed the absolute calibration of the data. Further details of the types of AUARs used, their location, deployment depth and recording settings can be found in

Appendix A. A detailed description of the characteristics and calibration of the 2003 acoustic recording equipment is provided elsewhere [Borisov et. al., 2004].

1.2 Low Frequency and High Frequency transducers and hydrological sonde

A low frequency (LF) resonant electromagnetic transducer and high frequency (HF) piezoelectric broadband transducer deployed from the *Nevelskoy* were used for sound propagation and TL studies at frequencies from 15-15000 Hz. The acoustic level of signals generated by the transducers was monitored using a calibrated hydrophone and recorded on the *Nevelskoy*[6]. An autonomous tonal transducer (CW-320) was also deployed for three days to study the variation in the acoustic field with time and space caused by velocity and tidal variations.

The LF transducer has a cylindrical container filled with gas[7], and a pair of identical closely spaced radiating pistons oscillating in opposite directions creating a volume displacement[8]. An electromagnetic controller controls the motion of the pistons; hydrostatic compensation is achieved using an air pump. The LF resonance transducer was deployed at a depth of 8 m from the anchored *Nevelskoy*. The 28 Hz acoustic signal has an intensity of 166 dB re 1 μPa^2/Hz at 2 m from the transducer.

The HF broadband piezoelectric (ceramic) transducer is cylindrical[9] and consists of 12 piezoelectric rings connected in parallel coated with a composite material and sealed at the ends. An autonomous electromagnetic resonant transducer was tested during the 2003 field season. The transducer consists of a transmitter, power amplifier and transformer. A voltage stabilizer is used to remove the variation in transmitted signal amplitude with the battery voltage (i.e. battery charge). The transmitter is housed in a sealed cylindrical container[10] with a transmitting diaphragm at one end, and is depth rated to 100 m. The transducer produces a continuous tonal signal with a power of 10 W at the center frequency. The acoustic pressure at 1 m from the transducer is 173 dB re 1 μPa-m. The

---

[6] While the transducers were operating the acoustic signal levels were measured using a calibrated hydrophone located 1 - 2 m away from the transducer.
[7] Dimensions are diameter 58 cm, height 15 cm, weight 48 kg in air, ~6 kg in water.
[8] Tests in the Sea of Japan using calibrated accelerometers, and conducted at a depth of 2 m, indicated that when the maximum number of springs (30) are used, the resonance frequency of the transducer is 20.2 Hz with marginal frequencies of 15.2 and 30.6 Hz (-3 dB).
[9] Dimensions are diameter 20 cm, height 1 m, weight ~ 20 kg in air, ~ 6 kg in water.
[10] Dimensions are diameter 30 cm, length 1 m, weight 100 kg in air, ~40 kg in water.

center frequency can be adjusted in steps over the frequency band 290-392 Hz using heavy disks attached to the diaphragm. The transducer can transmit at a pre-defined acoustic level for 72 hours.

In order to more accurately characterize the 2003 TL measurements, the hydrological characteristics (velocity, temperature, salinity and pressure) of the water layer were acquired using a newly acquired hydrological sonde. The sonde is powered by a set of D cells, providing approximately 180 hours of continuous operation.

1.3 Terminology and algorithms used in the report

Ambient and anthropogenic noise recorded by the AUARs was written to disc in microPascals (μPa)[11]. Acoustic spectra in decibels will be used to describe the variation in acoustic power as a function of frequency. In this report sound pressure power density spectra *G(f)* (μPa^2/ Hz)[12] will be used when spectral data are plotted. These spectra are often averaged over 10-300 one-second windows to improve the statistical stability of the ambient noise data[13]. The sonograms *G(f,t)* are plots of frequency vs. time, the scales generally run from ~37 to ~100 dB re 1 μPa^2/Hz. A detailed description of the methodology used for normalizing and calculating both the amplitude and spectral data is given in Borisov et.al. [2004], Appendix C.

1.4 Units

During the course of this report a number of different unit notations have been used. This is due to differences in standard notation between different disciplines and nationalities. The following are equivalent units using the different standard nomenclatures:

1 mkPa = 1 μPa and 1 mkV = 1 μV.

For spectral density plots: Although the units for power spectral density are μPa^2/(s Hz), μPa^2/s/Hz or μPa^2, it is common usage to define the units for power spectral density as μPa^2/Hz or $\mu Pa/\sqrt{Hz}$.

---

[11] The data was scaled (after incorporating hydrophone sensitivity and system gain) to convert the data to standard units of pressure (measured through an omni-directional hydrophone) in real time.
[12] Energy and power spectra are scaled to 1 Hz whatever the analysis length.
[13] Average of 10 or 300 1-second spectral realizations, the analysis window length is shown on the plot. Spectral averaging will lead to the cancellation of zero mean instrument noise leading to an improvement in the ambient noise/instrument noise ratio at low ambient noise levels.

2 Impact of weather conditions on the ambient acoustic field of the NE Sakhalin shelf

This section analyzes the ambient noise measurements recorded in 2003 and discusses the variation in ambient noise with meteorological conditions and Sea State.

In September 2002 sonobuoys were used to make ambient acoustic noise measurements in Chayvo and between Molikpaq and Piltun bay [Borisov et. al., 2003]. Analysis revealed that for a sea state of 4 the broadband spectral levels increased by 12 dB over the levels present during calm conditions. During a rainstorm the levels were ~16-18 dB above ambient and for frequencies greater than 2.5 kHz the spectral levels reached ~64 dB re 1 μPa^2/Hz (the level was ~56 dB re 1 μPa^2/Hz during a storm without rain).

Knudsen [Knudsen et. al., 1948] showed that the level of noise in the frequency band from 0.5-20 kHz is highly dependent on sea conditions. Perrone later discovered that noise level correlates not to wave height, but to local wind velocity [Perrone, 1969]. The noise level decreases steadily with frequency at 5-6 dB/octave ($\approx 1/f^2$), although a maximum is sometimes seen in the frequency band from 500-1000 Hz. The main source of this noise is surface splashes from waves and the pulsations and cavitations of subsurface bubbles.

Wind velocity is not homogeneous and consists of large number of wind gusts with a wide variety of spatial and temporal scales; this causes temporal variations in the noise level recorded by a stationary hydrophone. The spectrum of these variations depends not only on fluctuations in wind velocity, but on the ratio of the area of the squall to the area of the integrating surface that determines the noise received by a hydrophone [Furduev, 1998][14]. The area of the integrating surface is defined by a number of conditions including the wind speed profile and sound absorption as well as reflection and scattering of sound by the sea floor. The spectrum of the variation in wind velocity has a maximum at ~36 s (0.03 Hz), this is the maximum of wind squalls. This maximum is caused either by convection cells with unsteady atmospheric stratification (when the ocean is warmer than the air) or atmospheric internal waves (when the atmospheric stratification is steady).

[14] The integrating surface is the total area from which noise is received at the hydrophone.

Wind squalls have an average spatial scale of ~300-400 m; this is important for noise estimation. Noise modeling can be used for determining the relationship between noise level and wind velocity (the effective source level). This relationship[15] holds only for a homogeneous half-space, and, for a more general case, waveguide amplification should be considered [Kuryanov, 1998]. The first models of noise generated by the sea surface were based on the assumption that the ocean acts as an unbounded liquid with noise sources on the surface. These sources were specified either by their correlation functions or as a random group of independent sources whose noise propagated in a defined direction. All these models predicted that the energy would be focused (and therefore be at a maximum) in the vertical direction. Experimental measurements showed that this assumption was incorrect and that the energy (especially low frequency noise) was focused in the horizontal direction. Models taking into account not only source parameters, but propagation conditions, are now being actively pursued. These models, based on ray theory and mode theory of the noise field in a stratified inhomogeneous ocean, lead to a more accurate estimation of the noise and have emphasized the importance of transmission loss.

Calculations for shallow waveguides that take into account bottom conditions show that despite the incoherence of the source at the surface, interference can be seen in the sound field, especially near sharp changes in the waveguide parameters. Figure 2.1 shows sonograms *G(f,t)* of acoustic noise measured at the control station illustrating this phenomenon[16]. The time interval between 07:00 to 11:00 corresponds to approach of a storm and development of waves at the control station.

2.1 Measurements of acoustic noise generated by meteorological sources in 2003

Figure 2.2 displays a map showing the locations of the five points where AUARs were deployed and studies conducted between 15-21 August 2003[17]. The map also shows transects along which propagation studies were conducted from the proposed PA-B location using transducers deployed from the anchored *Nevelskoy*. Figure 2.3 displays sonograms *G(f,t)* that show the change of ambient noise during a storm. The spectra *G(f)* pictured in Figure 2.4 numerically describe this change for two points located more then 120 km apart.

---

[15] Modeling of the relationship for an infinite half space has become realistic with advances in computing power. This modeling is however only feasible for an infinite half space.
[16] Note that the left plot has a linear frequency scale and the right plot a logarithmic frequency scale.
[17] Control Point and Odoptu-N, PA-B-1, Piltun and Orlan monitor stations.

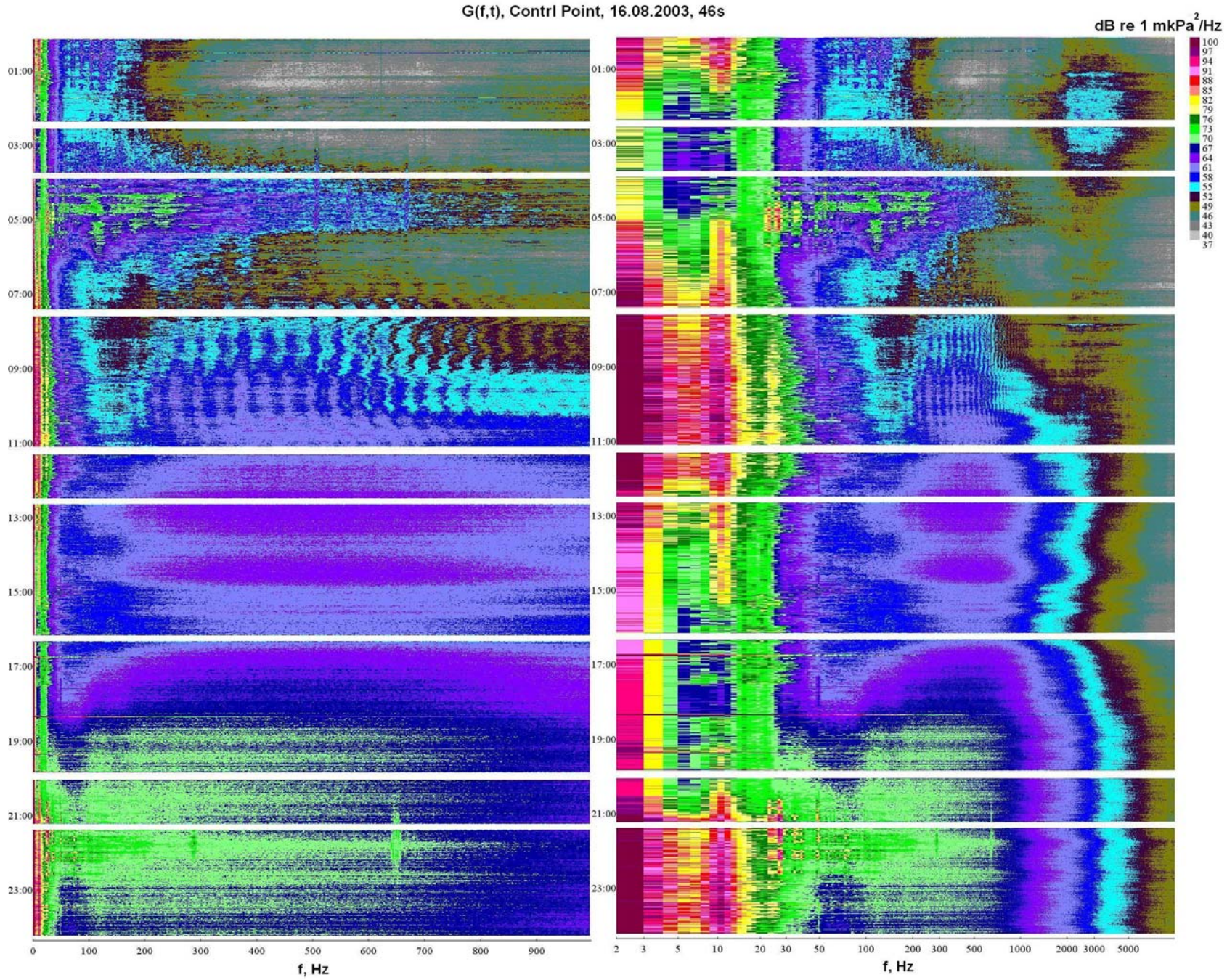

Figure 2.1 - Sonogram *G(f,t)* of data recorded at the control station on 16 August 2003 during the approach of a storm.

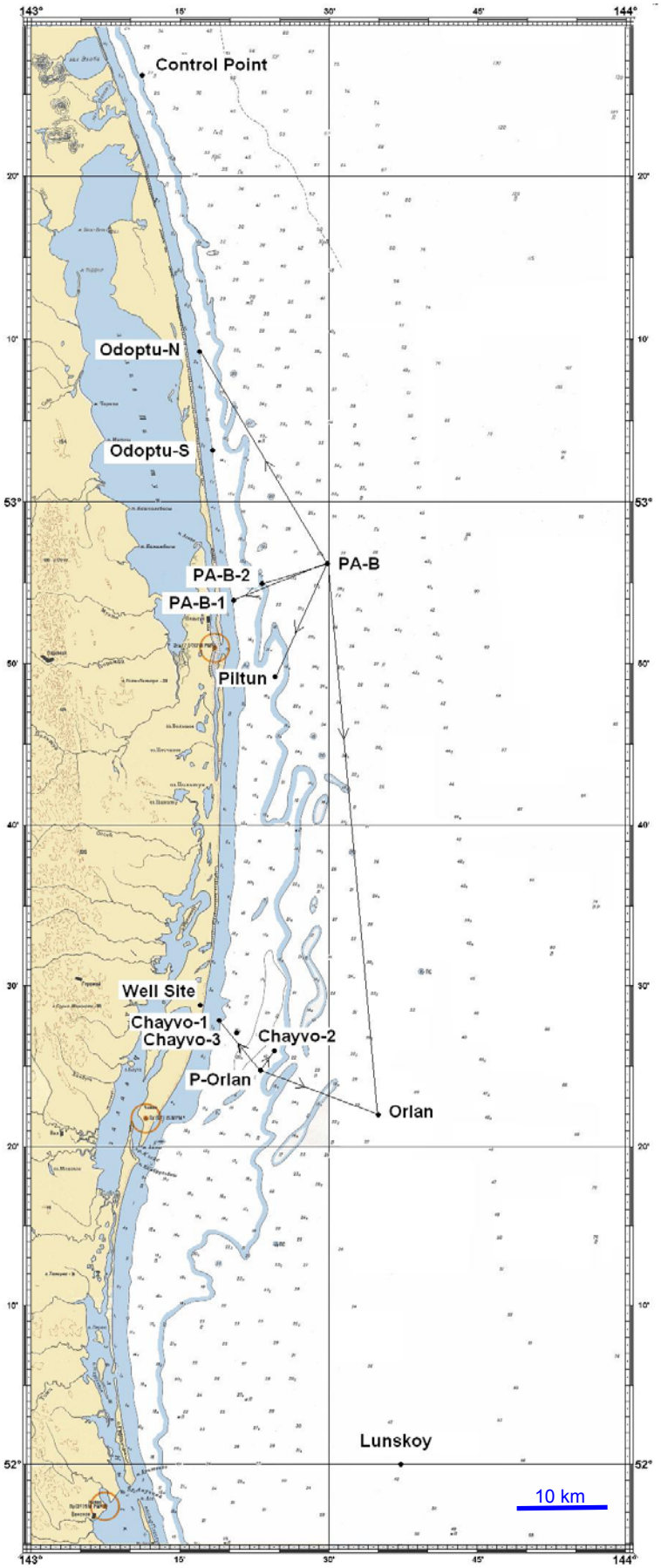

Figure 2.2 - Map showing the locations where AUARs were deployed during the 2003 acoustic program.

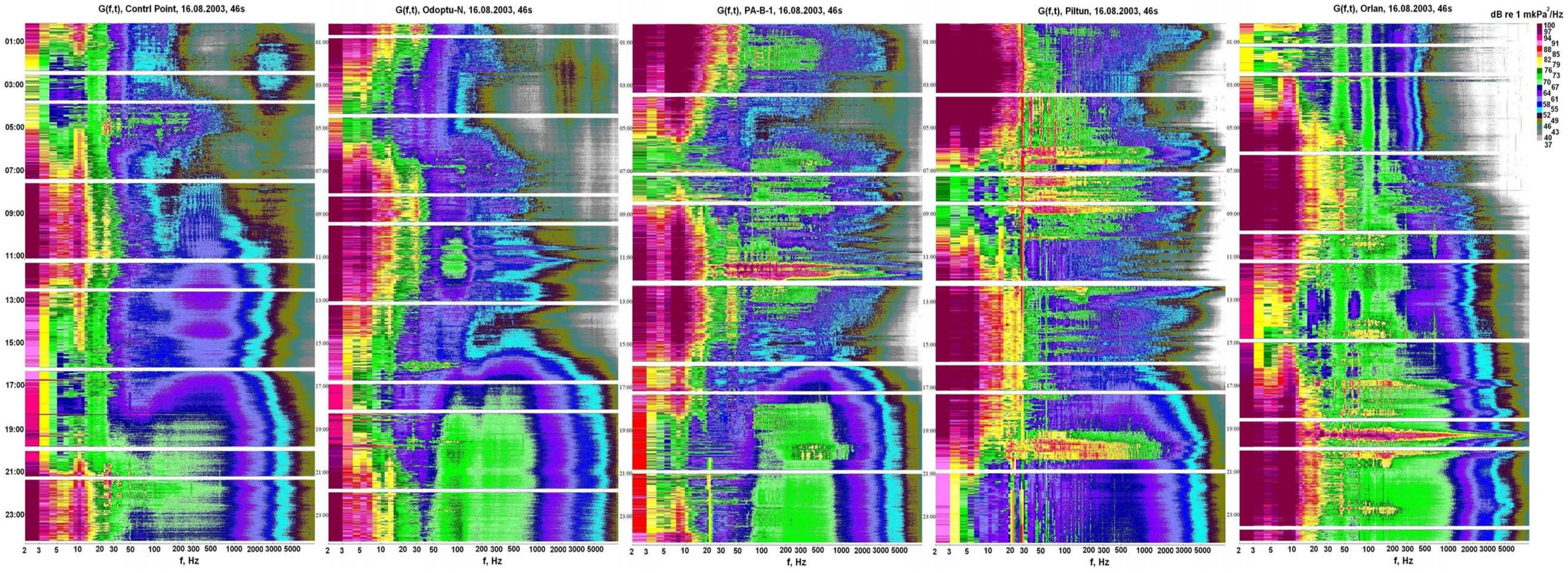

Figure 2.3 - Sonograms *G(f,t)* of noise synchronously recorded at the control point, Odoptu-N, PA-B-1, Piltun and Orlan on 16 August 2003.

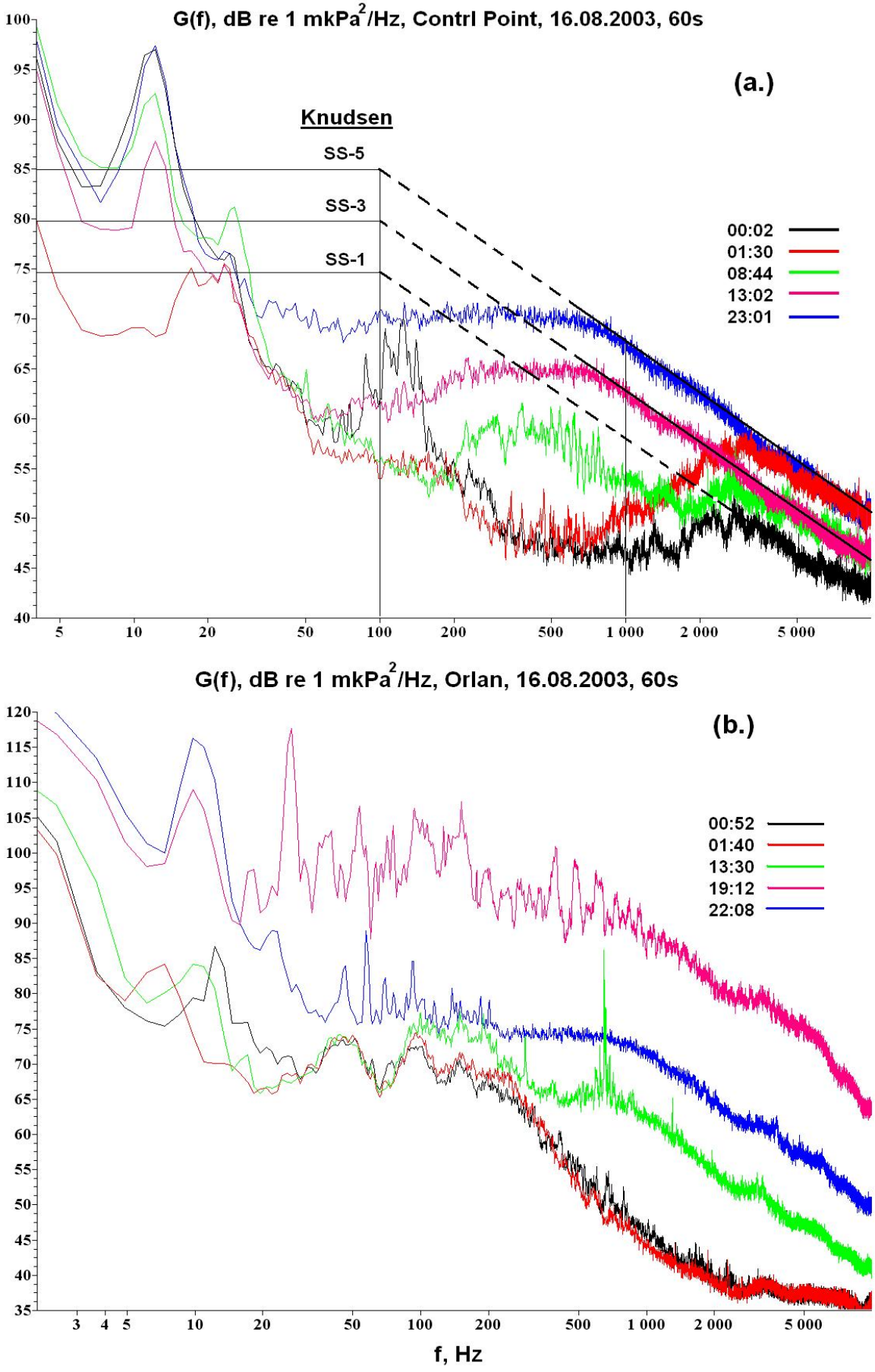

Figure 2.4 - Spectra *G(f)* of noise synchronously recorded 120 km apart at the control point (a) and Orlan monitor station (b) on 16 August 2003.

The three dashed lines on Figure 2.4(a) describe Knudsen's experimental relationship between sea state recorded at the surface and the spectrum of the noise field in the water noise [Knudsen et. al., 1948; Richardson et. al., 1995]. This relationship closely approximates the results observed at the control point. The Beaufort Sea State relates to the following wind speed and wave height:

Sea State 1 - Wind speed of 0.5-1.5 m/s and 0.1 m surface wave height.
Sea State 3 - Wind speed of 3.6-5.1 m/s and 0.5-1.2 m surface wave height.
Sea State 5 - Wind speed of 11.3-13.9 m/s and 2.4-4.0 m surface wave height.

The red and black spectra *G(f)* plotted in Figure 2.4 correspond to acoustic measurements taken at night in calm seas. The relatively high spectral level at frequencies greater than 2 kHz seen at the control point (Figure 2.4(a) - 01:30 and sonogram *G(f,t)* - Figure 2.3) is caused by an acoustic signal of biological origin and will be discussed further in chapter 4.

The spectral *G(f)* plot for 08:44 (Figure 2.4(a)) illustrates the frequency interference structure (300-1000 Hz) of the acoustic field produced by an approaching storm. The sonogram *G(f,t)* (Figure 2.3 (control station) - 07:00 to 11:00) displays its temporal variation. The spectral variation between 20-200 Hz shows evidence of both close and distant vessels. The spectrum *G(f)* (Figure 2.4(b) - 19:12) corresponds to a vessel under way close to Orlan and can be seen on the sonogram *G(f,t)* for Orlan monitor station (Figure 2.3 - 19:00).

During times of high tidal currents the power spectral density of flow noise at frequencies below 5 Hz can significantly increase and a peak emerges between 8-16 Hz (sonogram *G(f,t)* - Figure 2.1).

Figure 2.3 also indicates that vessels generated a significant part of the noise recorded at the Piltun and Orlan monitor stations. Spectral plots *G(f)* for calm seas (Figure 2.4(a) - 01:30 and Figure 2.4(b) - 00:52, 01:40 and 13:30) show that in the frequency band from 5-30 Hz, the level of noise generated by distant vessels and recorded at the control station reached 75 dB re 1 μPa^2/Hz and at Orlan reached 85 dB re 1 μ Pa^2/Hz. Spectral plots *G(f)* for the frequency band from 20-200 Hz (Figure 2.4(b) - 00:52, 01:40 and 13:30) have a

relatively stable interference structure which could be defined by the noise field generated by a distant stationary source.

Figure 2.5 presents the results of spectral analysis of the acoustic field measured at the control point on 3 September 2003. Sonograms *G(f,t)* illustrate the temporal variation in the spectral level of acoustic noise for frequencies from 2-15000 Hz, and spectra *G(f)* show the spectral density levels for differing times of day and meteorological conditions. The spectral *G(f)* plot at 11:02 is for calm seas and distant moving vessels. At 02:24 the low frequency tonal components are very clear, possibly caused by a distant vessel.

Figure 2.6 displays Sonograms of synchronous acoustic background measurements from Chayvo-1, Chayvo-2 and Lunskoye recorded on 10 September. They clearly illustrate the variation in the ambient acoustic field in shallowing water[18] as the weather conditions changed. From visual monitoring the weather was clear in the morning, and the waves did not have whitecaps. After midday the wind began to strengthen and a storm built.

Weather conditions during the measurements at Chayvo-1, Chayvo-2 and Lunskoye were:

9 September - Clear with good visibility in the morning, fog in the afternoon, Sea State 2.

10 September - Full moon, clear in the morning, wave height <1 m (no whitecaps). After 12:00 the wind strengthened and by evening there was a storm. The *Nevelskoy* rode out the storm.

11 September - Cloudy, stormy, Sea State 6. The *Nevelskoy* was riding out the storm, which ended in the afternoon. By evening, the *Nevelskoy* sailed to the coast to pick up AUARs at Chayvo-1 and Chayvo-2. By 22:30 the current at Chayvo-2 was zero.

[18] The water depths were Lunskoye 46 m, Chayvo-2 17 m and Chayvo-1 10 m.

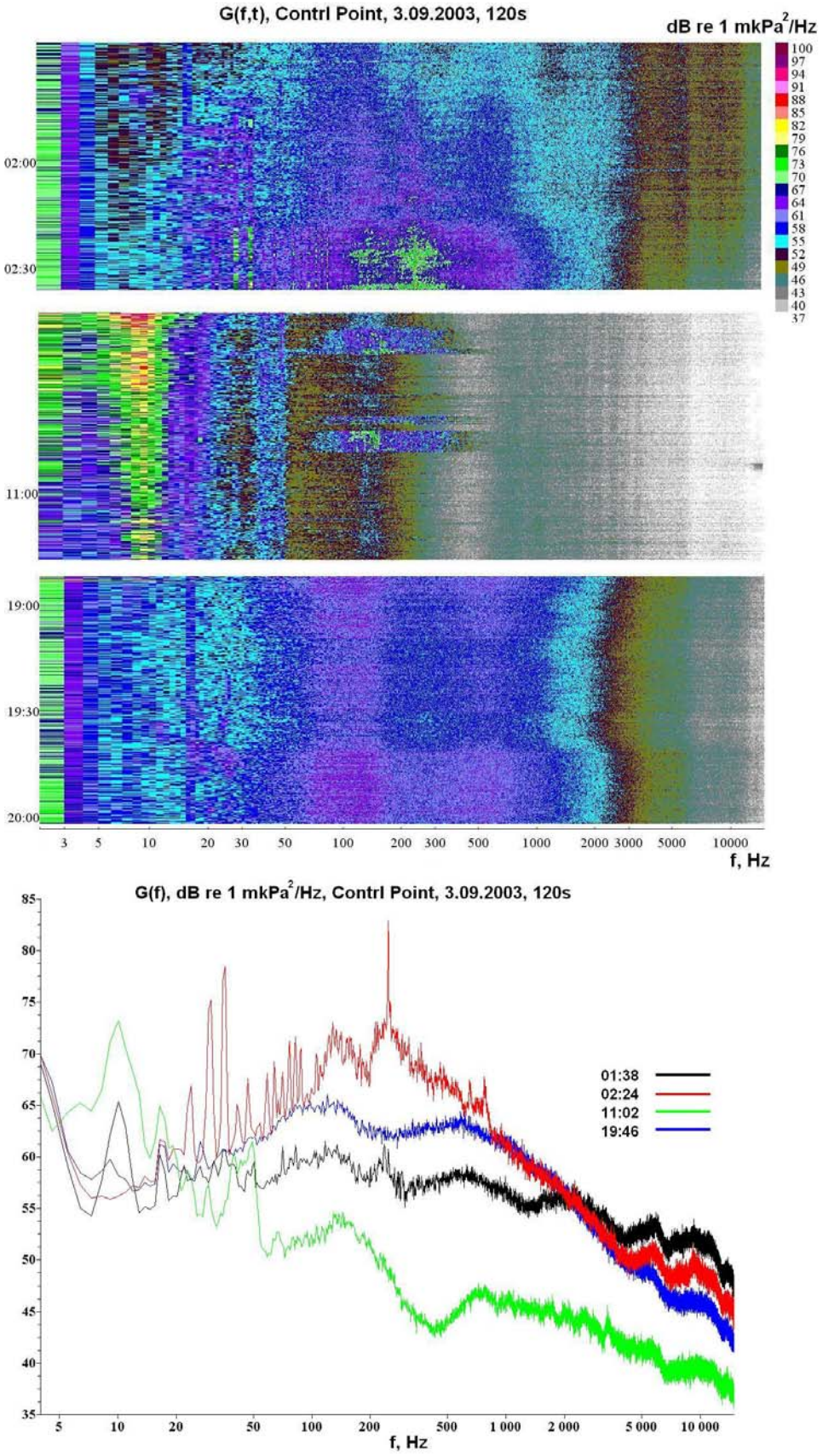

Figure 2.5 - Sonograms *G(f,t)* and spectra *G(f)* of acoustic noise recorded at the control station on 3 September 2003.

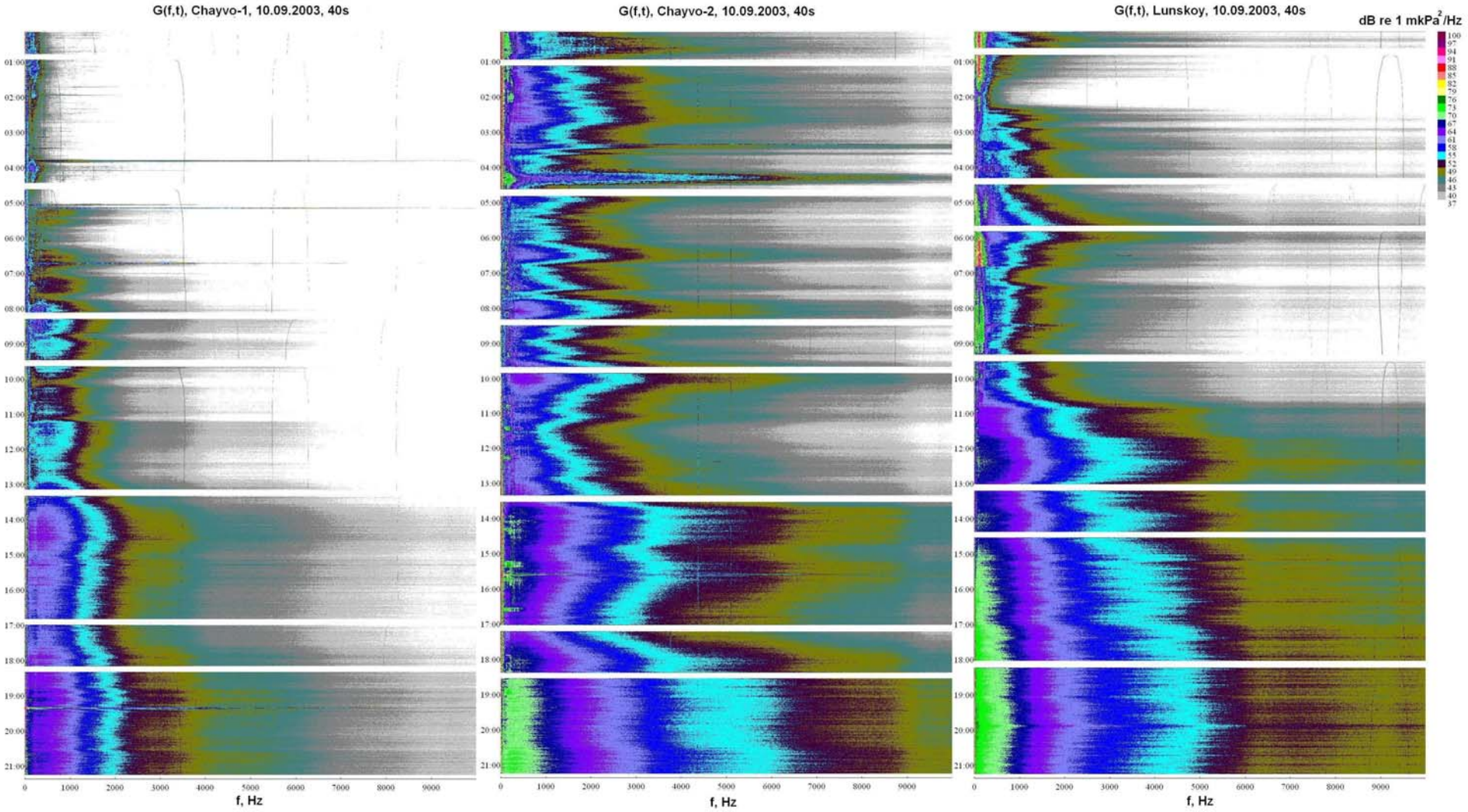

Figure 2.6 - Sonograms *G(f,t)* recorded at locations Chayvo-1, Chayvo-2 and Lunskoye on 10 September 2003, during a change in weather conditions from calm to storm.

3 Theoretical & experimental analysis of sound propagation at PA-B & Chayvo

This section analyzes the influence of the hydrodynamic field over acoustic propagation on the NE Sakhalin shelf and experimental analysis of sound propagation and TL in the PA-B and Chayvo areas.

3.1 Impact of the hydrodynamic field on sound propagation in the Chayvo area

Bondar [Bondar et al., 1993] presented the results of an experimental and theoretical study of the influence of surface tides on the hydrodynamic field and the impact of these disturbances on low frequency sound propagation over the shelf of the Japanese sea. Their study utilized numerical experiments (based on mode theory) and the analysis of measurements along a 23 km stationary profile oriented perpendicular to the shelf, to study the effects of surface tides and tidal internal waves (TIWs)[19]. Comparisons of measurements recorded during different hydrologic conditions allowed the effects of surface tides and temperature variations along the shelf caused by tidal internal waves propagating along the seasonal pycnocline to be estimated. Modeling results showed that a tidal change of 0.2 m at the surface has significantly less impact on sound propagation at a frequency of 315 Hz than an 8 m tidal internal wave. Measurements showed that up to 20 dB of variation could be seen in the amplitude of low frequency acoustic signals propagating over long profiles across the shelf. The variation in Intensity along these profiles correlate with the variation of waveguide parameters caused by tidal forces. However, this correlation is not present for refraction and scattering on spatial fluctuations of the velocity field induced by a number of hydrodynamic processes including internal waves. Phase variations in these signals, unlike intensity, have retained the correlation with the waveguide parameters and can be used as an indicator of integral change of waveguide parameters over the profile.

The impact of TIWs and related non-linear short wavelength internal waves[20] with known spatial and temporal parameters on the propagation of low frequency tonal and noise signals was studied on the shelf of the Japanese sea [Rutenko, 2003]. This paper stated that relatively short non-linear internal waves generated by the disruption of tidal internal waves in shallow water can significantly impact sound propagation on the shelf. Scattering

[19] Tidal internal waves have wavelengths of10's of kilometers and amplitudes of 7-14 m.
[20] Short wavelength internal waves have wavelengths of 80-300 m and amplitudes of ~15 m.

of propagating acoustic waves on spatial fluctuations in the velocity field formed by internal waves causes intensity variations and can cause significant transmission loss. This scattering results in the transfer of energy from lower modes to higher modes, which propagate with higher losses due to absorption by the bottom.

The height of the surface tide on the NE Sakhalin shelf is greater than 1 m and the velocity of the tidal current in shallow water exceeds 2 m/s. Figure 3.1 displays hydrologic measurements taken at the proposed PA-B location in August and September of 2003. The hydrologic data illustrates that in August, as the temperature of the surface layer increases, a steady seasonal pycnocline emerges. Within this pycnocline, the acoustic velocity changes from 1495 m/s at the surface to 1472 m/s at 28 m. In September as the surface temperature decreases and wave action causes mixing of the surface water a sharp pycnocline forms (with a velocity gradient of ≈-4 m/s per meter) and stretches along the shelf. Thus tidal flows interacting with the ocean bottom at the shelf edge generate long wavelength tidal internal waves that propagate along the pycnocline to the shore with their peaks oriented along the bathymetry. These can be transformed into short non-linear internal waves with their peaks also oriented approximately parallel to the shoreline. Sound propagating across the shelf dissipates on spatial fluctuations of the velocity field caused by internal waves at the pycnocline and it leads to interacting modes. This interaction can be resonant[21], causing variations in TL with time of >6 dB [Rutenko, 2003]. Sound propagating parallel to the shore (and to the internal waves) is affected by the spatial waveguide formed by the internal waves. However, the waveguide parameters only change the spatial interference structure, not the acoustic energy carried by normal modes. In this case the effects of internal waves are clearest in measurements of acoustic pressure using a hydrophone placed at the interference minimum of the acoustic field. Any TL measurements must comprehend a periodicity greater than the periodicity of the internal waves propagating perpendicular to the acoustic profile. If it is not practical to make continuous TL measurements over a period greater than the periodicity of the internal waves, a stationary transducer could be used to make measurements over an extended period or the measurements could be averaged in space by moving the transducer.

[21] The difference in wavenumbers of the interacting modes is equal to the wavenumber of the internal wave.

PA-B

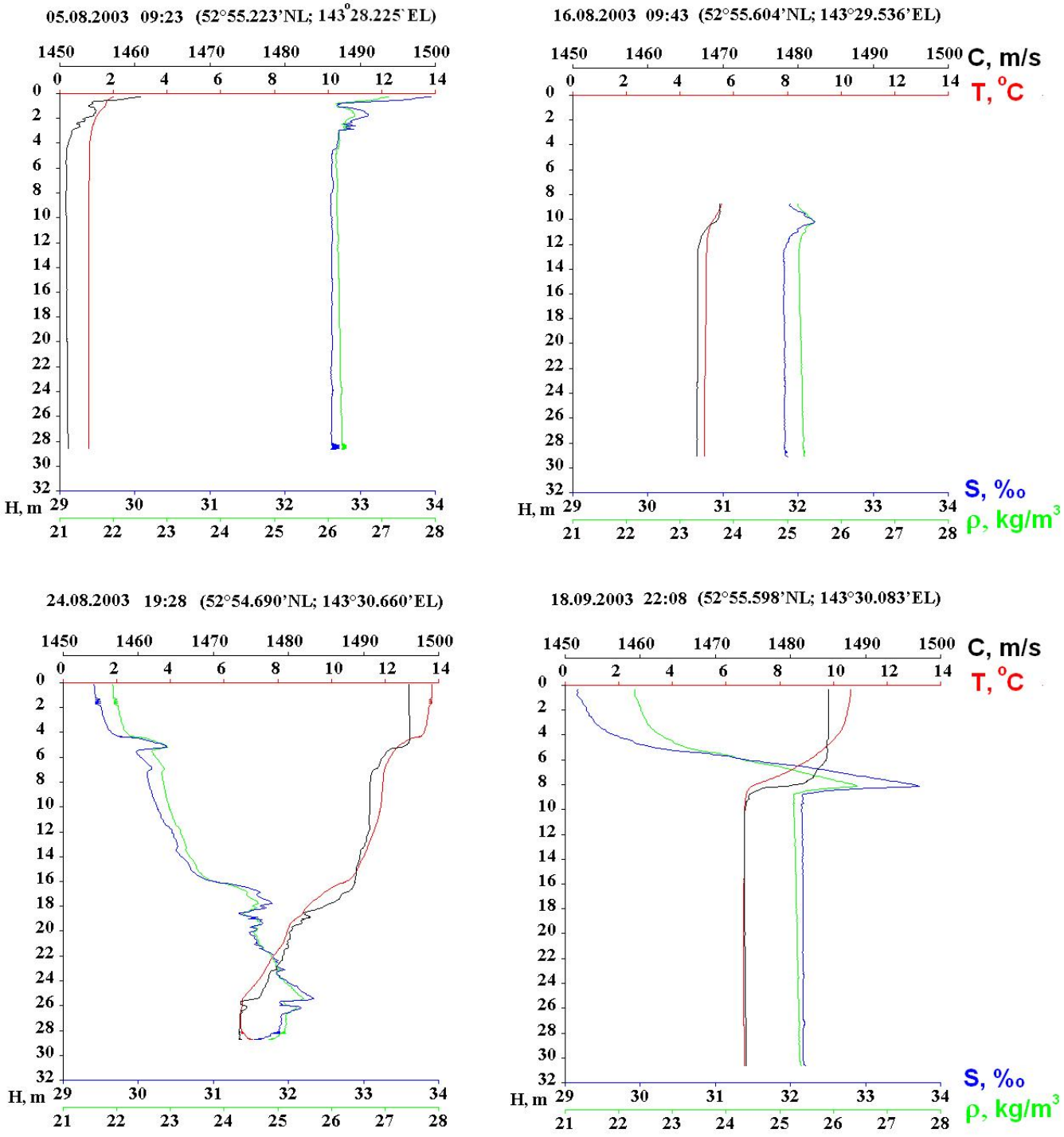

Figure 3.1 - Hydrological data acquired near the proposed PA-B location over August and September 2003.

In September 2003 an autonomous bottom transducer was placed on the sea floor close to the proposed location for the Orlan platform to estimate the impact of the hydrodynamic field on sound propagation. The autonomous CW-320 transducer produced a constant amplitude 320 Hz tonal signal for three days. Figure 3.2 gives a map of the area showing the location of the transducer and AUARs during the experiment (Chayvo-1, Chayvo-2 and Orlan).

Figures 3.3 and 3.4 present plots showing the variation in power spectral density (intensity *I(t)*) at 320 Hz. The intensity *I(t)* estimates are calculated by averaging the 320 Hz spectral density values from 120 one second FFT realizations. Figure 3.2 shows that the transect from the CW-320 transducer to Chayvo-2 is oriented approximately parallel to the coast and the 20 m contour. Internal waves produced by a tide at the edge of the shelf must therefore propagate perpendicular to the transect. Variations in *I(t)* measured at Chayvo-2 should therefore correlate to the variations in the internal wave parameters as they cross this profile. A quasi-periodic variation in the intensity measured at Chayvo-2 can be seen in Figures 3.3 and 3.4, with clear packets (labeled IW) of variations of *I(t)* with a period of approximately 40 minutes and a level of up to 14 dB (Figure 3.4: 9 September 2003 - 10:00). Six such IW packets were recorded in three days (Figure 3.3), giving support to the theory that these internal waves are generated by tidal flows interacting with the continental slope. Internal waves propagate to shore with a phase and group velocity that are dependent on the spatial distribution of the density field, which constantly changes in this area. Internal waves in the shallow part of the shelf therefore lose the harmonic shape of the tidal flow that sources them (Chayvo-1).

Two conclusions can be drawn from the data presented in Figures 3.3 and 3.4 and the previous discussion:

1. During the summer-fall season on the NE Sakhalin shelf hydrodynamic processes that destabilize the spatial and temporal density field along the seasonal pycnocline significantly affect sound propagation. The variations in Intensity *I(t)* of a 320 Hz signal propagating over 6 km to 13 km long profiles are 16 dB and 12 dB respectively, with periods of $\approx$12 and $\approx$24 hours.
2. The effect of tidal internal waves are distinct and at a maximum on a profile oriented perpendicular to their propagation direction, this result is in accordance with the

theoretically predicted impact of internal waves on sound propagation. For a 320 Hz tonal signal propagating along a 12 km profile Intensity *I(t)* variations of 10-14 dB with a period of 25-45 minutes were recorded.

These results must be considered when assessing the accuracy of TL experiments acquired using acoustic signals and known hydrologic and hydrodynamic conditions.

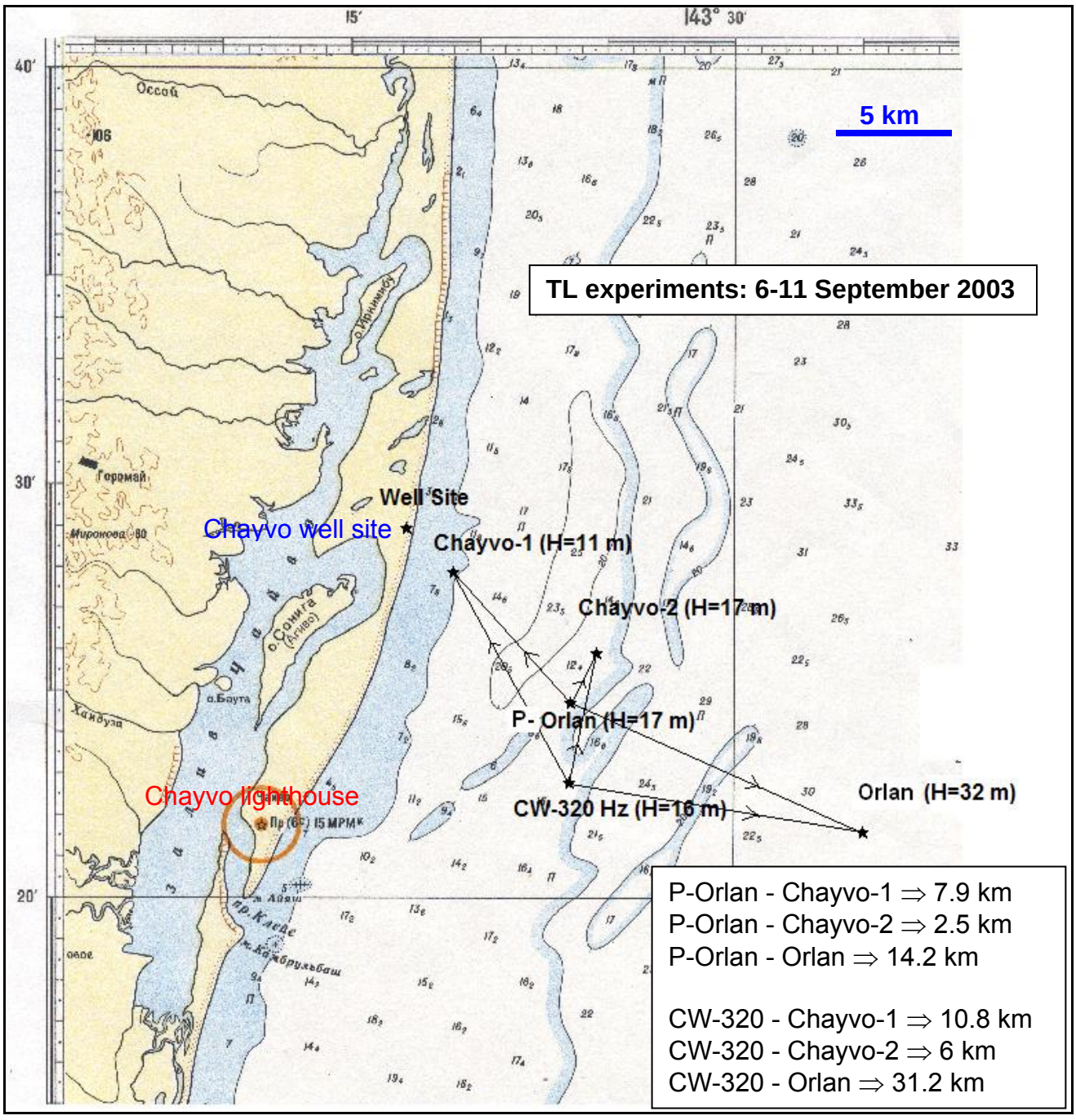

Figure 3.2 - Map showing the locations of the autonomous CW-320 transducer, the transducer at the proposed location of the Orlan platform (P-Orlan) and the Chayvo-1, Chayvo-2 and Orlan AUARs deployed on 6-11 September 2003.

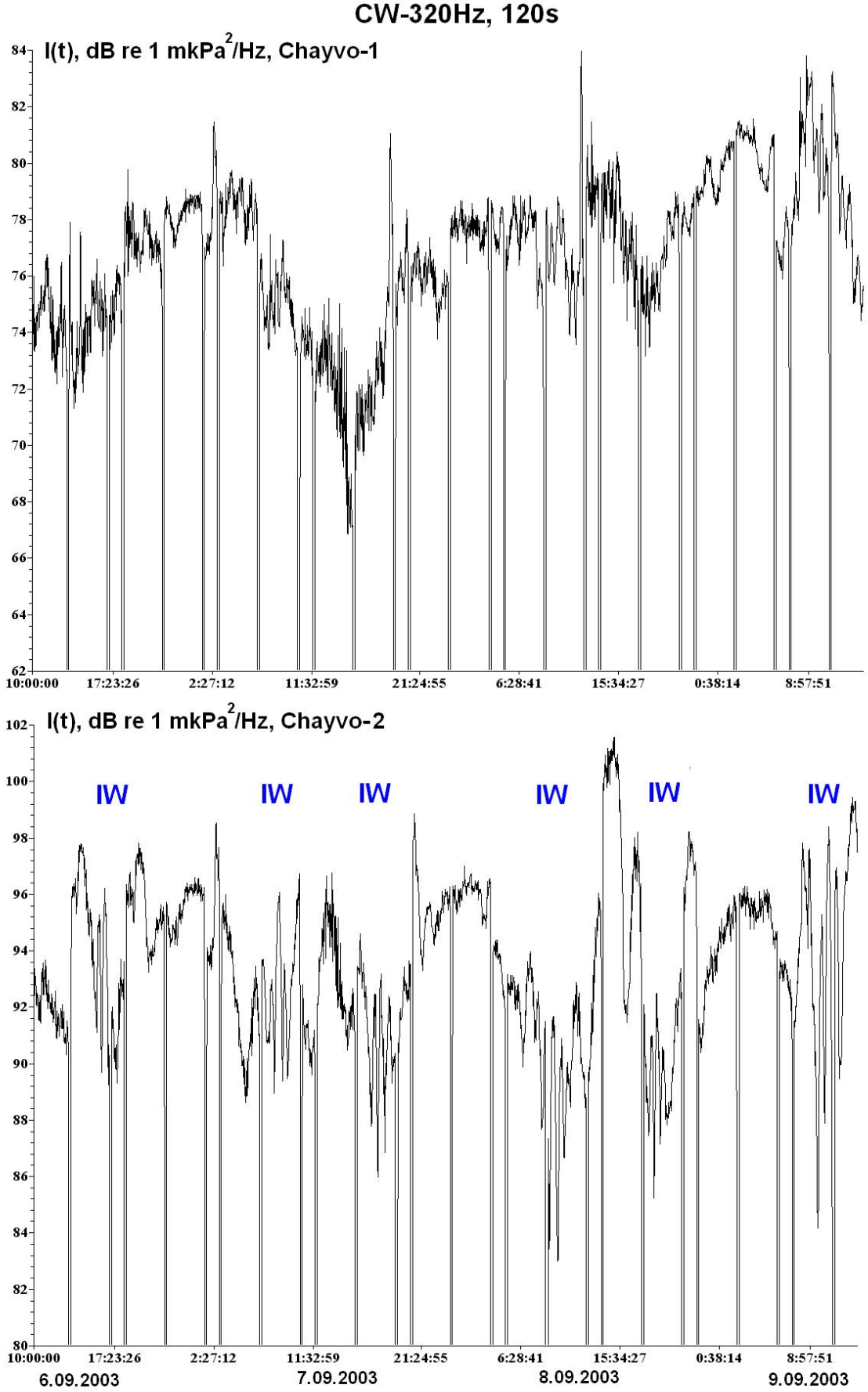

Figure 3.3 - Variations in the Intensity I(t) of the 320 Hz acoustic field synchronously measured at Chayvo-1 and Chayvo-2 when an autonomous transducer was deployed at point CW-320.

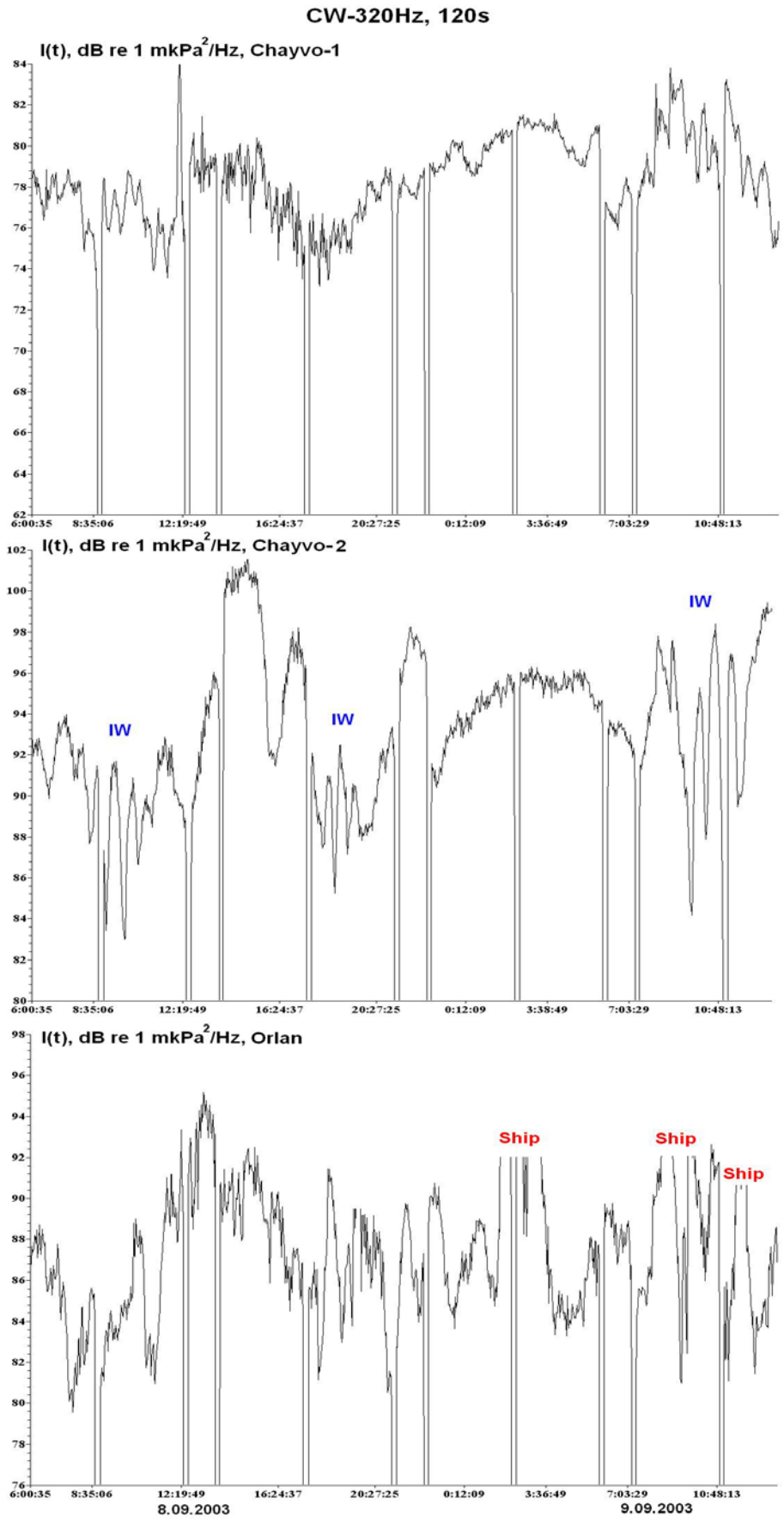

Figure 3.4 - Variations in the Intensity I(t) of the 320 Hz acoustic field synchronously measured at Chayvo-1, Chayvo-2 and Orlan when an autonomous transducer was deployed at point CW-320.

3.2 Analysis of sound propagation and TL from PA-B to the inshore feeding area

The goal of this study was to estimate the TL from the proposed location of the PA-B platform to the PA-B-1 and PA-B-2 monitor stations, located at the 10 m and 20 m contours within the inshore feeding area (Figure 3.5). The TL was estimated for frequencies from 15-15000 Hz using transducers deployed at 8 m from the anchored *Nevelskoy* and received by AUARs at PA-B-1 and PA-B-2. The source level of the transducer was monitored using a calibrated hydrophone at 1 m.

Figure 3.5 illustrates the profiles over which the TL experiments were conducted. Figure 3.6(a) shows a bathymetric profile from PA-B to PA-B-1 generated by the bottom profiler on the *Nevelskoy*, and Figure 3.6(b) gives the frequency dependent TL from PA-B to PA-B-1, PA-B-2 and Odoptu-N estimated from these field experiments. Figure 3.7(a) shows hydrologic data acquired during the experiment and Figure 3.7(b) hydrologic data acquired at the points shown on Figure 3.6(a) on 16 August 2003. Figure 3.6(b) illustrates that the TL values for propagation from PA-B to these stations are at a minimum between 100-200 Hz reaching approximately -60 dB at both PA-B-2 and PA-B-1 and -85dB at Odoptu-N. The TL increases sharply for frequencies below 80 Hz due to interaction with the sea floor. TL is significantly greater at PA-B-1 and Odoptu-N than at PA-B-2; for a frequency of 30 Hz the TL values at PA-B-1 and Odoptu-N are -95 and -117 dB respectively. For lower frequencies, acoustic energy propagates mainly through the earth rather than the bottom and TL decreases. For example at 15 Hz the TL at PA-B-1 is -78 dB, and there is a noticeable decrease of TL at PA-B-2 and PA-B-1 for 9-11 kHz (-62dB). For Odoptu-N (28 km from PA-B) there is a rapid increase in TL with frequency, and at 8 kHz TL $\approx$-115dB (attenuation coefficient $\beta \approx 2$ dB/km) due to absorption in the water and scattering.

Figure 3.8 compares theoretical and experimental TL results for the profiles from PA-B to PA-B-1, PA-B-2 and Odoptu-N. The theoretical TL values were estimated using the program MOATL[22] [Miller et.al., 1980] for the waveguide and parameters pictured in Figure 3.8(a). For a three-layer model with liquid bottom, elastic basement and transmitter and receivers as shown in Figure 3.8(a) the theoretical results approximately match the experimental results obtained during the experiment.

[22] MOATL is a mode theory approximation of acoustic propagation with non-interacting modes (adiabatic).

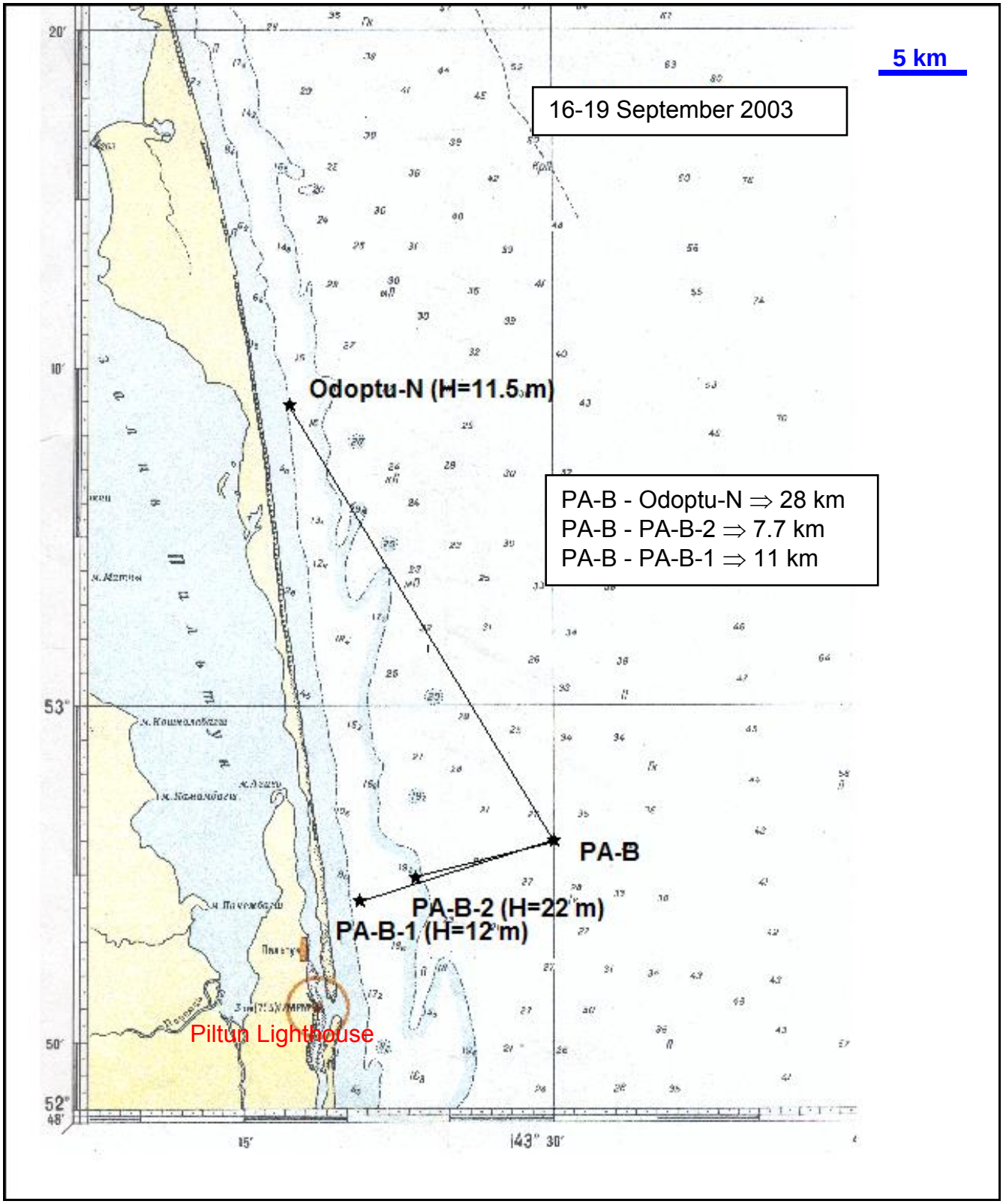

Figure 3.5 - Map showing the locations of the proposed PA-B platform and the Odoptu-N, PA-B-1 and PA-B-2 monitor stations 16-19 September 2003.

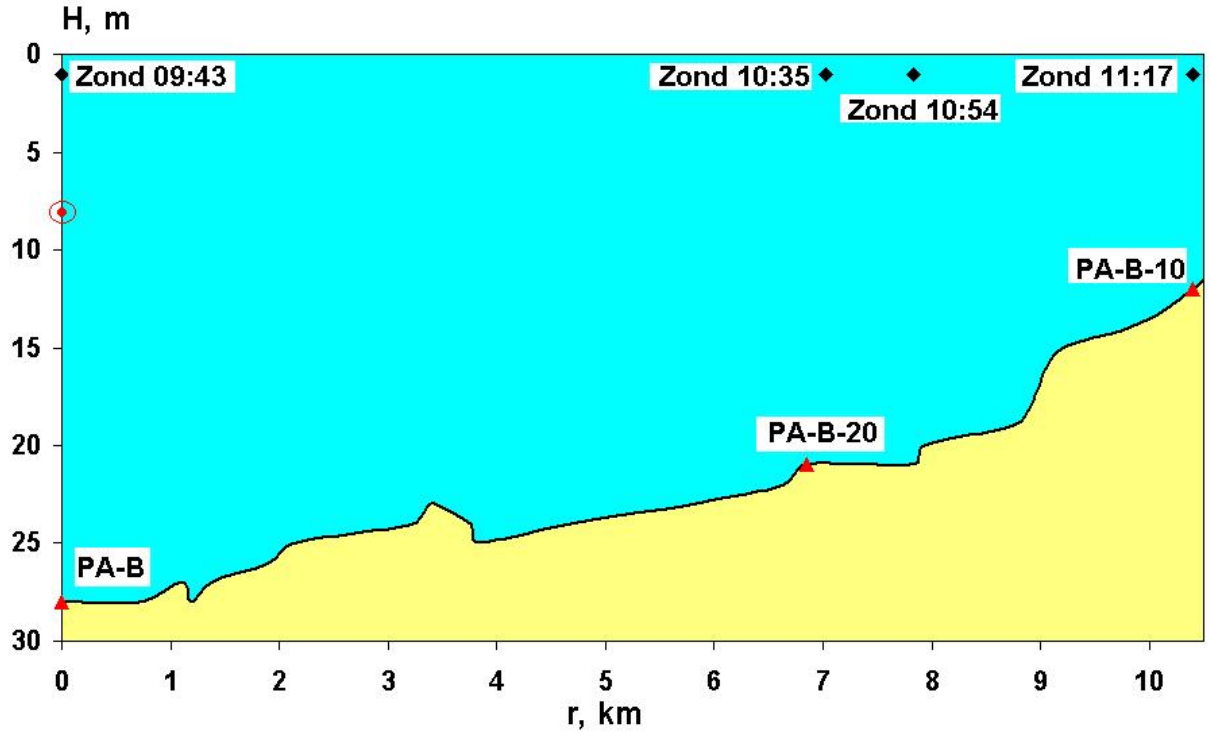

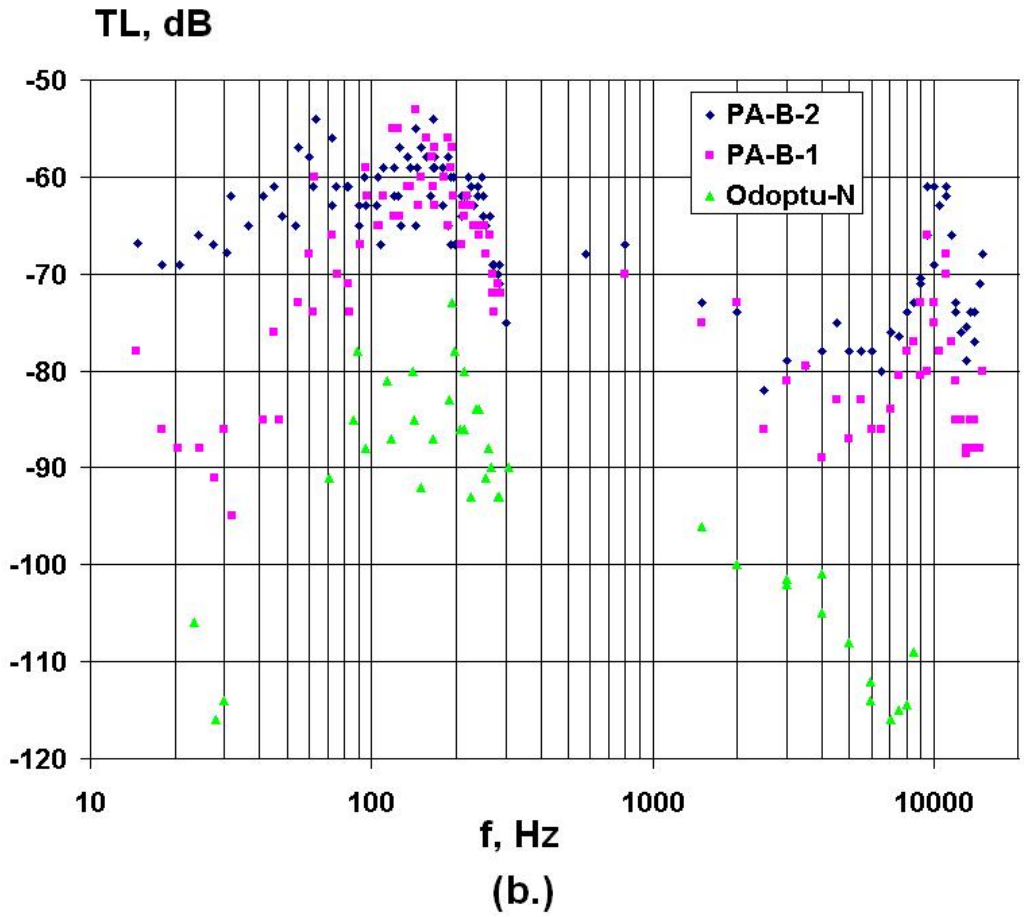

Figure 3.6 - (a) Bathymetric profile from PA-B to PA-B-1 showing the source, receiver and hydrologic data locations (b) Frequency dependent TL data from the proposed PA-B location to PA-B-1, PA-B-2 and Odoptu-N acquired on 16 September 2003.

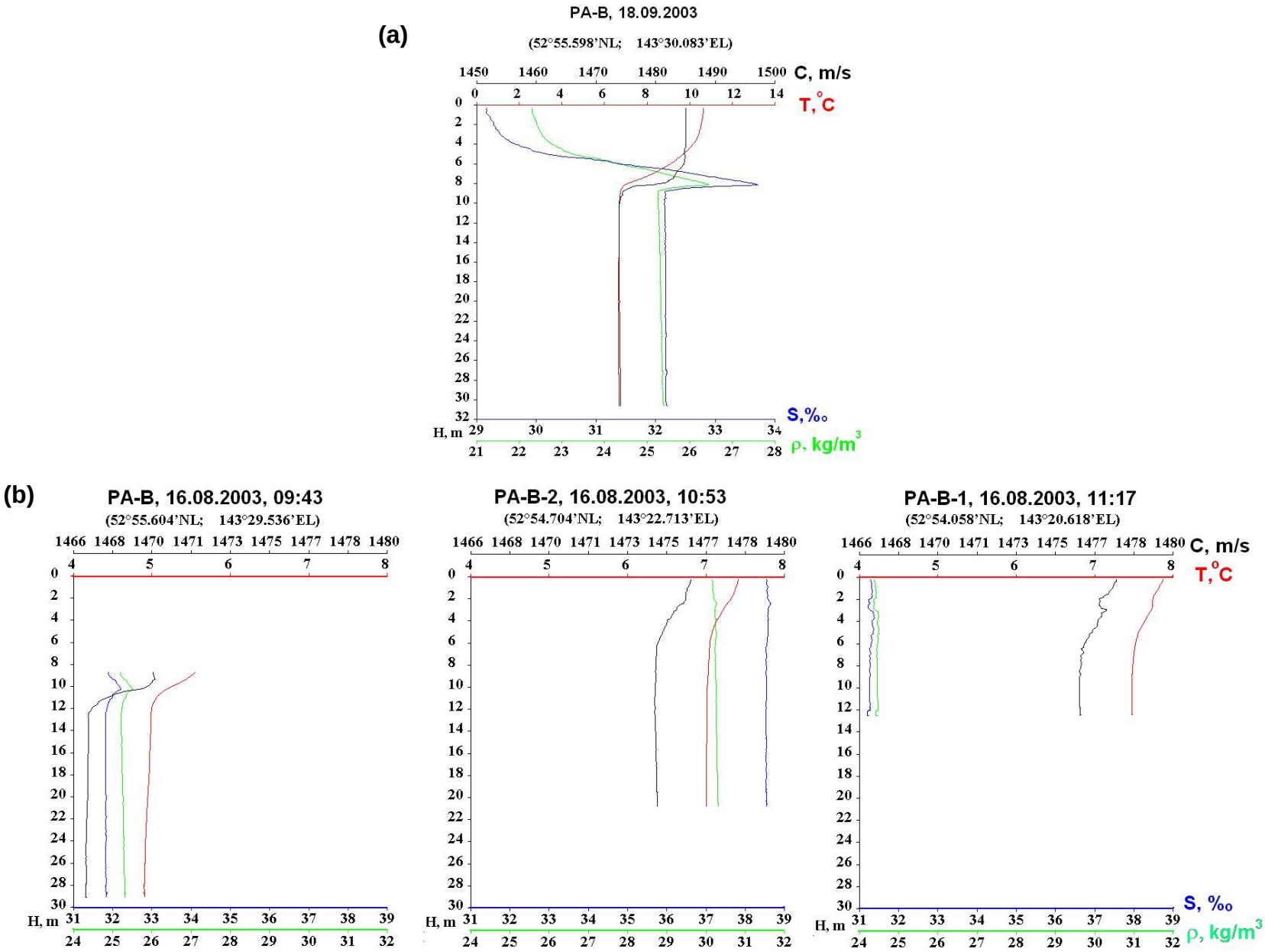

Figure 3.7 - Hydrologic data acquired at (a) PA-B on 18 September 2003 (b) PA-B, PA-B-1 and PA-B-2 on 16 August 2003.

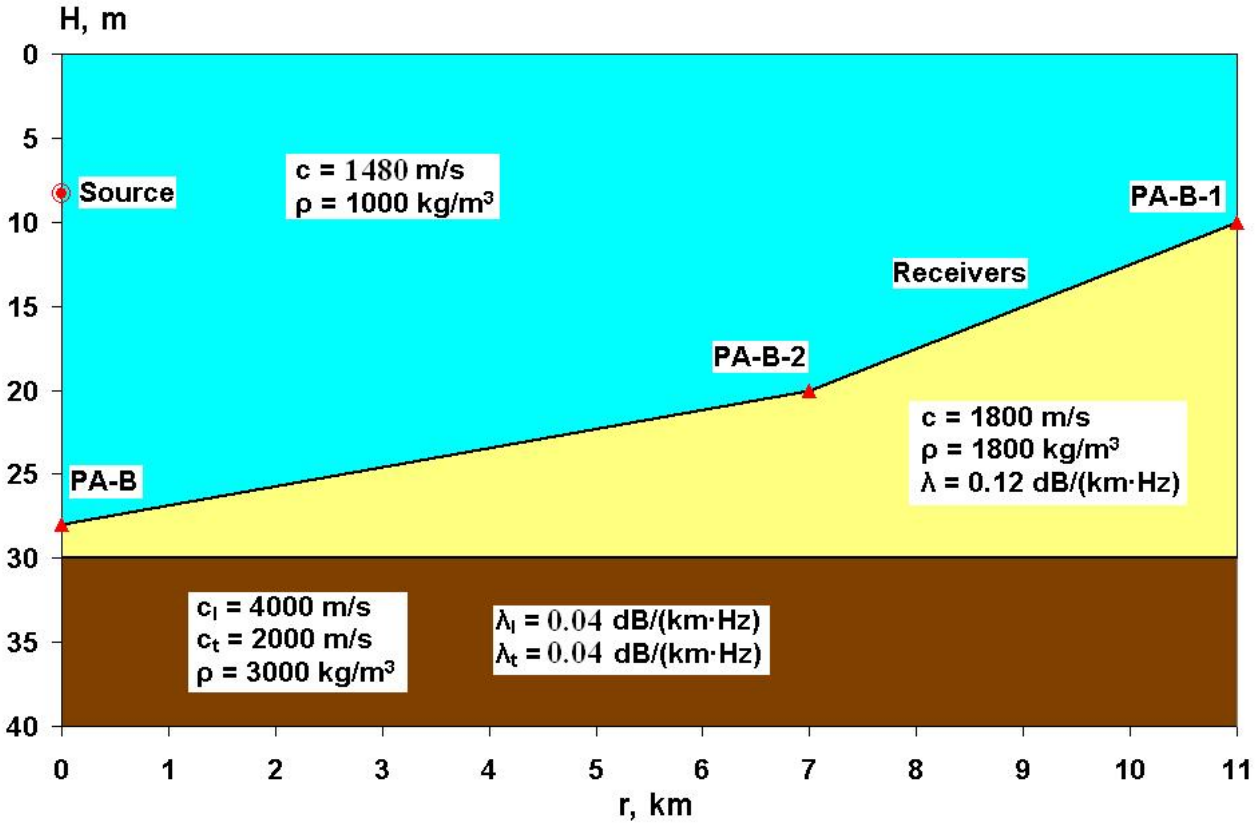

(a.)

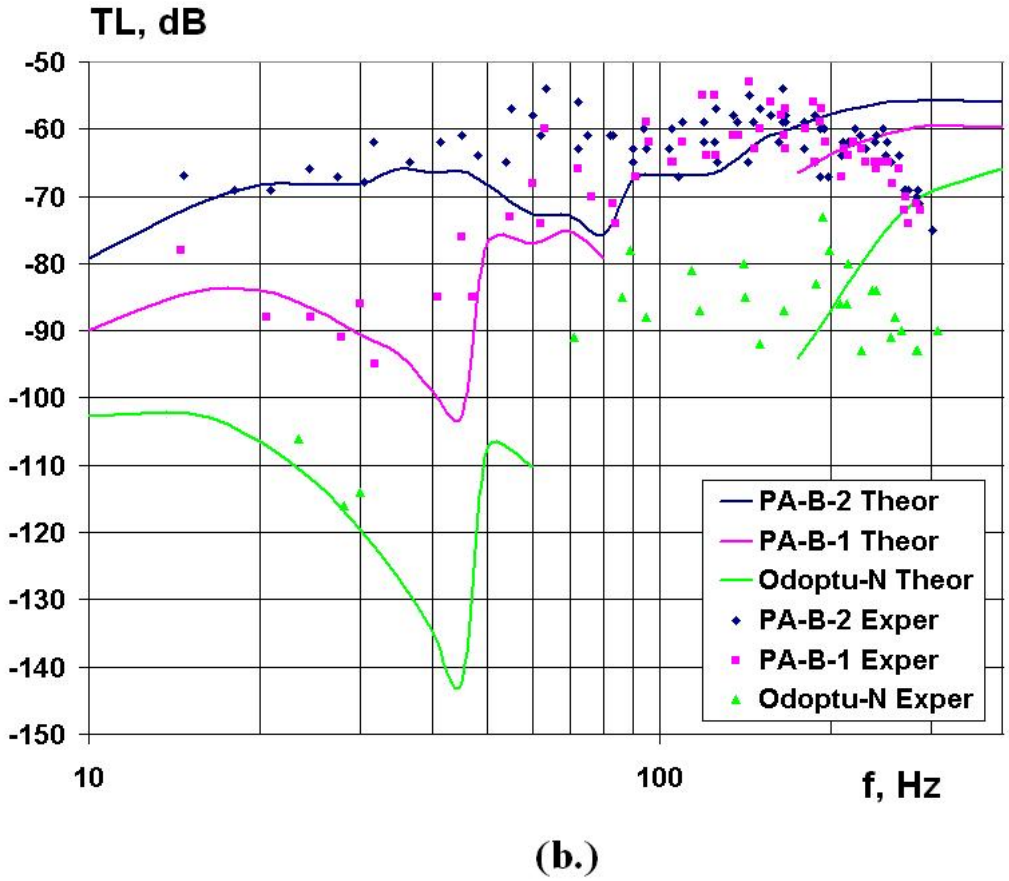

(b.)

Figure 3.8 - (a) Bathymetric profile from PA-B to PA-B-1 showing the source and receiver locations and parameters used in the modeling (b) Theoretical and experimental frequency dependent TL from PA-B to PA-B-1, PA-B-2 and Odoptu-N.

The theoretical TL values to PA-B-1 and Odoptu-N show an increase in TL for the frequency band from 25-50 Hz; this agrees with the experimental data. The shape of these curves is characteristic of the behavior of the zero and first mode, the zero mode emerges at 'zero frequency' and propagates along the bedrock surface, while in this case the first mode emerges at 30 Hz. Below 30 Hz sound propagates only in the zero mode whose attenuation has a significant increase with frequency (slope of the TL function from 20-40 Hz). The group velocity of the zero mode is 1700-1900 m/s. At higher frequencies the zero mode slows down to 1400-1470 m/s and the first mode appears at the source

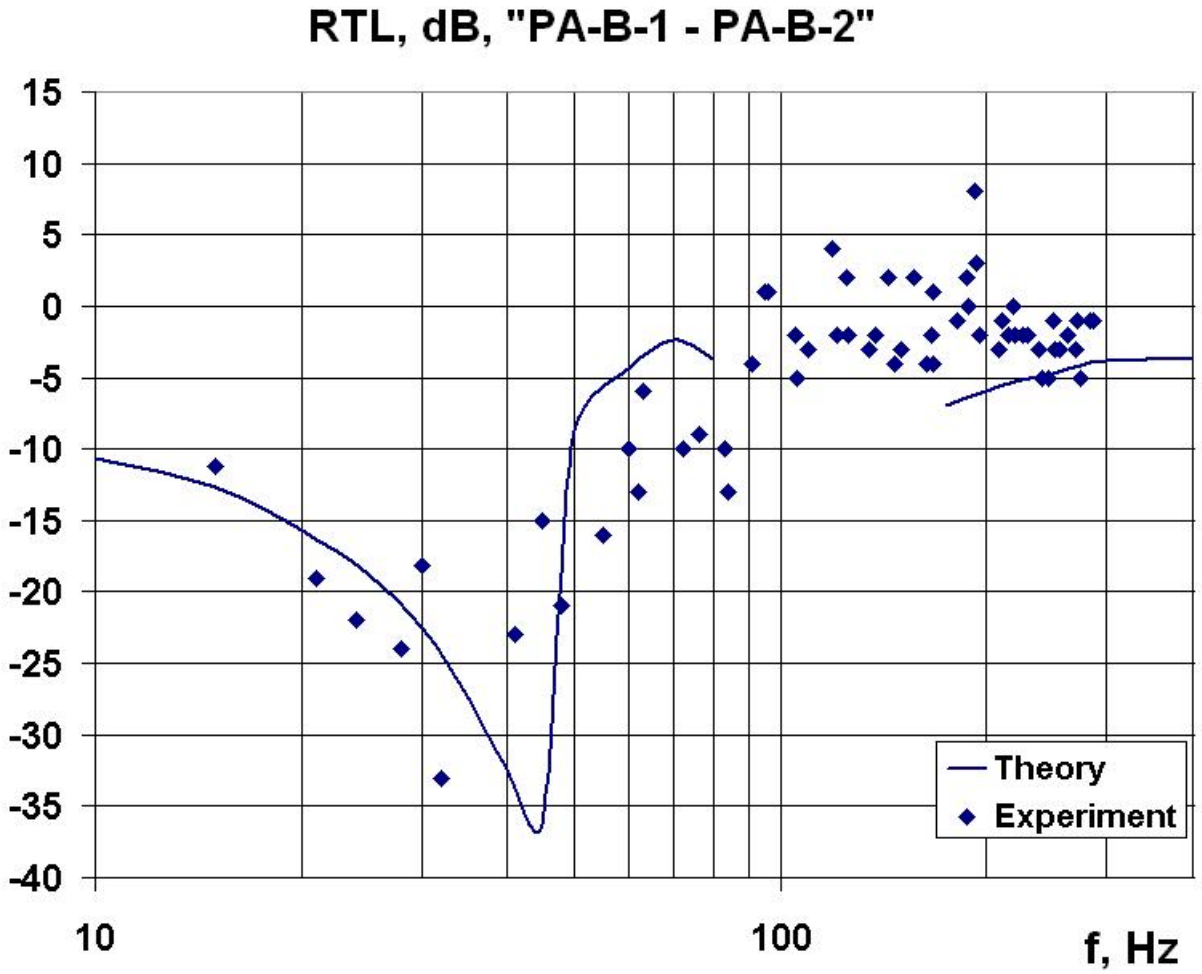

Figure 3.9 - Theoretical (line) and experimental (diamond) values of frequency dependent Relative Transmission Loss (RTL) between PA-B-2 and PA-B-1 for acoustic signals transmitted from PA-B.

However, due to the wedge shape of the waveguide this mode can be cut off and not reach the receivers. The highest relative losses occur when the first mode reaches the first

receiver (PA-B-2), but is cut off before reaching the second receiver (PA-B-1 or Odoptu-N). This occurs because the attenuation coefficient[23] of the first mode at a frequency of 40-45 Hz is 2-3 times lower than for the zero mode. Figure 3.9 shows experimental values and the theoretical Relative Transmission Loss (RTL) curve for sound propagating from PA-B-2 to PA-B-1. It is clear that since the first mode dies in the bathymetric wedge the RTL for distances greater than 4 km may reach -35 dB.

On 16 August 2003 tonal acoustic signals at 2, 3, 4 and 5 kHz transmitted from the PA-B location were recorded by the AUAR at the Orlan monitor station. Figure 3.10 shows spectra *G(f)* of signals recorded at this station and illustrates that acoustic signals can propagate along a 64 km profile with an average depth of 30 m. The main causes of signal attenuation over this profile are wave front spreading, absorption and scattering. At frequencies over 1 kHz most of the attenuation (apart from spreading loss) is absorption[24], which is proportional to f^2. This is demonstrated in Table 3.1 where the RTL (γ) $\approx f^2$ {kHz}.

Table 3.1 - TL and absorbtion loss over the PA-B to Orlan profile.

***f* (kHz)**	**2**	**3**	**4**	**5**
TL (dB)	-92	-103	-108	-119
γ = TL-TL$_{2\ kHz}$ (dB)	0	-11	-16	-27
f^2 (kHz)		-9	-16	-25

Figure 3.11 gives the experimental TL results for acoustic signals propagated from PA-B to Orlan, Odoptu-N, Piltun and PA-B-1 on 16 August 2003 (Figure 2.2)[25]. Despite a seasonal change in the hydrophysical field, the TL differences measured at PA-B-1 and Odoptu-N between summer and fall (Figures 3.11 and 3.6(b)) are not significant. Figure 3.11 shows that for frequencies from 2-6 kHz the TL from PA-B to Odoptu-N (28 km, narrowing wedge) is similar to that from PA-B to Orlan (63.4 km, flat bathymetry). This illustrates that the TL due to mode stripping by the inclined bottom is equivalent to absorption.

[23] β - Attenuation coefficient with range.
[24] Acoustic energy is absorbed in interactions with water & salt molecules, plankton, gas bubbles etc.
[25] 3.7 gives Figure the hydrologic taken between PA-B and PA-B-.

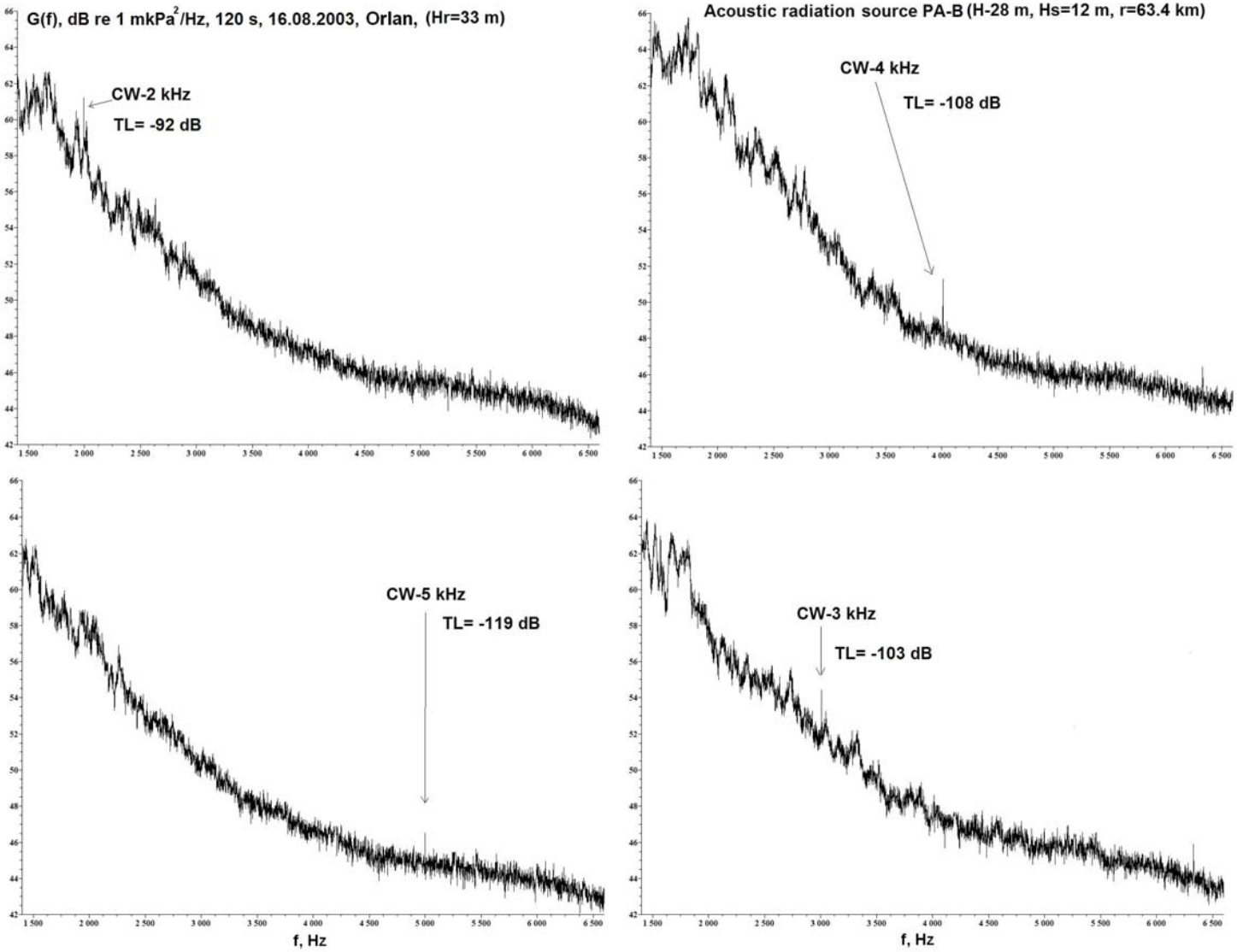

Figure 3.10 - Spectra *G(f)* of tonal signals transmitted from the proposed PA-B location and received at the Orlan monitor station on 16 August 2003.

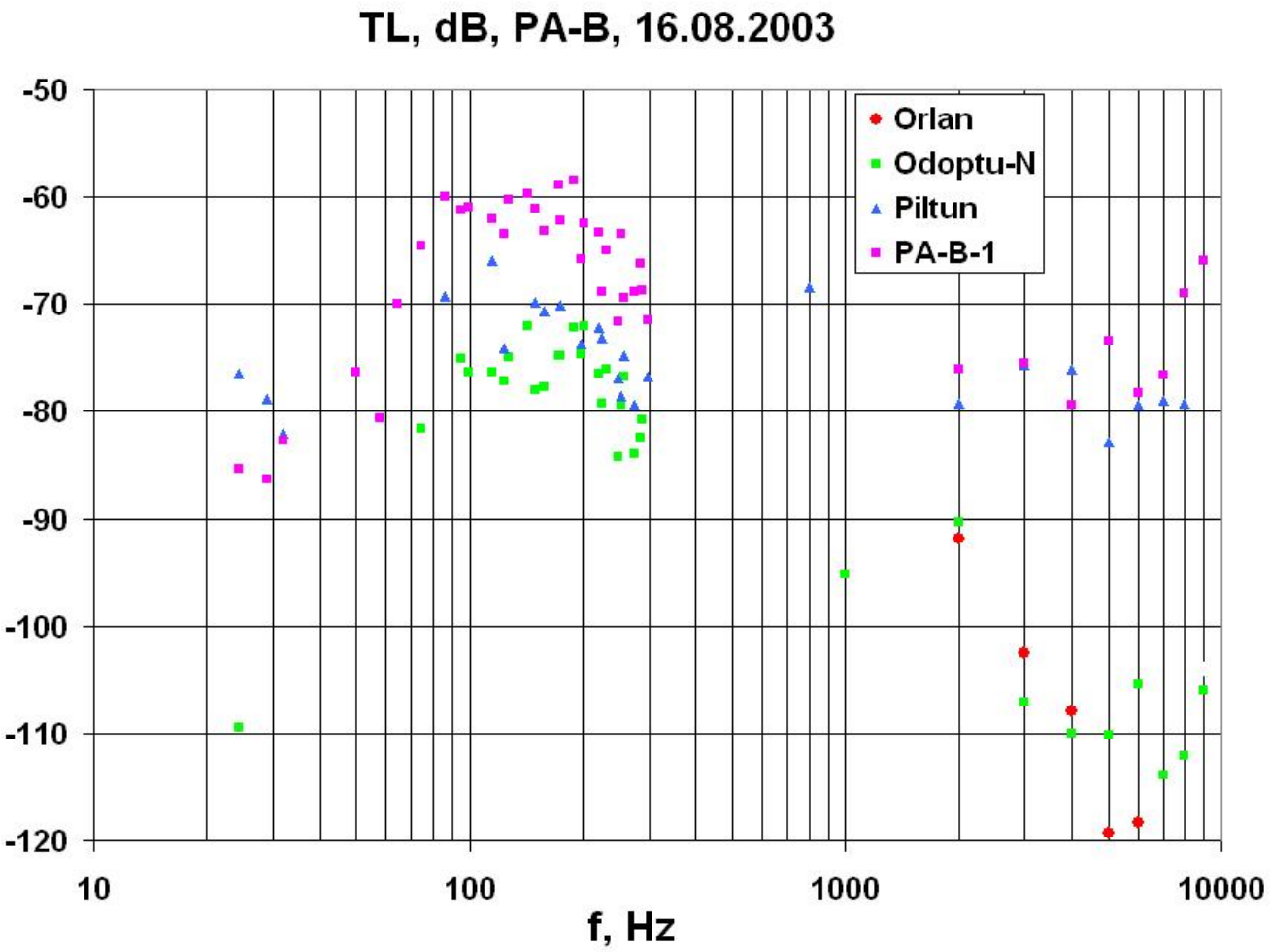

Figure 3.11 - Frequency dependent TL between PA-B and the PA-B-1, Odoptu-N, Piltun and Orlan monitor stations for acoustic signals transmitted from PA-B on 16 August 2003.

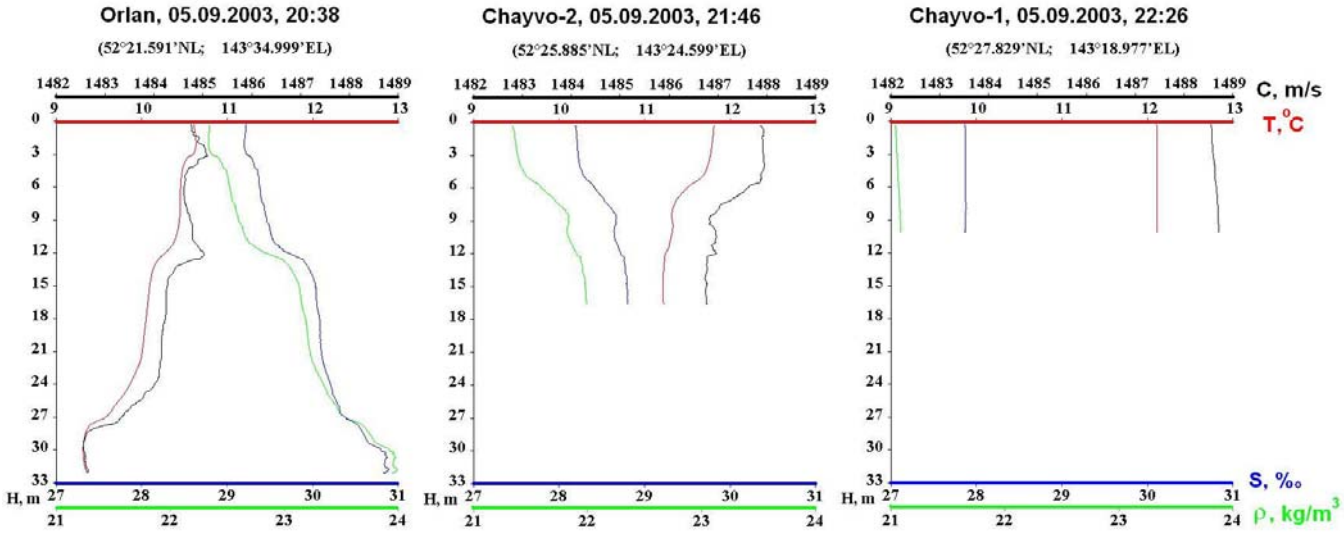

Figure 3.12 - Hydrologic data acquired at Orlan, Chayvo-2 and Chayvo-1 on 5 September 2003.

3.3 Analysis of sound propagation and TL from Orlan to the offshore feeding area

This experiment was conducted to estimate the TL from the proposed location of the Orlan platform to the Orlan monitor station located at the closest 95% kernel probability contour to the offshore feeding area in approximately 30 m water depth (Figure 3.2). The TL was estimated for frequencies from 15-15000 Hz using transducers deployed at 8 m from the anchored *Nevelskoy* and received by AUARs at Orlan, Chayvo-1 and Chayvo-2. The signal level of the transducer was monitored by a calibrated hydrophone at 1 m.

A profile from the Chayvo well site to the Orlan monitor station was used to investigate anthropogenic sound propagating offshore from the Chayvo well site (Figure 3.2), two acoustic monitor stations (Chayvo-1 and Chayvo-2) were located on this profile. Figure 3.12 presents the hydrologic measurements taken near the AUAR deployment sites on 5 September 2003. Figure 3.13(a) gives the bathymetric profile between Chayvo-1 and Orlan generated by the bottom profiler on the *Nevelskoy*.

Figure 3.13(b) shows the measurements obtained from a TL experiment during which signals were transmitted from the proposed Orlan platform location to Chayvo-2 (2.5 km, flat waveguide), Chayvo-1 (7.9 km, narrowing wedge waveguide) and Orlan (14.2 km, widening wedge waveguide). It is noticeable that the TL is approximately the same for acoustic propagation to Chayvo-1 and Orlan even though the second profile is approximately twice as long. The results from figures 3.13 and 3.6 can be compared (the acoustic profile from PA-B to PA-B-1 is 11 km long). Sound travels from PA-B to PA-B-2 in an approximately constant depth waveguide and from PA-B-2 to PA-B-1 in a 3.3 km long shallowing waveguide. TL values to PA-B-1, Chayvo-1 and Orlan are approximately the same for all frequencies except infrasonic. The experimental data for Chayvo-2, Chayvo-1 and Orlan do not show the reduction in TL for frequencies below 35 Hz that is clearly seen in experimental and theoretical data for the profile from PA-B to PA-B-1 (Figures 3.8 and 3.9).

Operational difficulties prevent the deployment of the transducers in water depths less than 10 m (the minimum operating depth of the *Nevelskoy*). The TL from the Chayvo well site to the offshore feeding area would however be a valuable component in the overall understanding of sound propagation in the area.

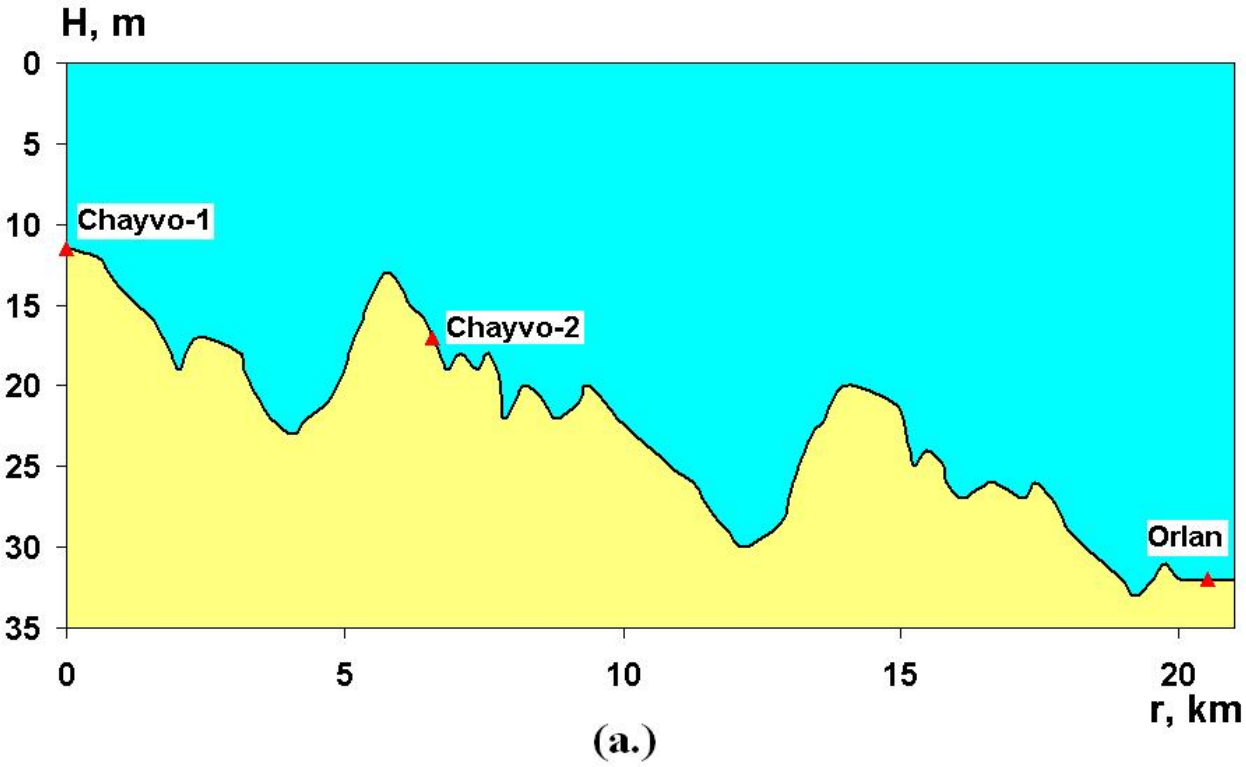

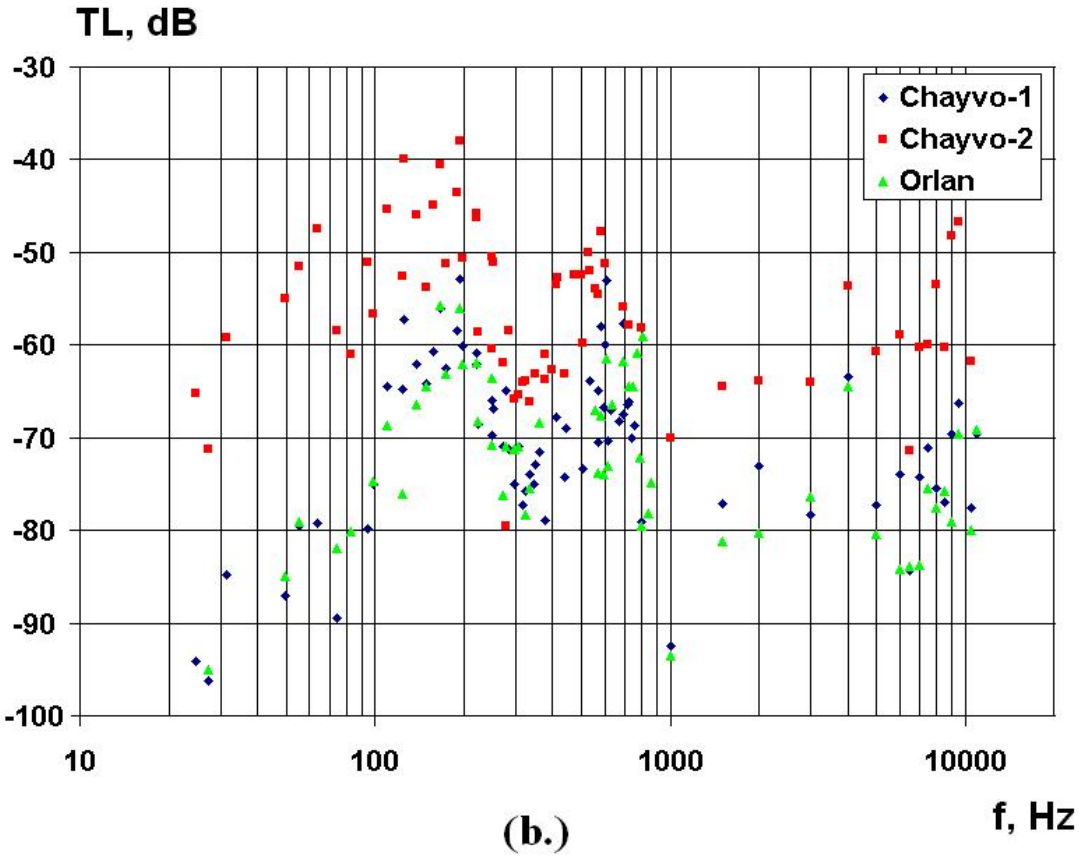

Figure 3.13 - (a) Bathymetric profile from Chayvo-1, through Chayvo-2 to Orlan showing the locations of the monitor stations (b) Experimental frequency dependent TL between the proposed Orlan platform location and Chayvo-1 (7.9 km), Chayvo-2 (2.5 km) and Orlan (14.2 km).

Modeling was therefore used to estimate acoustic propagation along the profile from Chayvo-1 to Orlan for sound generated close to shore. Figure 3.14(a) is a map showing the AUAR deployment locations (Chayvo-1, Chayvo-2 and Orlan), the location of the tonal signal source in the model (Source) and points (marked with crosses) where bathymetric measurements were taken as the *Nevelskoy* sailed along the profile. Figure 3.14(b) shows the geometry of the waveguide and the parameters used in the modeling; the model was based on the bathymetric measurements from the *Nevelskoy*. The waveguide is a three-layer model with liquid sediment layer and elastic basement. This model was used to estimate TL for sound generated at 1 m depth and propagating offshore. Figure 3.14(c) gives TL (at 1 m depth) versus range for three frequencies (30 Hz, 50 Hz and 200 Hz) estimated using the program MOATL with adiabatic approximation. The first frequency (30 Hz) corresponds to the zero mode that propagates along the boundary between the basement and the sediment layer and attenuates mostly in the sediments. The second frequency (50 Hz) corresponds to the addition of the first mode and the third (200 Hz) to propagation of the first four modes. For the TL estimate at a frequency of 200 Hz the basement properties were not taken into account[26] and the plot for 200 Hz shows decreasing modal interference with distance. The weak modal interference on the 50 Hz plot is most probably because the zero mode attenuates more rapidly with distance than the first mode. However, at 200 Hz, higher modes have greater attenuation. On the plots for 50 Hz and 200 Hz there are TL fluctuations at ranges of 9 km and 17 km that correspond to a shallowing of the bathymetry at that point along the acoustic profile.

Figure 3.14(d) shows the estimated frequency dependent TL for sound propagating from the source to the Chayvo-1, Chayvo-2 and Orlan monitor station locations. For computational efficiency the low frequency (<100 Hz) TL was estimated taking the elastic properties of the basement into account, while the high frequency TL does not. At low frequencies there is a sharp change in slope near the frequency at which the first mode appears, which is normal for waveguides with an elastic basement. For high frequencies the majority of TL occurs in the near shore part of the profile. The RTL (100-600 Hz) for propagation from Chayvo-1 to Chayvo-2 and Chayvo-2 to Orlan is approximately equal, decreasing slightly with frequency.

[26] At this frequency the basement properties have insignificant impact on acoustic propagation.

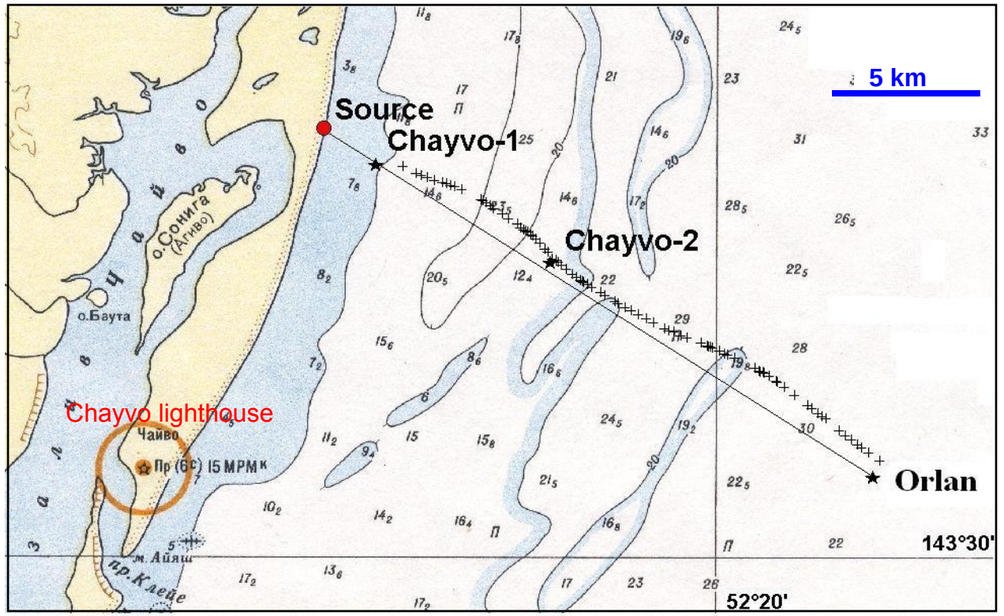

(a.)

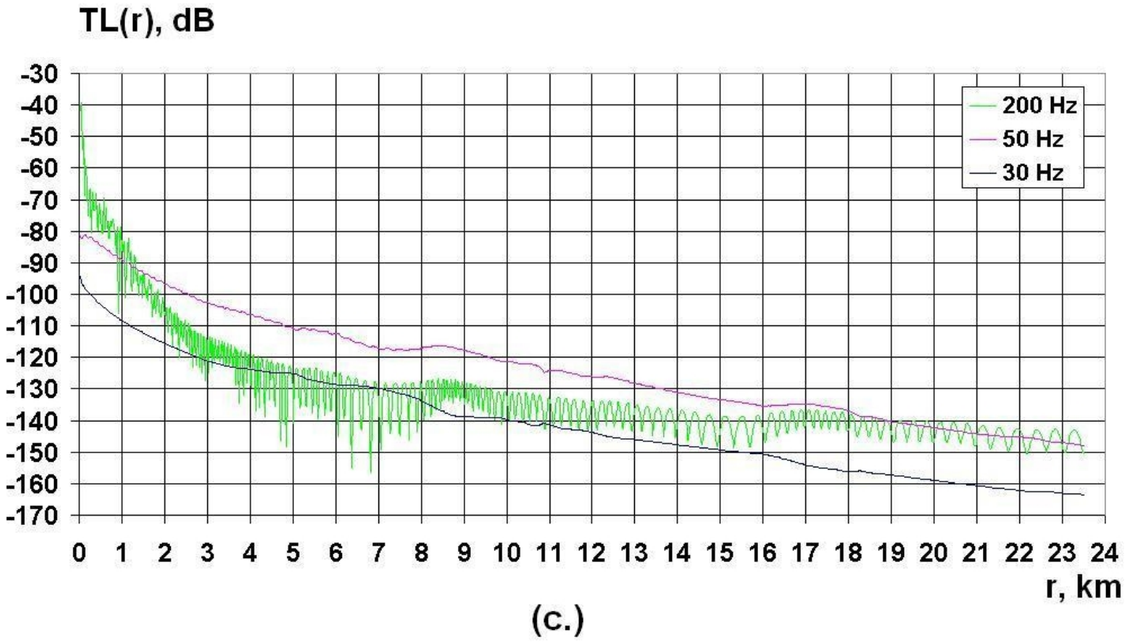

(c.)

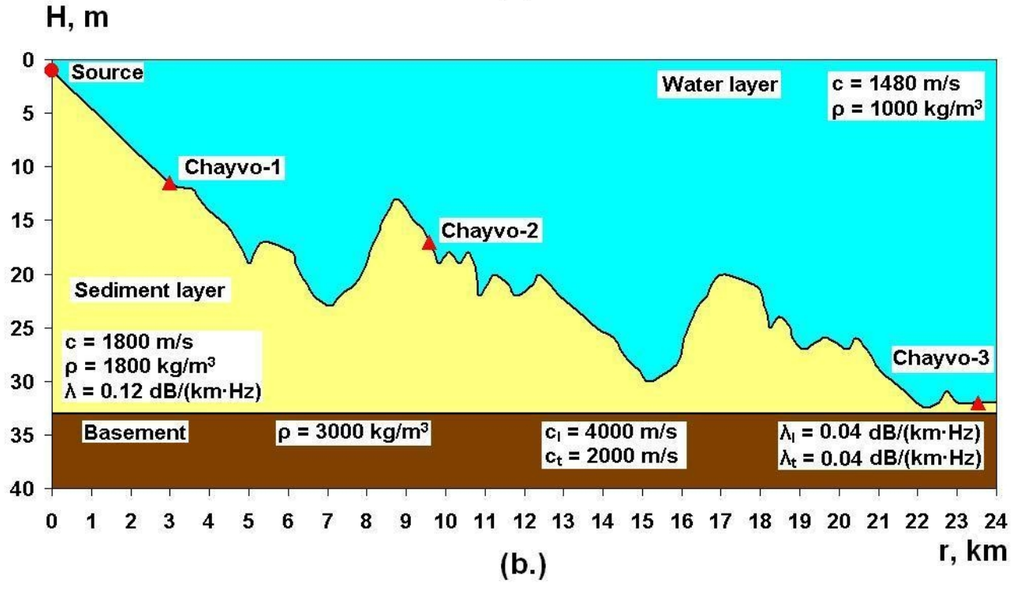

(b.)

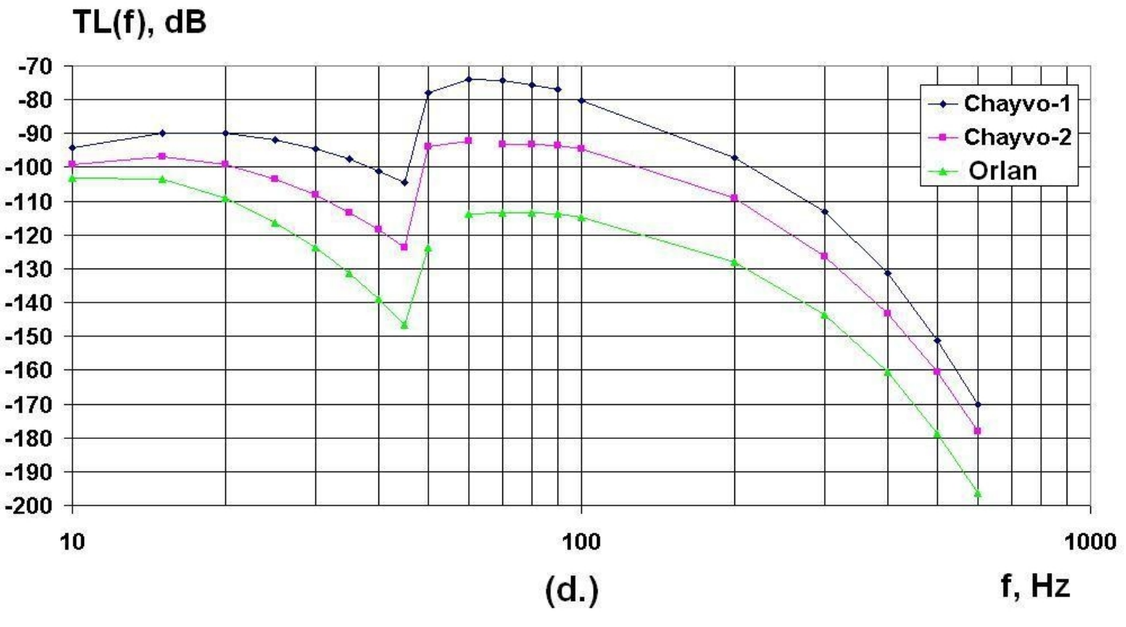

(d.)

Figure 3.14 - (a) Map showing the profile from the Chayvo well site to Orlan (b) Bathymetric profile from the Chayvo well site to Orlan showing the model parameters (c) Theoretical range dependent TL profiles for 30 Hz, 50 Hz and 200 Hz (d) Theoretical frequency dependent TL profiles for Chayvo-1, Chayvo-2 and Orlan.

4 Analysis of sound propagating from the Chayvo well site

The Odoptu field will be developed using deviated wells drilled from well pads on the coast (Figure 1.2). There has been some concern that the noise from this development may propagate to the inshore feeding area, disturbing the gray whales that feed there. The Chayvo well site was regarded as a viable analog to the Odoptu conditions and the noise propagating from the Chayvo well site was monitored for a variety of drilling activities to determine if significant noise would propagate offshore from a land based drilling operation.

Figure 4.1 shows the recording schedule for the four AUARs that were deployed in the area. The Chayvo-1 acoustic station was closest to the well site (3 km from the Chayvo well site, 11 m water depth)[27], the Chayvo-2 farther away (11 km, 17 m water depth) and the Orlan AUAR at the closest 95% kernel probability contour to the offshore feeding area (24 km, 32 m water depth). After the initial data had been evaluated an acoustic station was added between the Chayvo-1 and Chayvo-2 stations and was designated Chayvo-3 (5.5 km, 17 m water depth).

Figure 4.1 also shows the drilling operations being conducted at the Chayvo well site while the AUARs were operational. Four major categories of operations were evaluated, these were:

- **Drilling operations -** This is the time when the rig was actually drilling the well (both 17.5" and 12.25" diameter well bores were drilled during the evaluation time).
- **Casing operations -** These include running casing in the well bore, cementing and cutting the casing (the 13 5/8" casing was run during the evaluation time).
- **Tripping -** This includes the time when drill pipe was being run into or out of the well bore.
- **Other operations -** This is a category that includes a variety of topside operations including circulating bottoms-up, washing and reaming, testing, cleaning shakers and setting up for other processes.

[27] Due to operational constraints it was not possible to deploy an AUAR closer to the well site than the Chayvo-1 acoustic station.

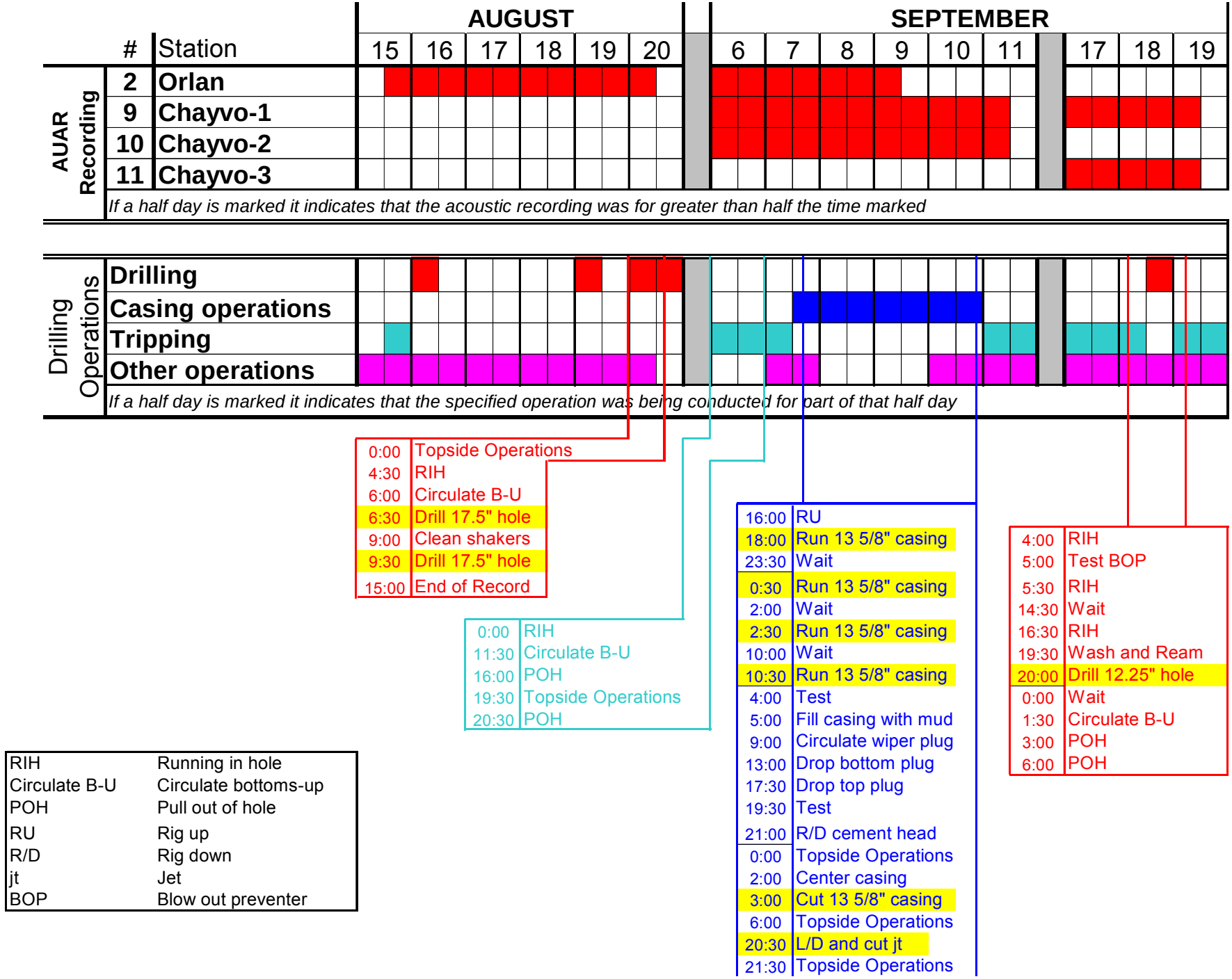

Figure 4.1 - AUAR recording schedule and Chayvo drilling operations log for the evaluation period.

4.1 Experimental analysis of acoustic level vs. drilling operations at Chayvo

Figure 4.1 shows the broad categories of drilling operations and the times when AUARs were operational at the acoustic monitor stations. Figure 4.1 also shows increased operational details for four periods of time selected to represent different categories of drilling operations. These four periods will be used to determine what level of noise propagated offshore from drilling operations at Chayvo during these times.

Figures 4.2 to 4.8 are sonograms *G(f,t)* recorded at the specified acoustic or monitor stations during the detailed time periods. The broad categories of drilling operations being conducted at that time are shown on the left-hand side of each plot. Each figure is displayed twice; the first plot (a) displays frequencies from 0-1 kHz and the second (b) from 2 Hz to 10 kHz. The color scales remain the same for all the plots[28].

4.1.1 Acoustic monitoring (Orlan monitor station) - 20 August 2003

Figures 4.2(a) and 4.2(b) are sonograms *G(f,t)* showing the received level recorded at the Orlan monitor station between midnight and 15:00 on 20 August 2003. During this time the rig at the Chayvo well site was preparing to drill or drilling a 17.5" well bore. Approximately five hours of drilling was conducted while the AUAR was recording on this day.

There is no indication of an increase in the acoustic level received at the Orlan monitor station during this time. The broad burst of noise seen on the sonogram between 12:00 h and 14:00 h was caused by the Nevelskoy as it recovered the AUAR.

4.1.2 Acoustic monitoring (Chayvo-1, Chayvo-2 & Orlan) - 6 September 2003

Figures 4.3(a) and 4.3(b) are sonograms *G(f,t)* showing the received level recorded at the Chayvo-1 and Chayvo-2 acoustic stations as well as the Orlan monitor station between 01:00 h and 22:00 h on 6 September 2003. During this time the rig at the Chayvo well site was conducting tripping operations at the Chayvo well site, running into the hole (RIH) and pulling out of the hole (POH) as well as circulating bottoms-up. These operations were being conducted for almost all of the displayed time.

[28] Unfortunately the very low frequency (0-10 Hz) part of the spectrum is dominated by flow noise. POI plan to conduct experiments to determine how to reduce this noise for the 2004 expedition.

The sonogram shows a broadband increase in acoustic level at approximately 08:30 h. This is not correlated with any operations at the Chayvo well site and has higher levels at the stations farthest from the well site; it is probably therefore associated with regional weather events. The high amplitude tonal signal at 320 Hz is a signal generated by the CW-320 autonomous transducer. The high frequency events visible at approximately 08:15 h on Figure 4.3(b) and marked with red ellipses are signals generated by the high frequency transducer. These signals were generated during the course of propagation and TL experiments.

The transient high-amplitude broadband events seen most clearly at the Orlan monitor station are generated by moving vessels. These vessels are transiting in deeper water as the received levels at the Orlan monitor station are higher than at the Chayvo-2 acoustic station. As before, the variable amplitude low frequency noise visible from 2-10 Hz is related to flow noise caused by strong current action.

There is no indication of an increase in the acoustic level received at the Chayvo-1 and Chayvo-2 acoustic stations or the Orlan monitor station and correlated to activities at the Chayvo well site during this time.

4.1.3 Acoustic monitoring (Chayvo-1, Chayvo-2 & Orlan) - 7 to 10 September 2003

Figures 4.4(a) to 4.7(a) and 4.4(b) to 4.7(b) are sonograms *G(f,t)* showing the received level recorded at the Chayvo-1 and Chayvo-2 acoustic stations as well as the Orlan monitor station between 16:00 h on 7 September and 21:30 h on 10 September 2003. The Orlan monitor station was recovered on 9 September 2003 and after this time only the Chayvo-1 and Chayvo-2 acoustic stations recorded acoustic data. During this time the rig at the Chayvo well site was conducting 13 5/8" casing operations at the Chayvo well site. These included running the 13 5/8" casing into the well bore, cementing and cutting the casing. These operations were being conducted for almost all of the displayed time (Figure 4.1).

The sonograms show similar broad characteristics to the previous figures. These include the high amplitude tonal signal at 320 Hz generated by the CW-320 autonomous transducer, transient high-amplitude broadband events from moving vessels and variable amplitude low frequency flow noise.

The higher amplitude lines visible on the Chayvo-1 plot of Figure 4.4(a) are instrument noise, which is visible at very low signal levels. This is an instrument artifact caused by the dynamic range of the AUAR and will be corrected for the 2004 field season.

Figures 4.4(b) and 4.5(b) show 10 to 20 minute duration narrow band (10-50 Hz) acoustic events with amplitudes 10 to 20 dB above background. These events are not correlated with drilling operations at Chayvo and have higher amplitude at Chayvo-2 than at Chayvo-1 indicating that the source of the noise is offshore. The source of this noise is unknown and was only recorded during the evenings of 7 and 8 September 2003.

Again there is no indication of an increase in the acoustic level received at the Chayvo-1 and Chayvo-2 acoustic stations or the Orlan monitor station and correlated to activities at the Chayvo well site while casing operations were being conducted.

4.1.4 Acoustic monitoring (Chayvo-1 & Chayvo-3) - 18 to 19 September 2003

Figures 4.8(a) and 4.8(b) are sonograms *G(f,t)* showing the received level recorded at the Chayvo-1 and Chayvo-3 acoustic stations between 04:00 h on 18 September and 06:00 h on 19 September 2003. During this time the rig at the Chayvo well site was preparing to drill or drilling a 12.25" well bore, approximately four hours of drilling was conducted while the AUAR was recording on this day.

Since previous recordings had not indicated any appreciable levels of noise propagating from the Chayvo well site an AUAR was deployed at a new location between the Chayvo-1 and Chayvo-2 stations and was designated Chayvo-3.

Apart from a vessel travelling close to Chayvo-3 and some low frequency flow noise the sonogram is relatively quiet. There is no indication of an increase in the acoustic level received at the Chayvo-1 and Chayvo-3 acoustic stations and correlated to activities at the Chayvo well site during this time.

Figures 4.9(a) and 4.9(b) are power spectral density plots *G(f)* analyzed at regular intervals over this time frame and showing frequencies from 0-800 Hz. These plots show similar results to the Sonograms *G(f,t)* of Figures 4.8(a) and 4.8(b).

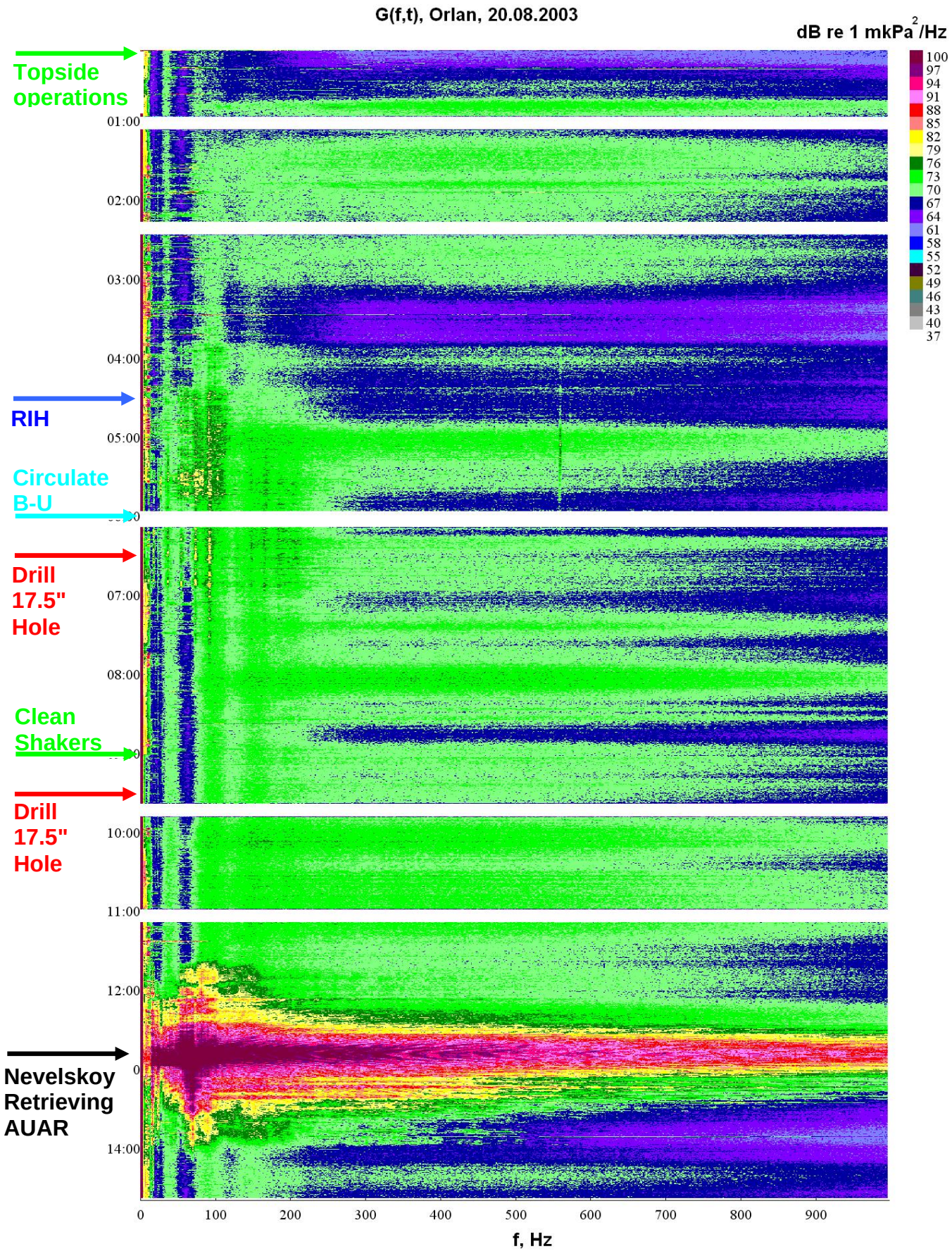

Figure 4.2(a) - Sonogram *G(f,t)* [0-1 kHz] recorded at Orlan on 20 August 2003, while the Chayvo rig was drilling a deviated well.

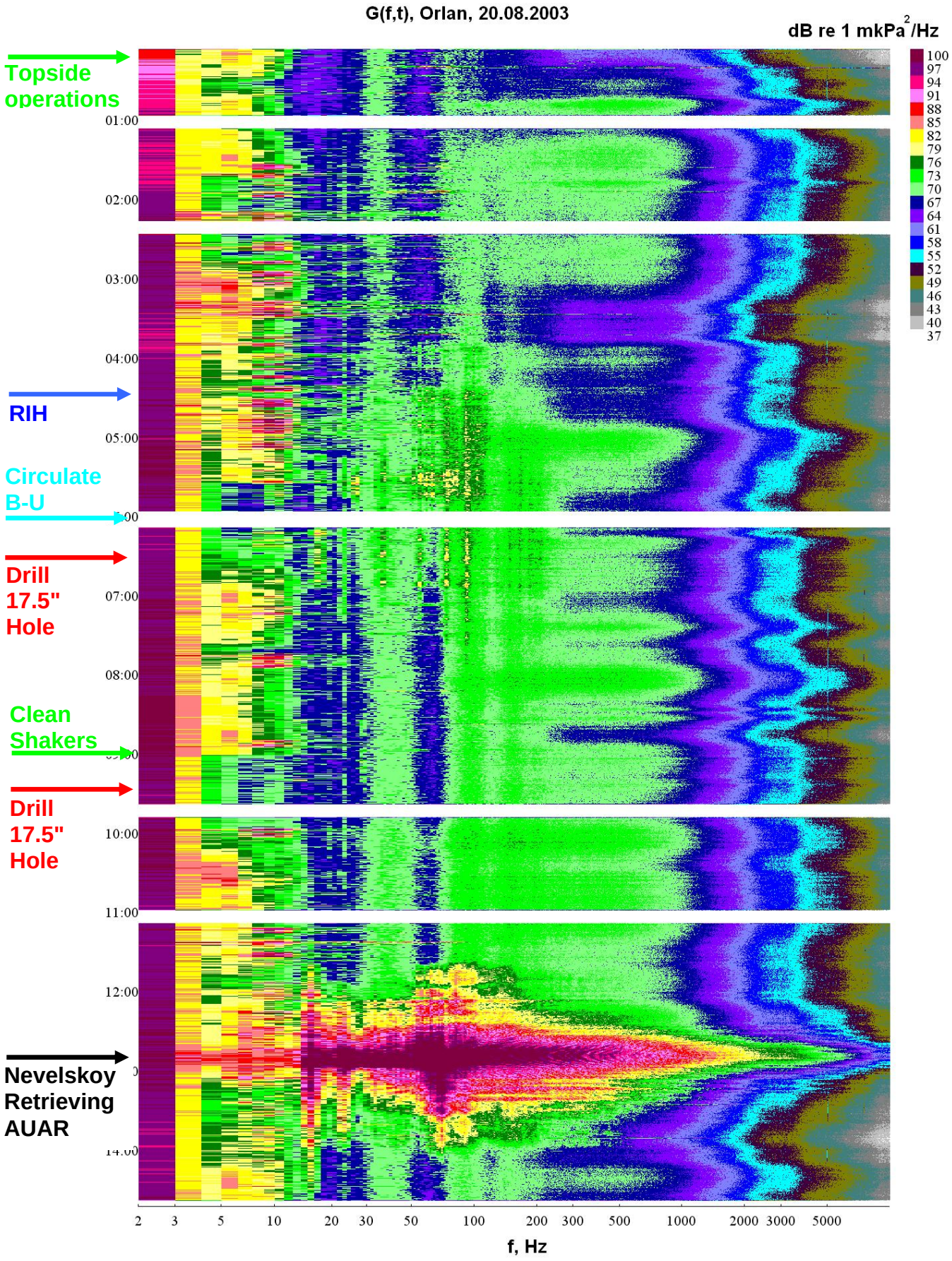

Figure 4.2(b) - Sonogram *G(f,t)* [0-10 kHz] recorded at Orlan on 20 August 2003, while the Chayvo rig was drilling a deviated well.

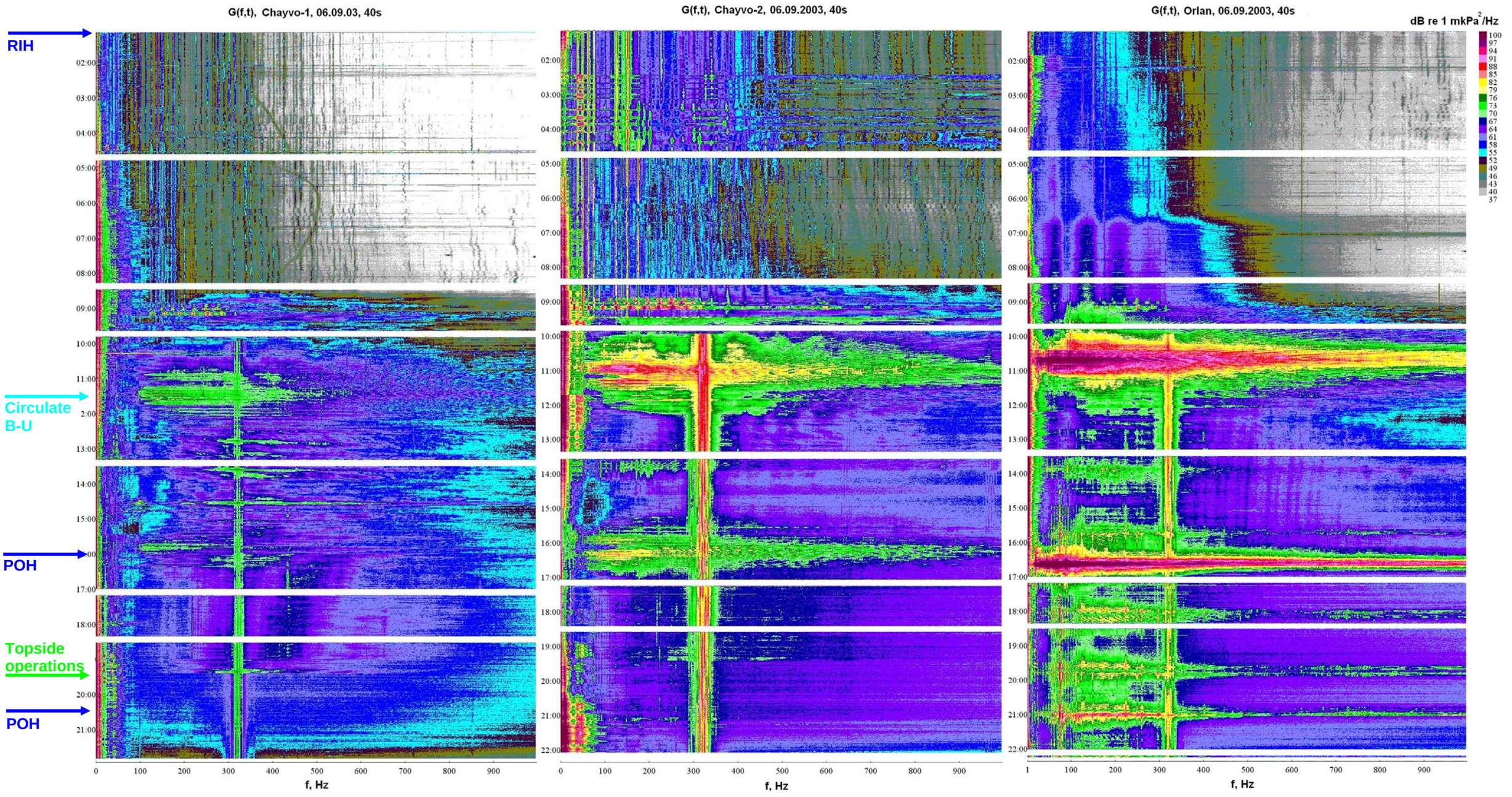

Figure 4.3(a) - Sonograms *G(f,t)* [0-1 kHz] recorded at Chayvo-1, Chayvo-2 and Orlan on 6 September 2003, while the Chayvo rig was conducting tripping operations.

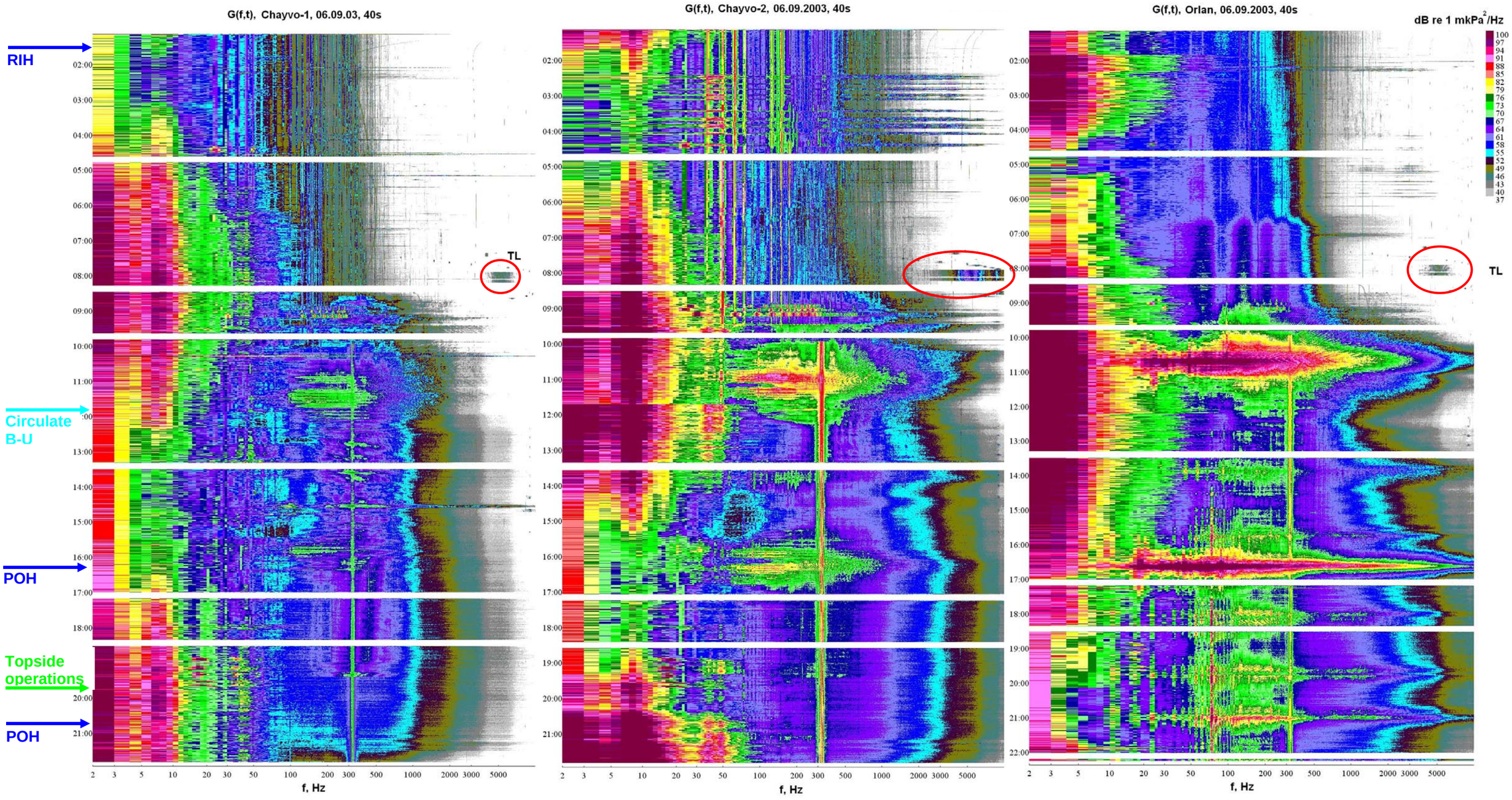

Figure 4.3(b) - Sonograms *G(f,t)* [0-10 kHz] recorded at Chayvo-1, Chayvo-2 and Orlan on 6 September 2003, while the Chayvo rig was conducting tripping operations.

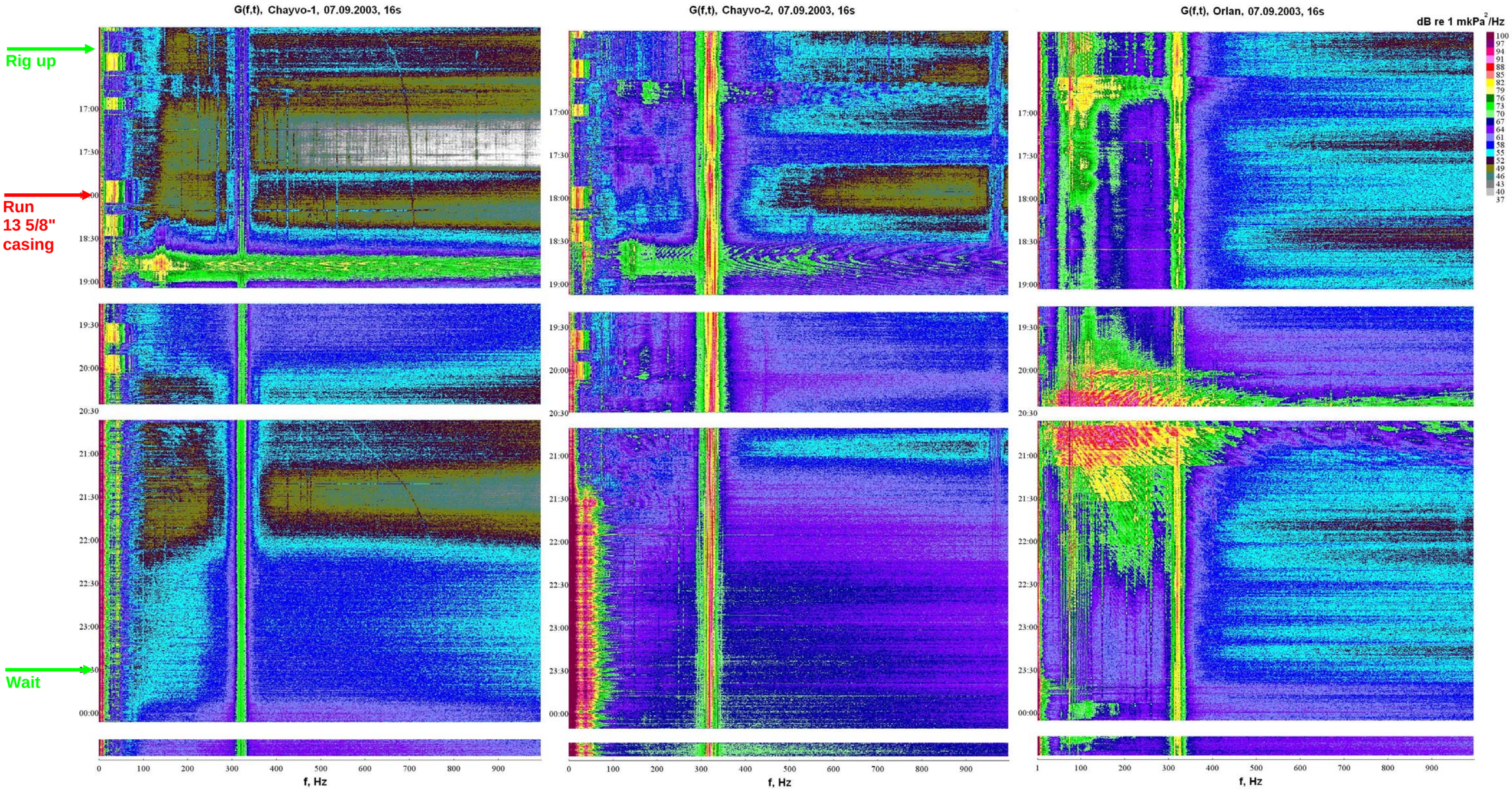

Figure 4.4(a) - Sonograms *G(f,t)* [0-1 kHz] recorded at Chayvo-1, Chayvo-2 and Orlan on 7 September 2003, while the Chayvo rig was running casing and conducting topside operations.

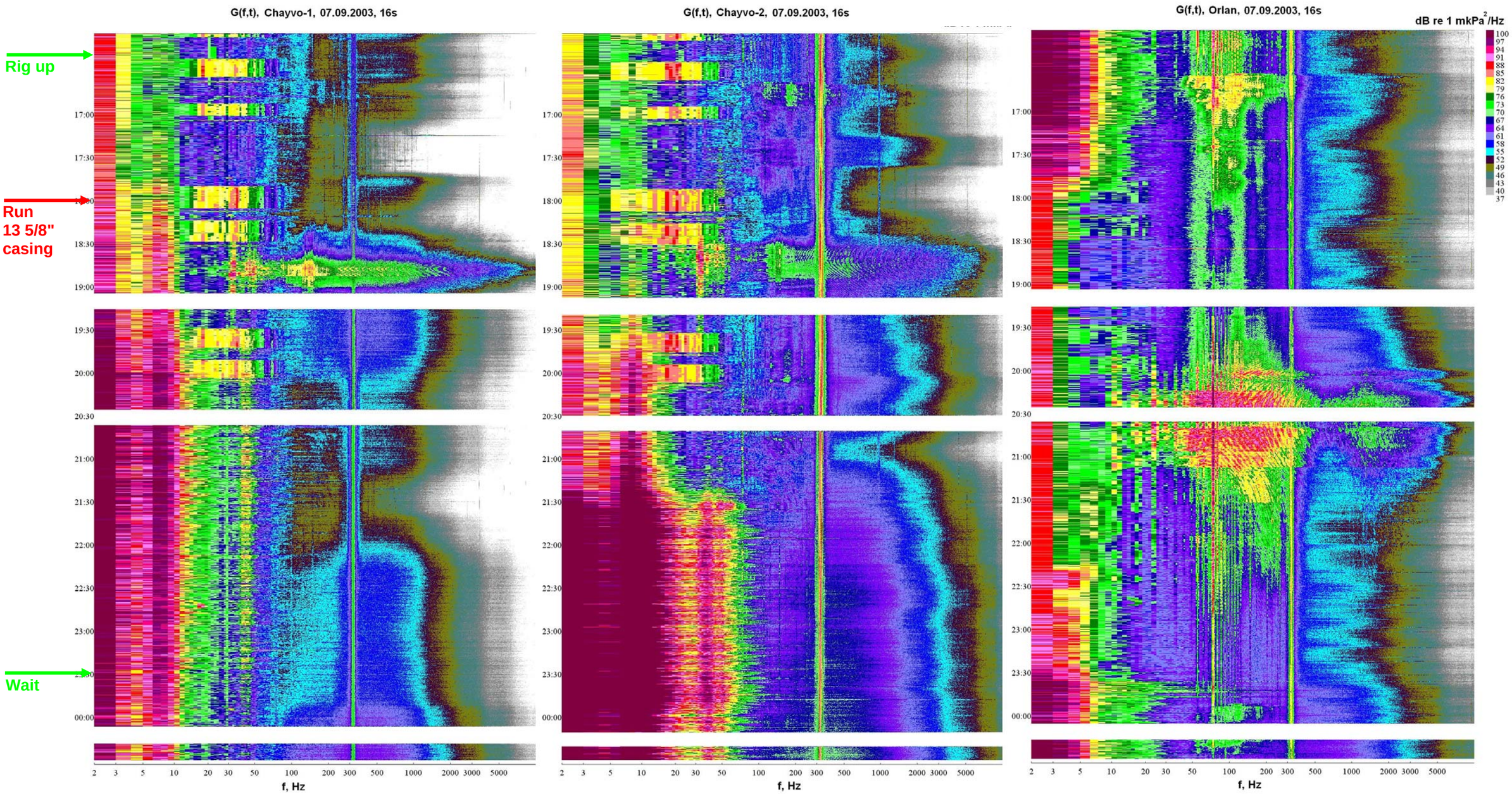

Figure 4.4(b) - Sonograms *G(f,t)* [0-10 kHz] recorded at Chayvo-1, Chayvo-2 and Orlan on 7 September 2003, while the Chayvo rig was running casing and conducting topside operations.

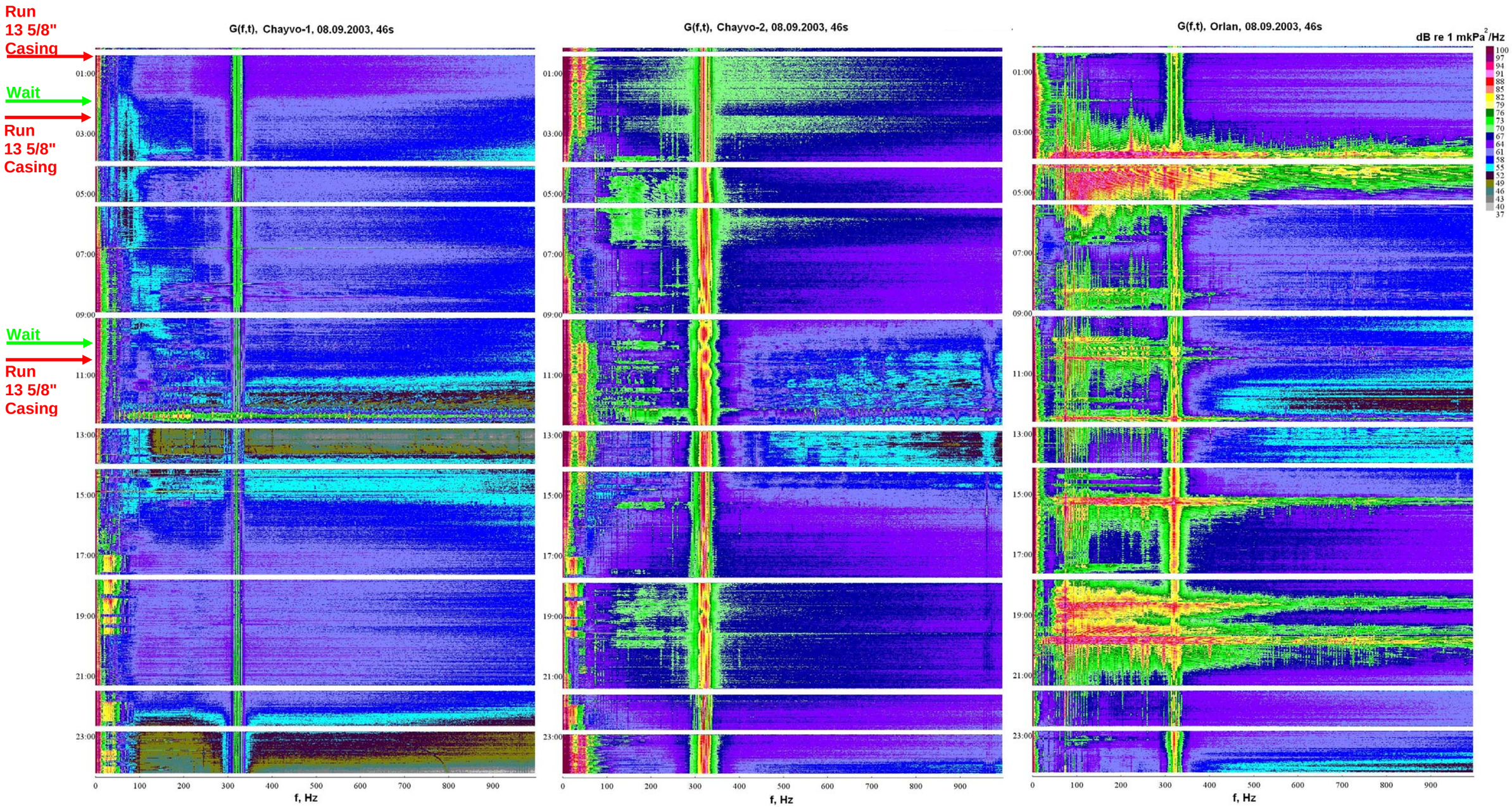

Figure 4.5(a) - Sonograms *G(f,t)* [0-1 kHz] recorded at Chayvo-1, Chayvo-2 and Orlan on 8 September 2003, while the Chayvo rig was running casing and conducting topside operations.

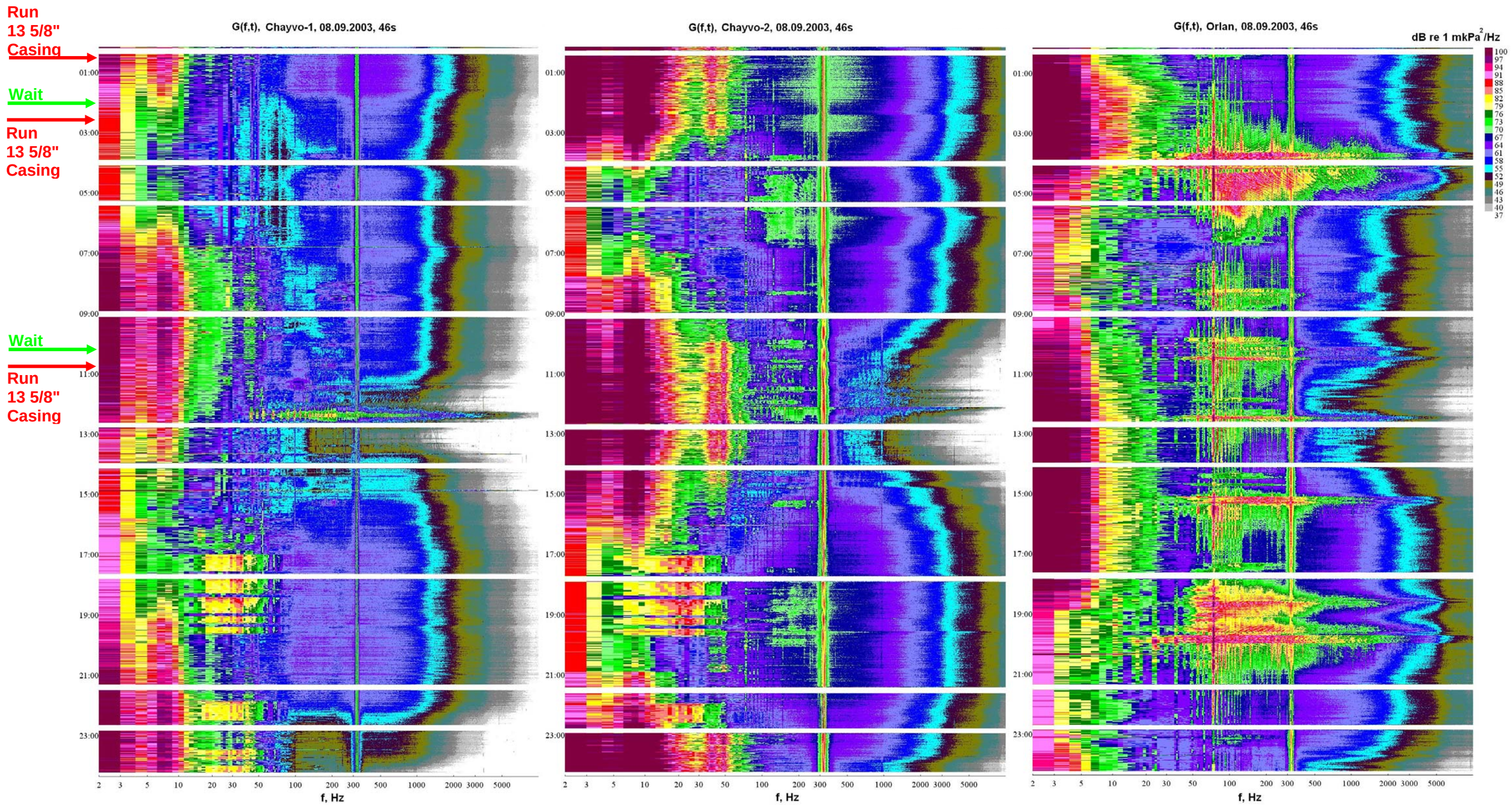

Figure 4.5(b) - Sonograms *G(f,t)* [0-10 kHz] recorded at Chayvo-1, Chayvo-2 and Orlan on 8 September 2003, while the Chayvo rig was running casing and conducting topside operations.

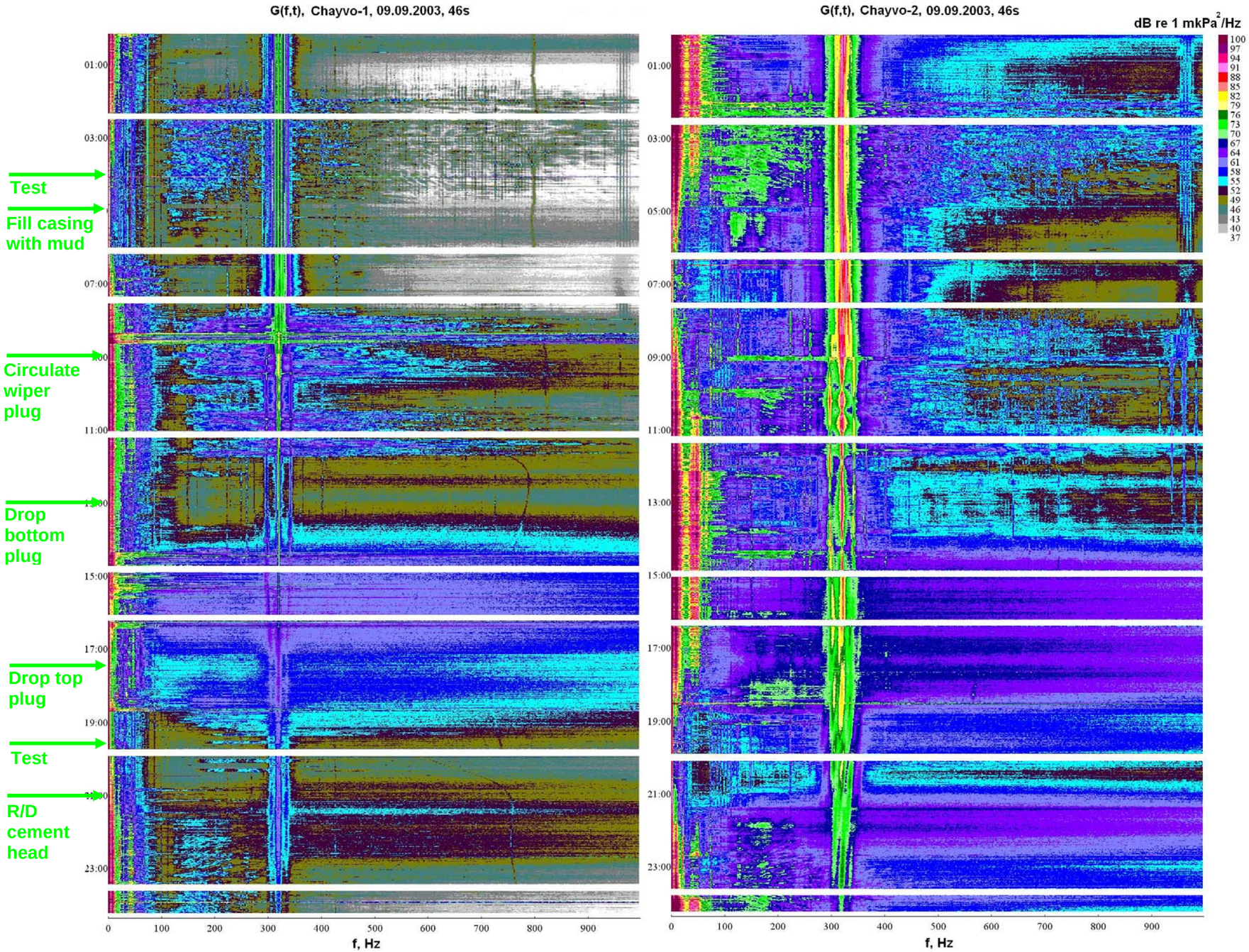

Figure 4.6(a) - Sonograms *G(f,t)* [0-1 kHz] recorded at Chayvo-1 and Chayvo-2 on 9 September 2003, while the Chayvo rig was conducting casing and topside operations.

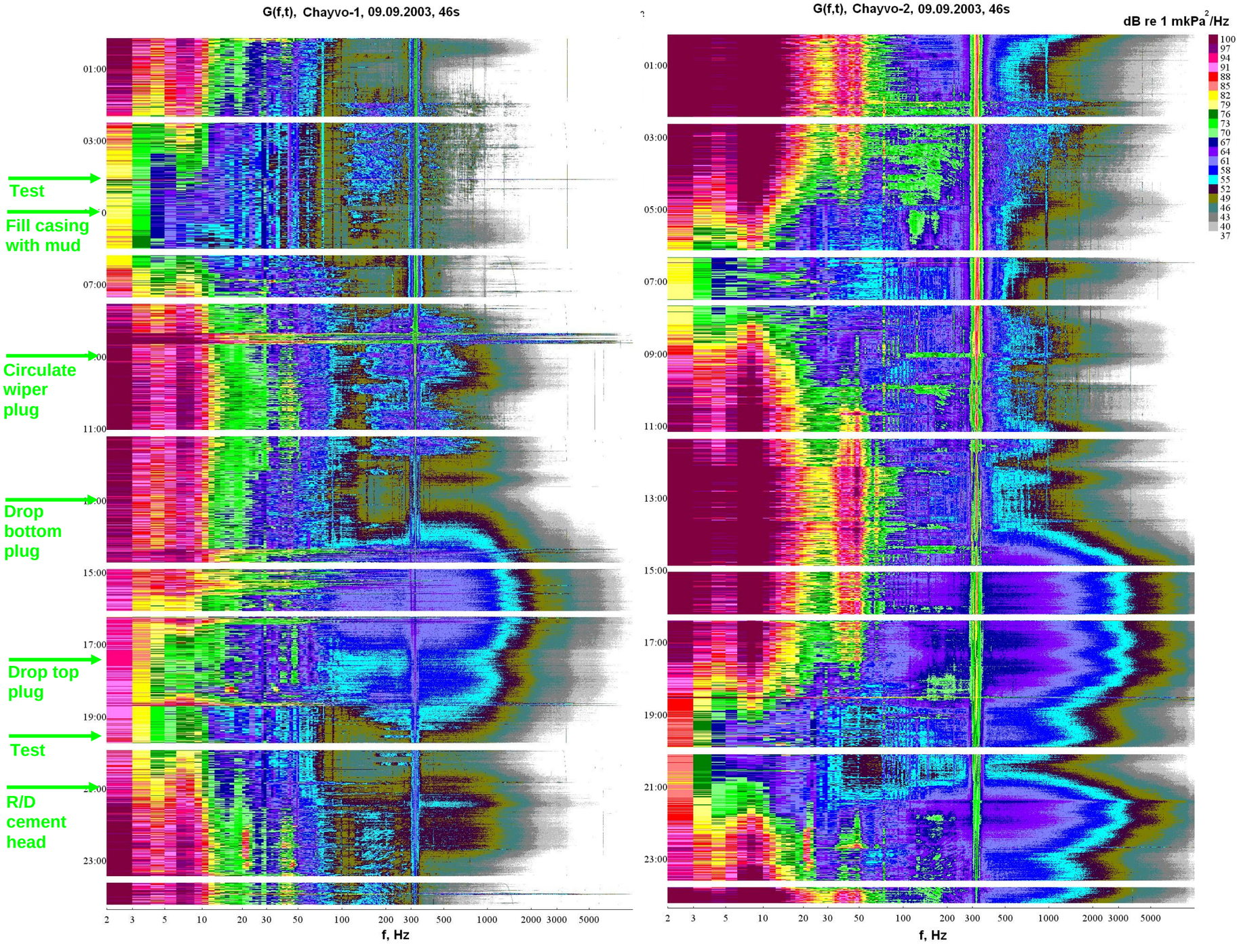

Figure 4.6(b) - Sonograms *G(f,t)* [0-10 kHz] recorded at Chayvo-1 and Chayvo-2 on 9 September 2003, while the Chayvo rig was conducting casing and topside operations.

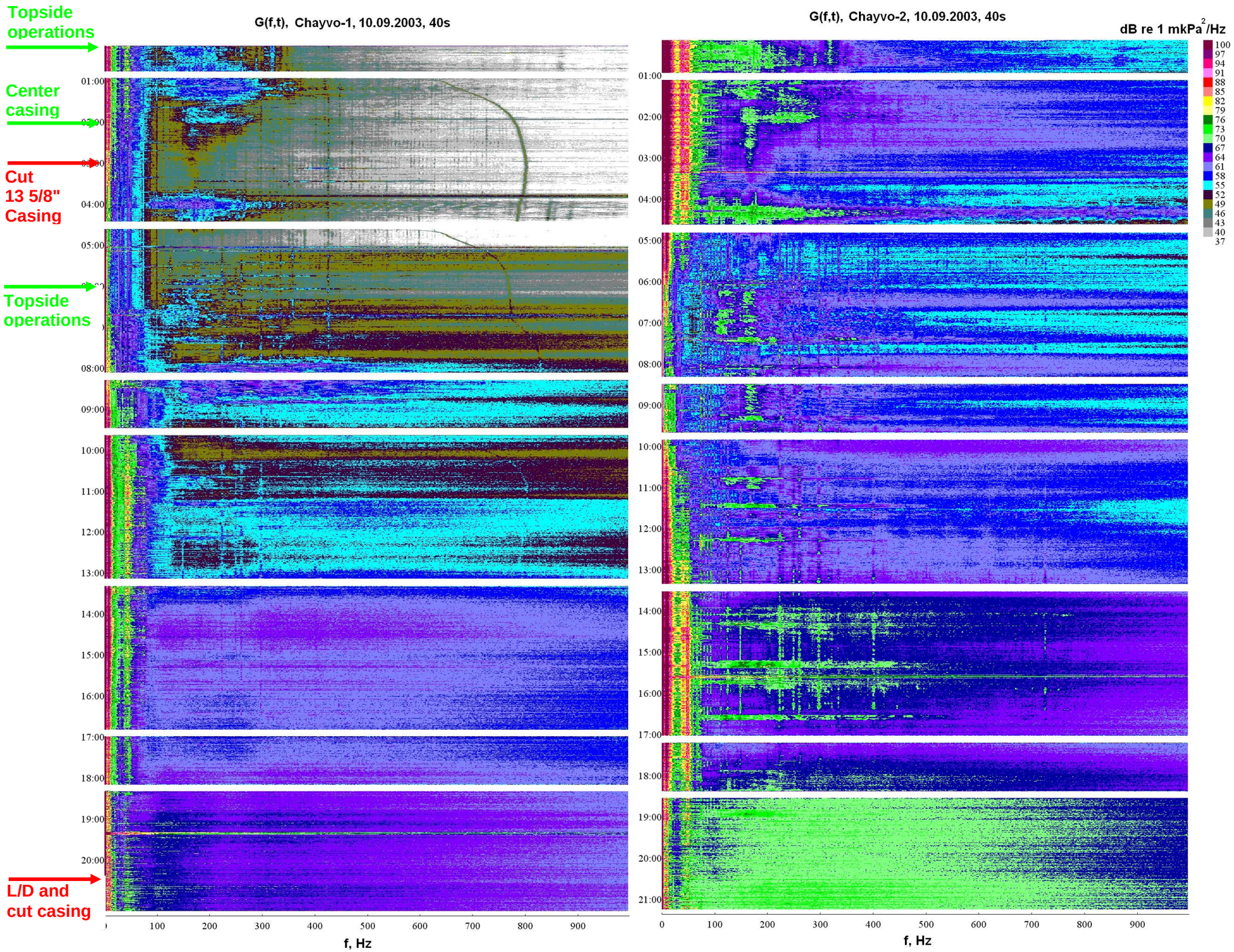

Figure 4.7(a) - Sonograms *G(f,t)* [0-1 kHz] recorded at Chayvo-1 and Chayvo-2 on 10 September 2003, while the Chayvo rig was conducting casing operations.

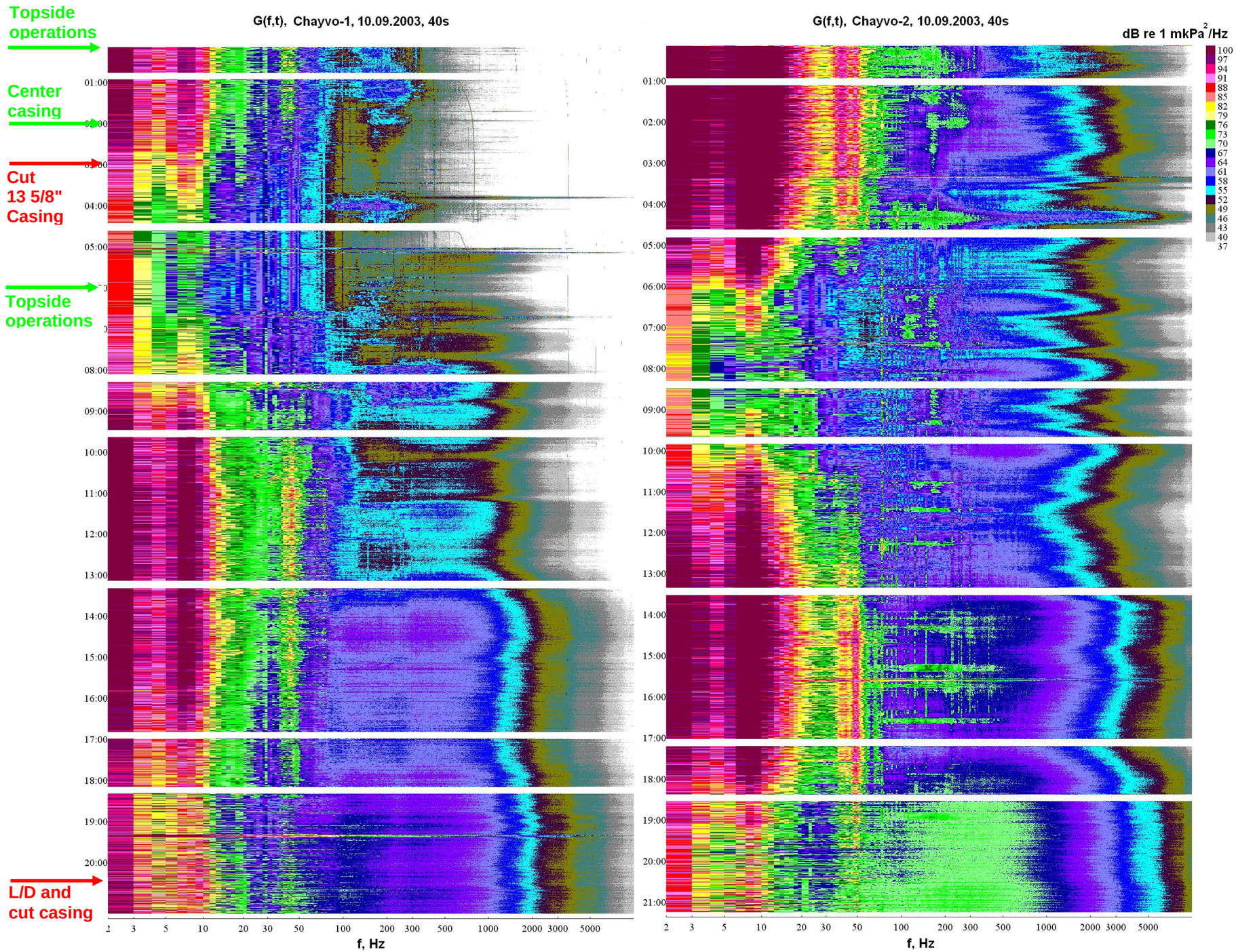

Figure 4.7(b) - Sonograms *G(f,t)* [0-10 kHz] recorded at Chayvo-1 and Chayvo-2 on 10 September 2003, while the Chayvo rig was conducting casing operations.

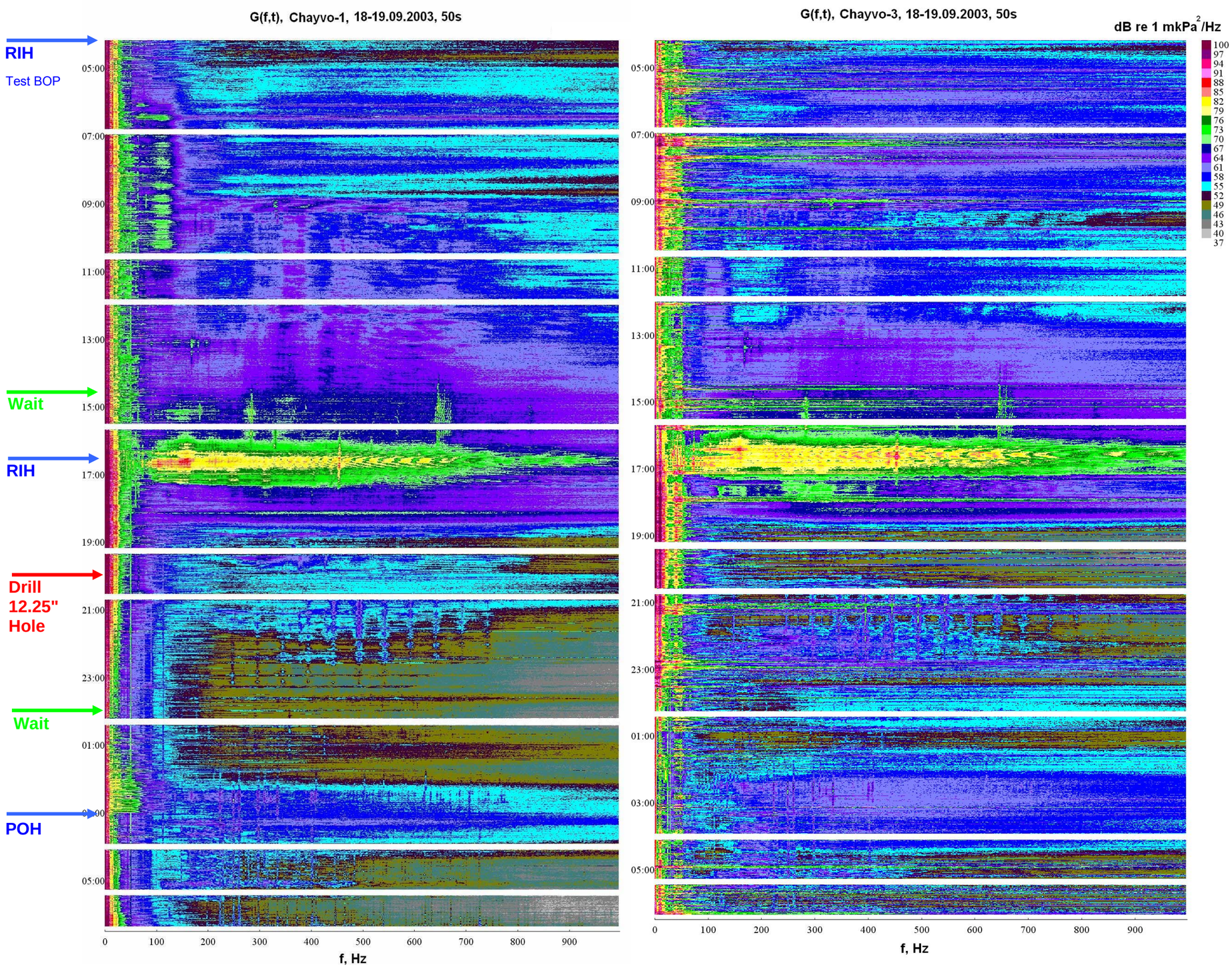

Figure 4.8(a) - Sonograms *G(f,t)* [0-1 kHz] recorded at Chayvo-1 and Chayvo-3 on 18-19 September 2003, while the Chayvo rig was drilling a deviated well.

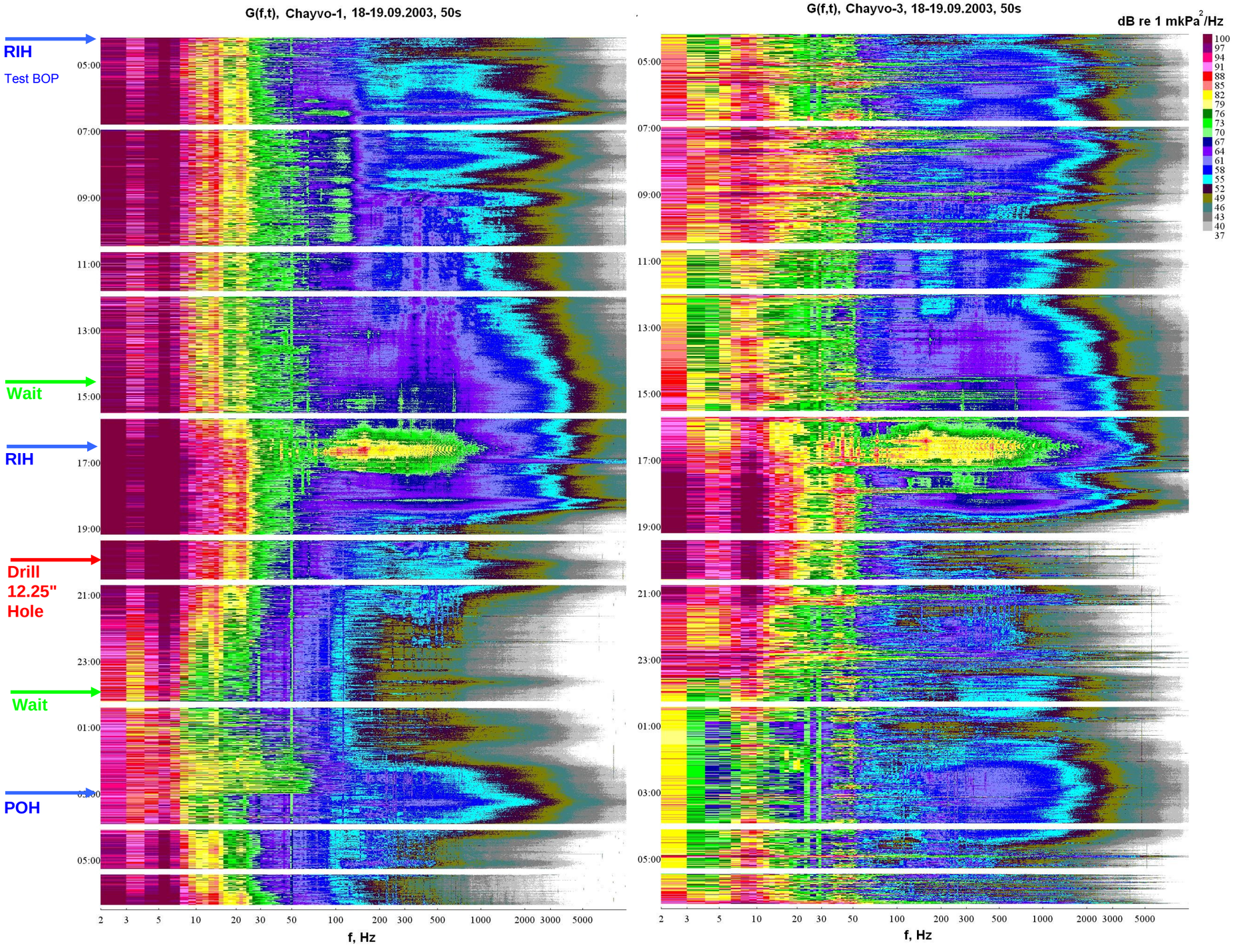

Figure 4.8(b) - Sonograms *G(f,t)* [0-10 kHz] recorded at Chayvo-1 and Chayvo-2 on 18-19 September 2003, while the Chayvo rig was drilling a deviated well.

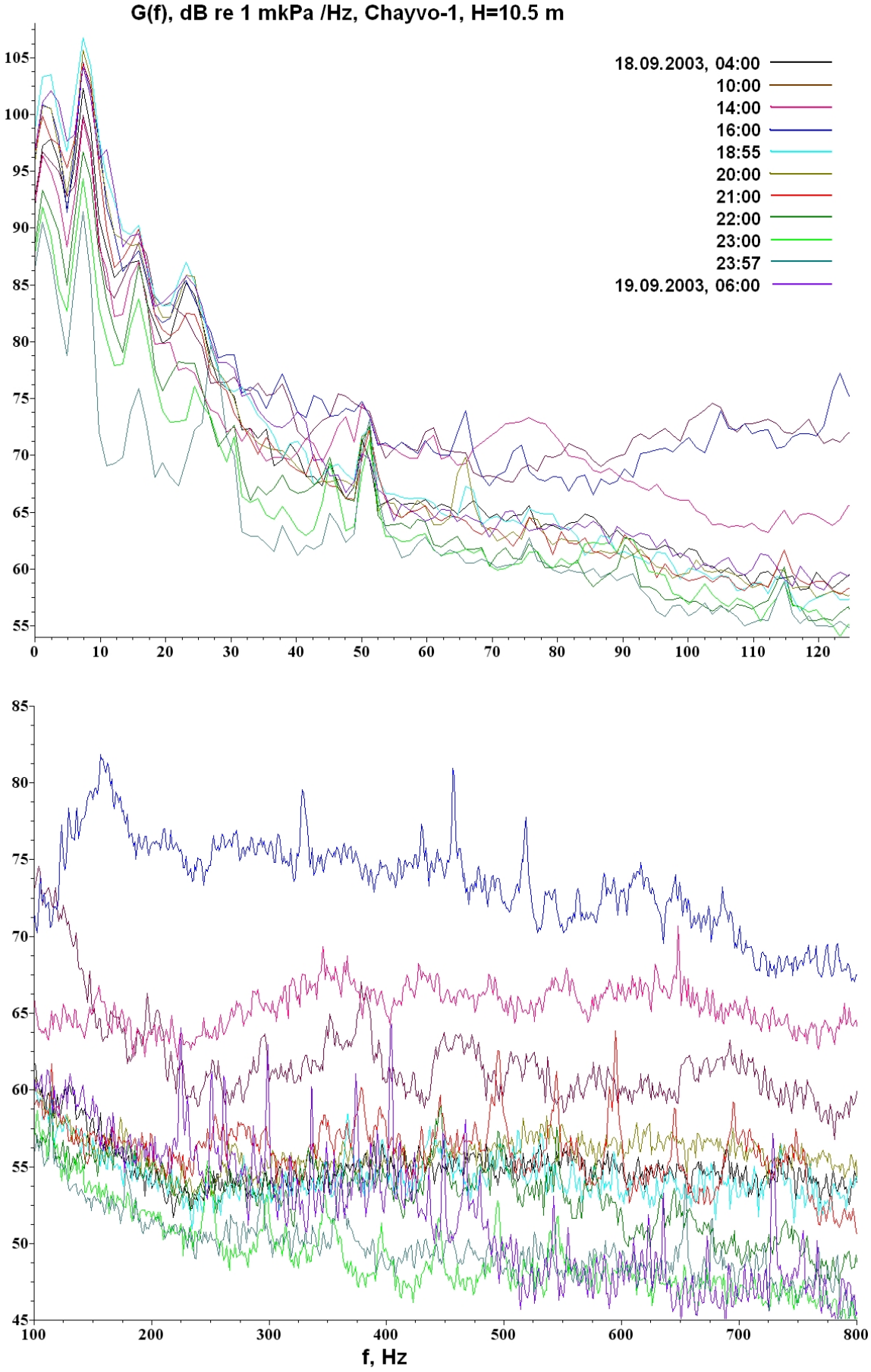

Figure 4.9(a) - Chayvo-1 spectral density, recorded on 18-19 September 2003, while the Chayvo rig was drilling a deviated well.

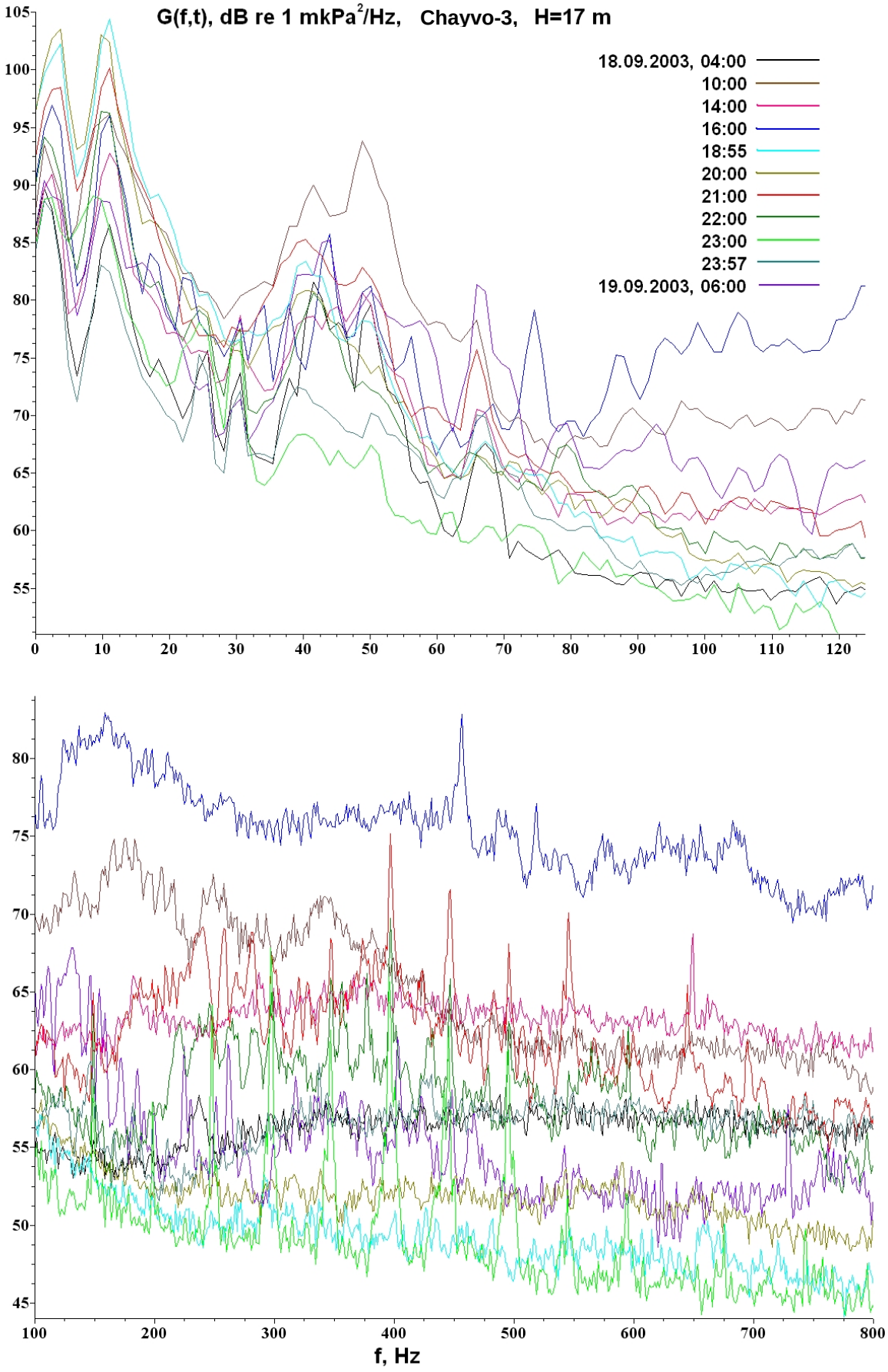

Figure 4.9(b) - Chayvo-3 spectral density, recorded on 18-19 September 2003, while the Chayvo rig was drilling a deviated well.

4.2 Results of the analysis of acoustic level vs. drilling operations at Chayvo

Drilling operations being conducted at the Chayvo well site were analyzed to determine if noise generated by these operations would couple into the water and propagate seawards from the well site. A number of typical operations were evaluated; these included drilling, casing, tripping and general topside drilling operations (Figure 4.1).

The sonograms show ambient and anthropogenic acoustic signatures generated by weather, moving vessels and the transducers used for propagation experiments. They also show artifacts due to instrument and flow noise.

None of the sonograms *G(f,t)* or spectra *G(f)* show any evidence of an increase in the anthropogenic acoustic level received at the Chayvo-1 and Chayvo-2 acoustic stations or the Orlan monitor station due to activities at the Chayvo well site. No correlation could be found between drilling operations at the Chayvo well site and the level of the acoustic field monitored offshore[29].

[29] 10 to 20 minute duration narrow band (10-50 Hz) acoustic events with amplitudes 10 to 20 dB above background were noted for part of two days. These events were not correlated with drilling operations at Chayvo and if possible will be investigated further in the 2004 field season.

5 Analysis of acoustic pulses from marine life, anthropogenic and natural seismicity

This section describes the temporal and spectral characteristics of impulses recorded on the NE Sakhalin shelf at different locations and times. These impulses include those originating from the seismic operations at Lunskoye, as well as impulses with biogenic and natural seismicity origins. The source of some of the impulses recorded in 2003 could not be determined and will be investigated further in 2004.

5.1 Impulses generated by the seismic survey at Lunskoye

On 9 September 2003 an AUAR was deployed at the Lunskoye monitor station which was located near the southern edge of the offshore gray whale feeding area. At this time the Ocean Explorer was acquiring a seismic survey in the Lunskoye license area. Figure 5.1 shows a sonogram *G(f,t)* of data from the Lunskoye monitor station recorded during the evening of 9 September 2003. The acoustic spectra of signals received during the acquisition of a seismic line can be clearly seen on the sonogram. Figure 5.2 displays time domain plots of impulses recorded in Lunskoye; the impulse at 03:47 shows a sharp impulse followed by a continuous 3 Hz tonal signal. Figure 5.3 clearly shows the repetitive signature of the impulses generated by the seismic survey, it also shows other impulses that are believed to be biologic in origin. These impulses were recorded at the Lunskoye monitor station even when the amplitude of the seismic impulses originating from the Lunskoye seismic survey reached ~10 Pa (141 dB_{peak} re 1 μPa). Figure 5.4 illustrates the difference in time domain character between acoustic pulses of biologic origin and those generated by a seismic air gun array. Figure 5.5 plots the peak and rms[30] values calculated for the data received at the Lunskoye monitor station from a line shot on 9 September 2003. The maximum rms level of this data was 135 dB_{rms} re 1 μPa, significantly below the level of impulsive noise known to cause a disturbance to 10% of feeding gray whales (163-164 dB_{rms} re 1 μPa).

[30] The rms was calculated using a window defined by the 5% and 95% energy levels for each impulse. This procedure was described in greater detail in Borisov et.al. 2002. It should be noted that the gain of the AUAR was set to record ambient noise levels, and the peak amplitude was sometimes clipped for short periods of time, this clipping only effects a limited number of samples and does not have a significant effect on the rms estimate.

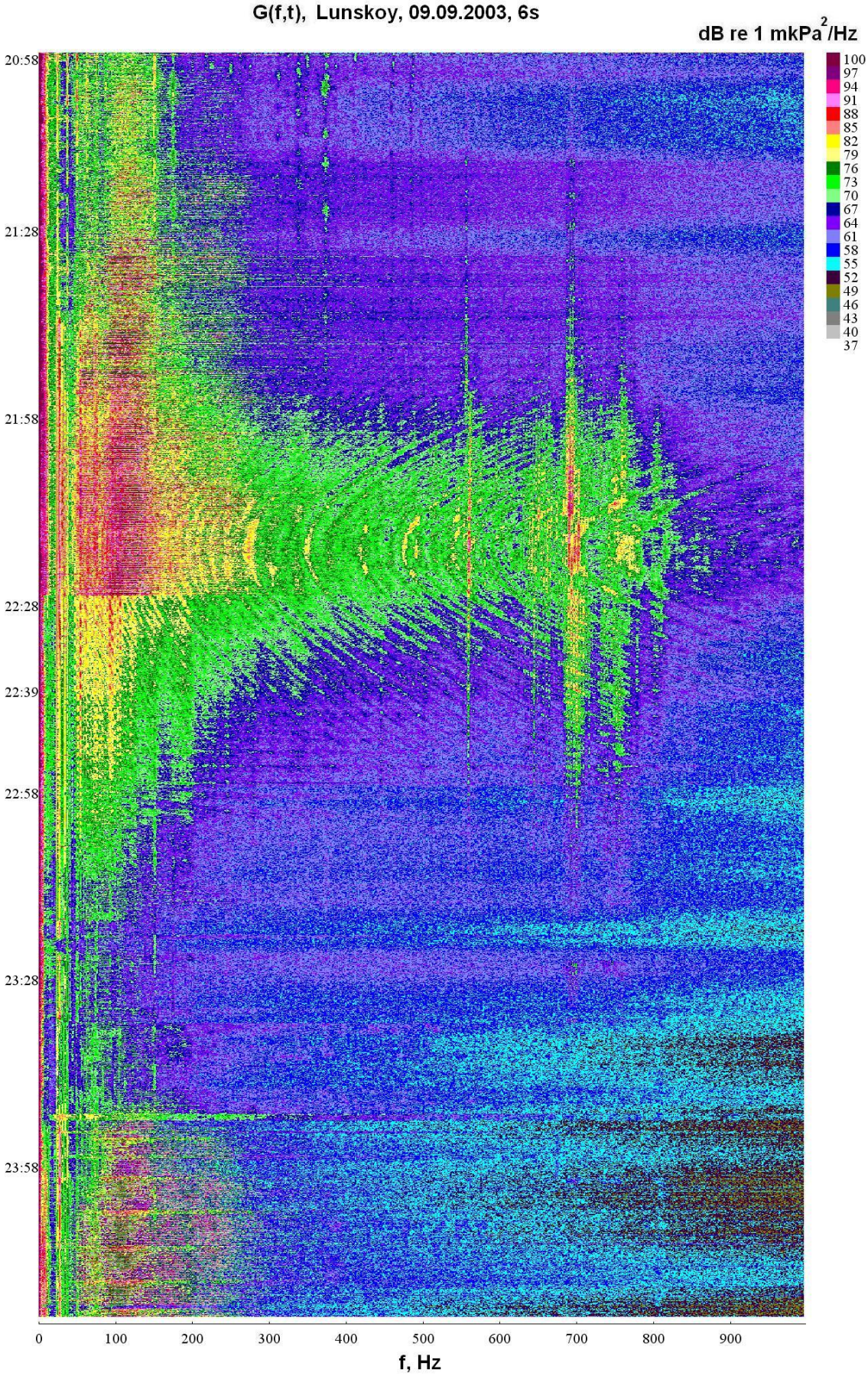

Figure 5.1 - Sonogram *G(f,t)* recorded at Lunskoye on 9 September 2003, showing the signals generated by a seismic survey in the Lunskoye license area.

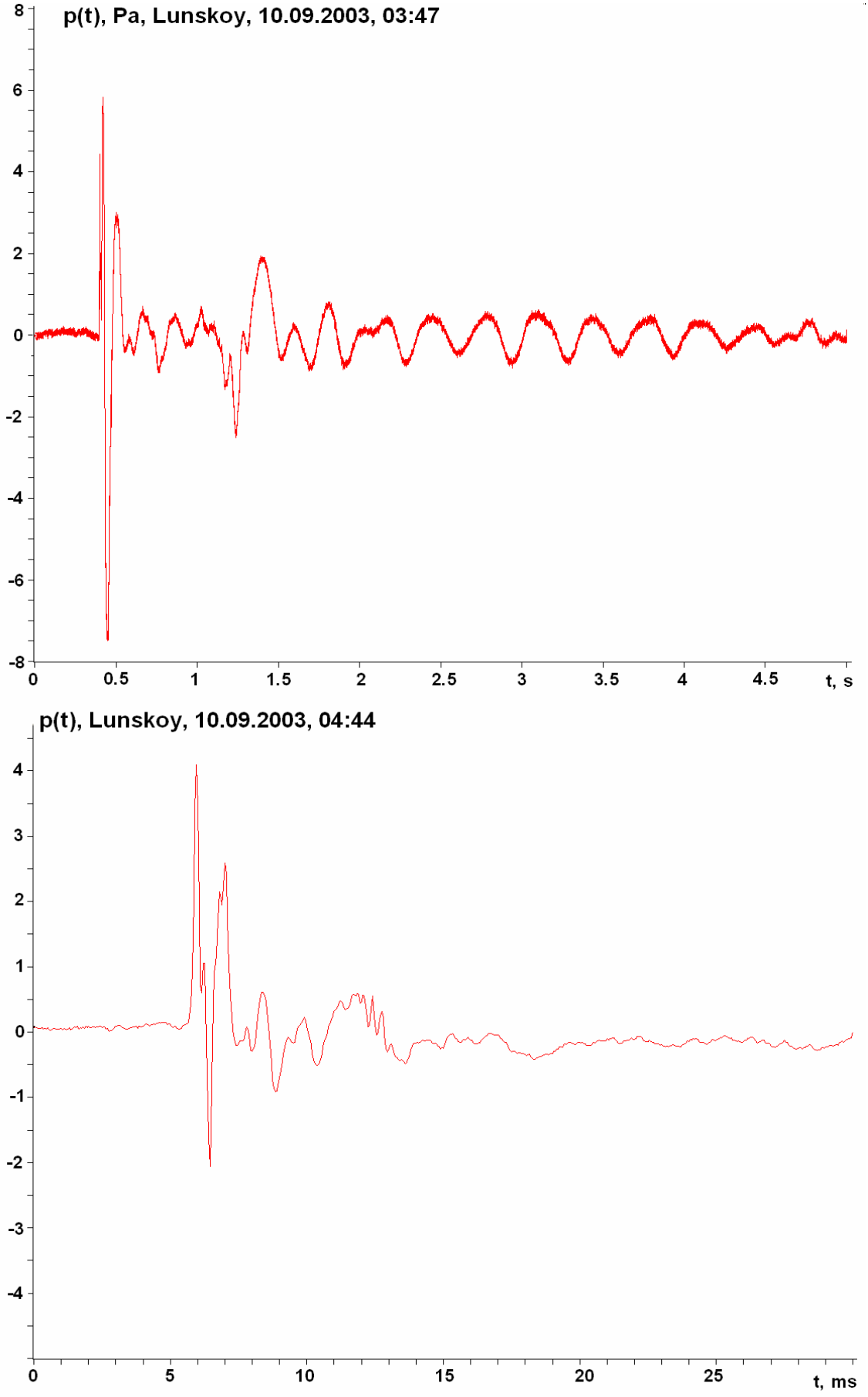

Figure 5.2 - Impulses recorded at the Lunskoye monitor station on 10 September 2003.

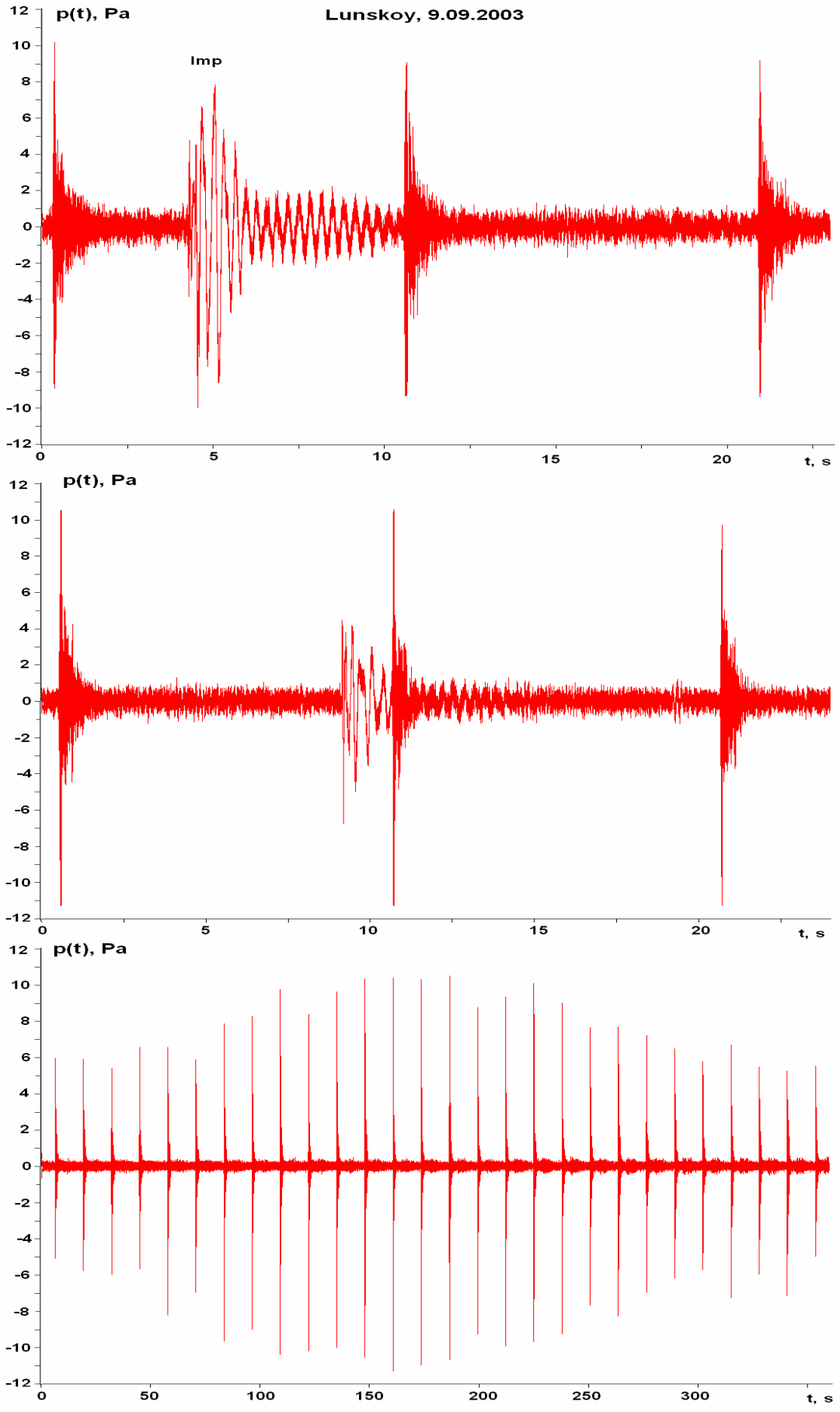

Figure 5.3 - Repetitive seismic impulses (and impulses of biogenic origin) recorded at the Lunskoye monitor station on 9 September 2003.

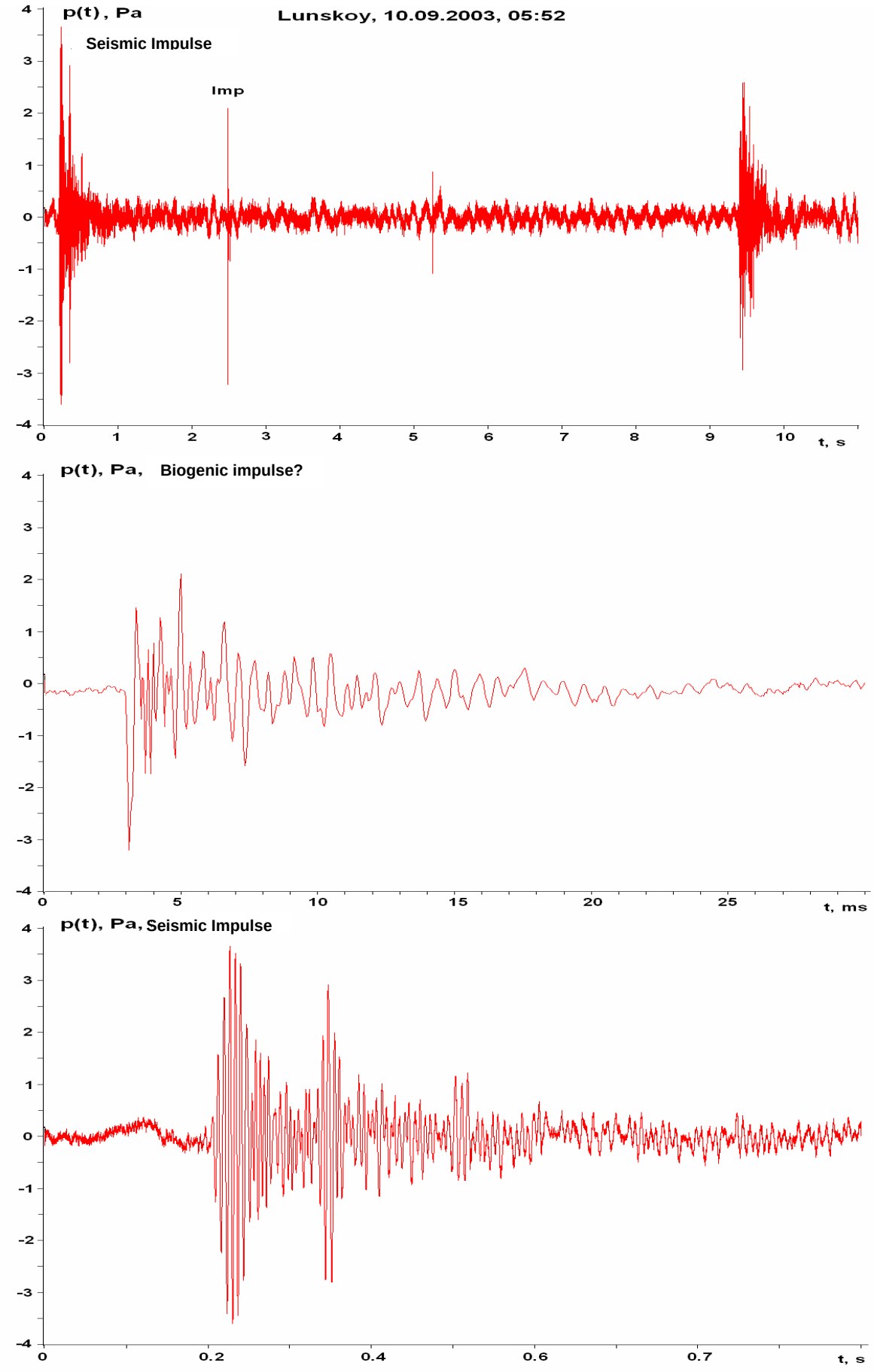

Figure 5.4 - Comparison of seismic impulses and impulses of biogenic origin recorded at the Lunskoye monitor station on 10 September 2003.

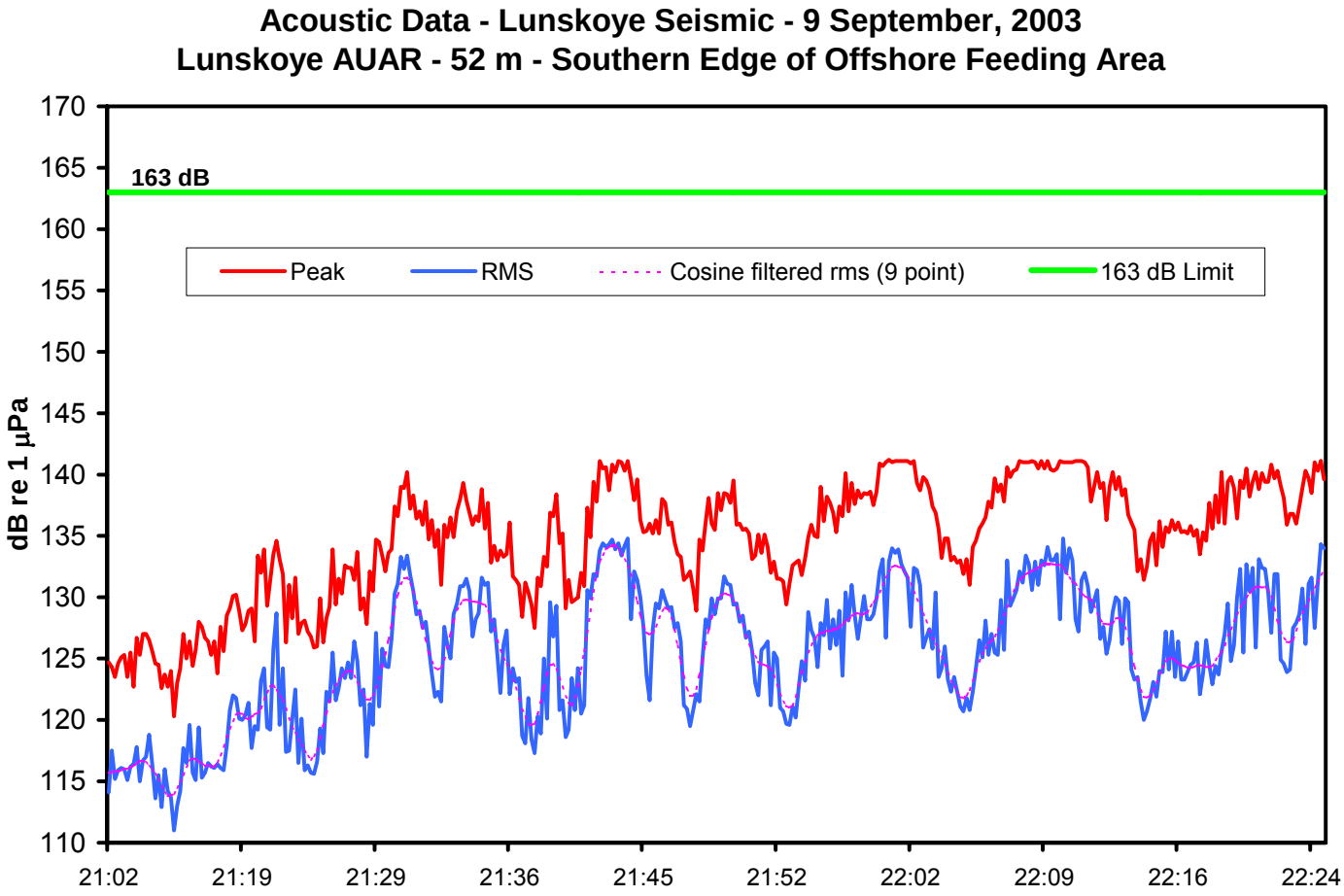

Figure 5.5 - Plot of the received level [peak, rms and cosine filtered rms (~250 m filter length)] of impulses from the Lunskoye seismic survey received at the Lunskoye monitor station on 9 September 2003.

5.2 Impulses of possible biogenic origin recorded in 2003

During analysis of data recorded at the control station on 16 August 2003 and displayed as sonograms *G(f,t)* on Figure 2.1, it was observed that from 01:00 to 03:00 in the frequency band from 1500-6000 Hz the acoustic level was higher than the background. This acoustic signal was probably generated by the activity of a marine animal.

Figure 5.6 shows time domain plots of a group of high amplitude acoustic signals recorded at the control station at 01:33 on 17 August 2003. Figure 5.7 displays four pulses from this group in greater detail. A distinguishing feature of these signals is the combination of relatively high (≈1.2 kHz) and low (≈70 Hz) frequencies, the amplitude of the high frequency impulse 1.2 reached 12 Pa (142 dB re 1µPa). Impulses plotted in Figure 5.6 and marked as 1.1 and 1.2 resemble the broadband signals often used by marine mammals (whale or killer

whale) for echolocation. Because the time difference (Δt) between them is 0.2 s the object was probably a distance of approximately 150 m[31] from the marine mammal. The animal may be using the subsequent impulses to investigate the object.

Figure 5.8 illustrates the complex acoustic signal that can be produced by a marine mammal. The impulse labeled Imp-1 is more than 20 dB above an acoustic background that is dominated by the regular seismic impulses originating at Lunskoye. Imp-1 starts with a complex low frequency signal. In the middle is a modulated tonal signal at ~2.5 kHz (plotted in the bottom panel) and ends with a 3 Hz tonal signal. Figures 5.9 and 5.10 show further acoustic signals that may be biologic in origin. The impulses on Figure 5.10 were recorded with the HF channel of the AUAR at a sample rate of 30 kHz. Figure 5.10 illustrates that the dominant frequency of the acoustic energy for the impulse at 05:28 was $\approx$8 kHz.

5.3 Natural seismicity of the Sakhalin area

It has been assumed that the sporadic series of pulses (often several hours long) usually generated at night are biological in origin. However, research conducted at Lake Mikizha on Kamchatka in March 2004, showed that such pulses can be produced by natural seismic activity caused by tectonic movement before an earthquake [Kuptsov et.al., 2003]. The long term compression of rocks can lead to a build up of stress that is rapidly released causing the cascaded formation of small fractures [Rice, 1982] and an accompanying geoacoustic emission. There have been doubts about the possibility of acoustically monitoring this activity at high frequencies as they are strongly attenuated by the earth; at 3 kHz the attenuation coefficient for sedimentary rock is 206 dB/km. However, for basalt it is only 0.15 dB/km, therefore if it is assumed that acoustic signals from an earthquake travel the majority of their path in basalt and pass through sedimentary rock at the receiving end, it may be possible to detect these high frequency signals[32] at long distances. Since the NE Sakhalin shelf is a seismically active zone, it is probable that many pulses recorded by the AUARs were generated by natural seismic activity.

---

[31] $r \leq \frac{c\Delta t}{2} \approx 150\,\text{m}.$

[32] The high frequency signals are produced by crack development.

The following figures give examples and quantitatively illustrate the characteristics of signals from natural seismic events recorded in spring 2004 at Lake Mikizha on Kamchatka. The signals were synchronously recorded at three locations using hydrophones deployed through holes in the ice. The distance between Point 1 and Points 2 and 3 was 110 m and between Point 2 and Point 3 was 50 m. Figure 5.11 impulses Imp-1.1 and Imp-1.2 were probably generated by the same source, however because of the different propagation velocities for compressional and shear wave in hard rock they are separated in time[33]. Figure 5.11 shows that the dominant frequency of these pulses is approximately 4 kHz, synchronous spatial measurements of geoacoustical signals (e.g. Figure 5.12) can be used to estimate the direction to the source.

[33] This time delay should allow the distance to their point of origin to be estimated.

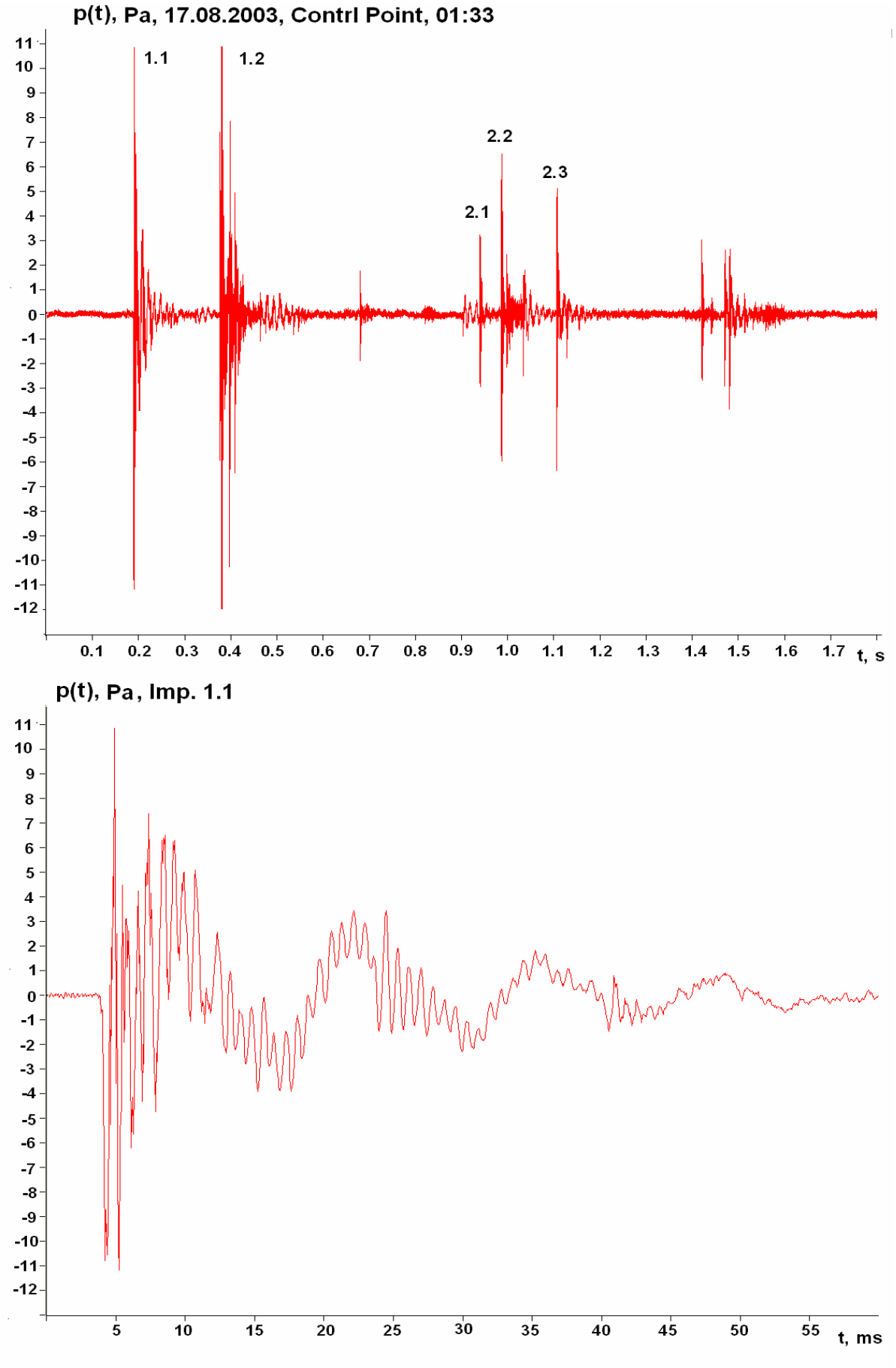

Figure 5.6 - Biogenic impulses recorded at the control station on 17 August 2003.

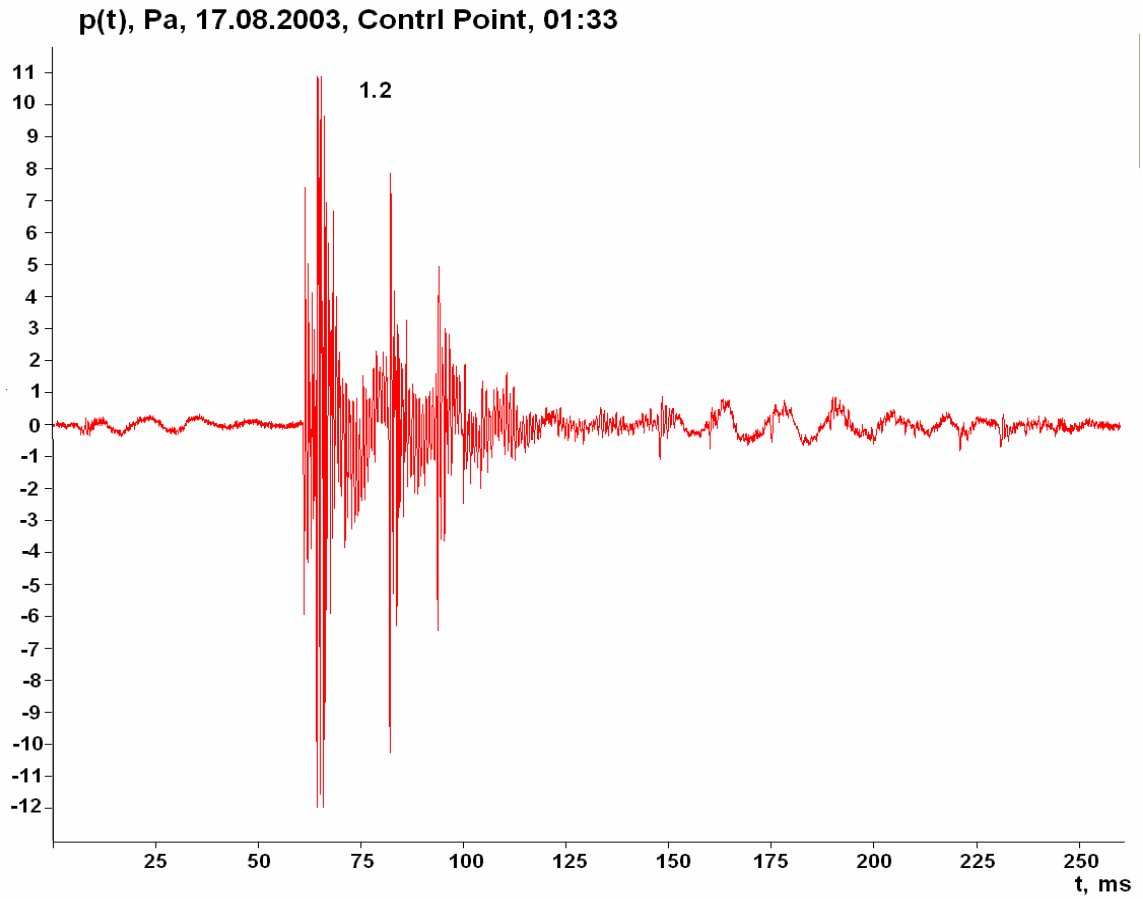

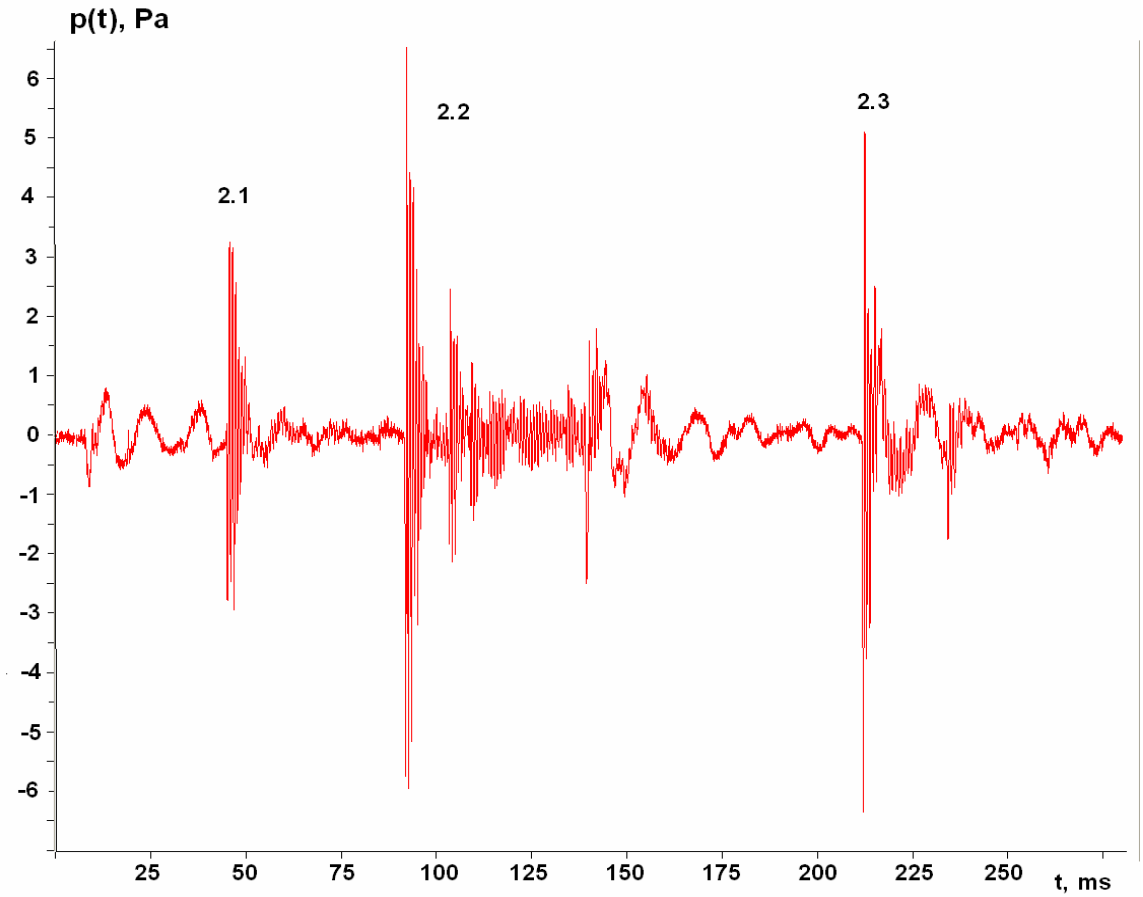

Figure 5.7 - The plots from Figure 5.5 at a larger scale.

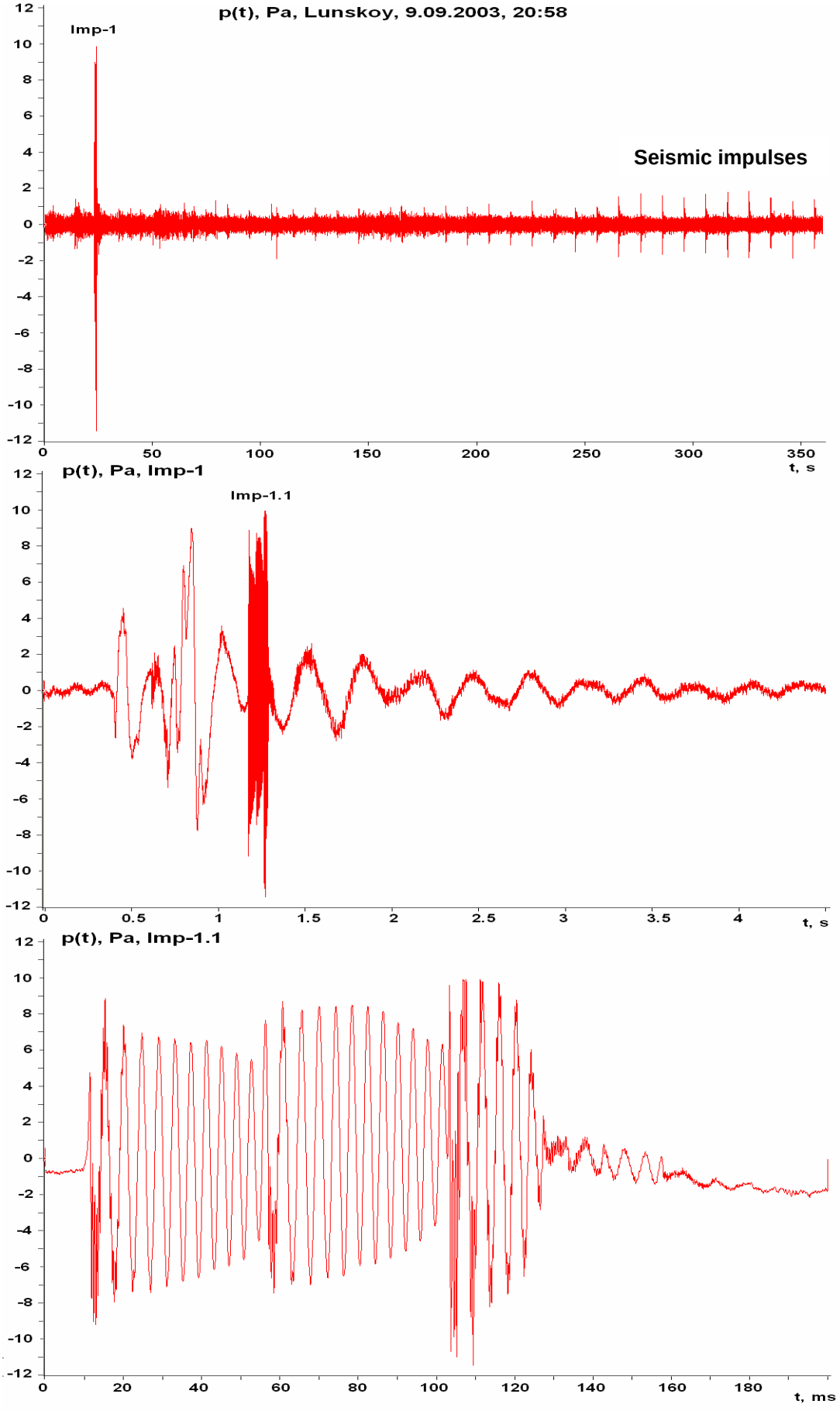

Figure 5.8 - Detailed analysis of a biogenic impulse recorded at the Lunskoye monitor station on 9 September 2003.

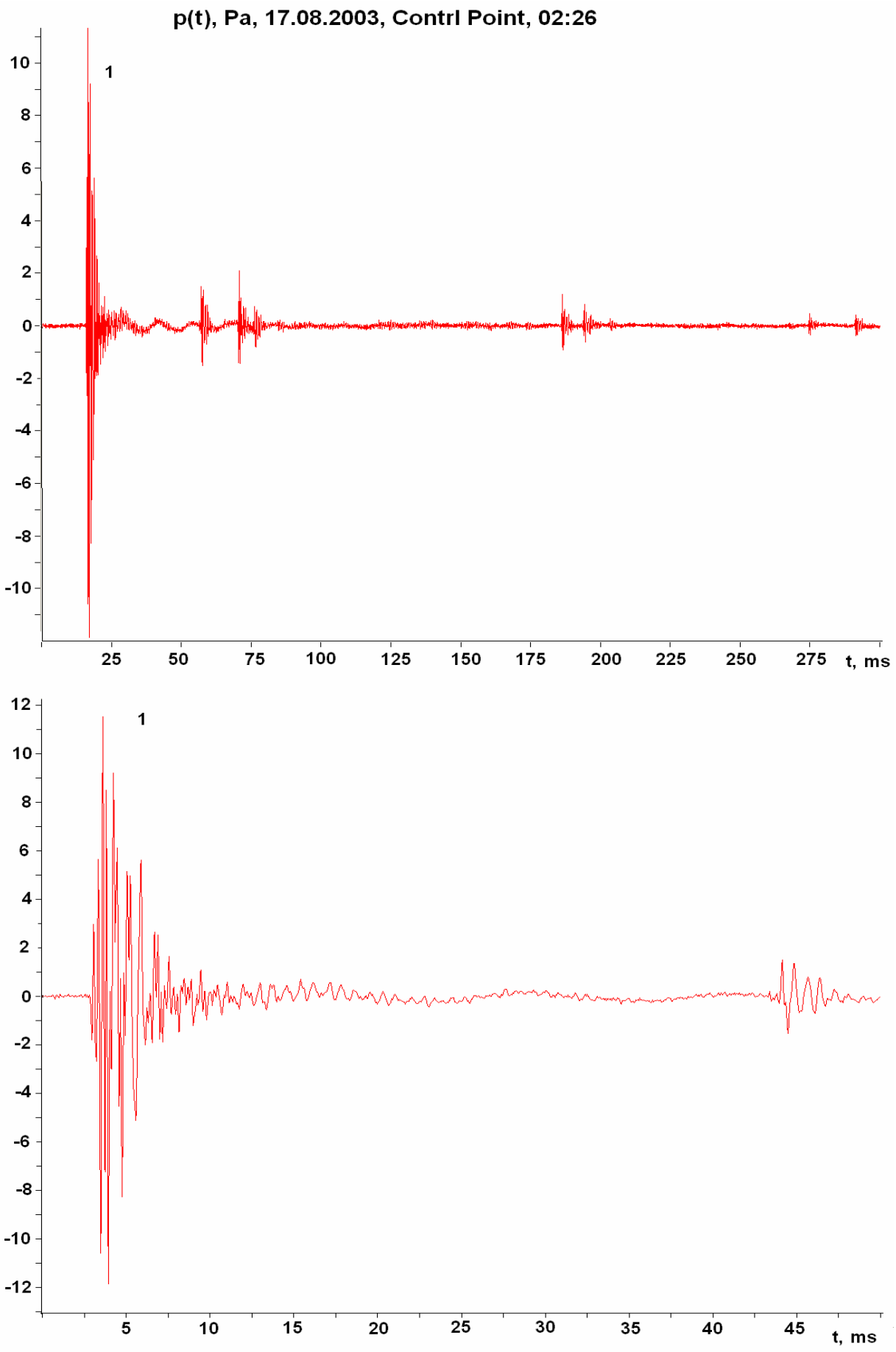

Figure 5.9 - Further biogenic impulses recorded at the control station on 17 August 2003.

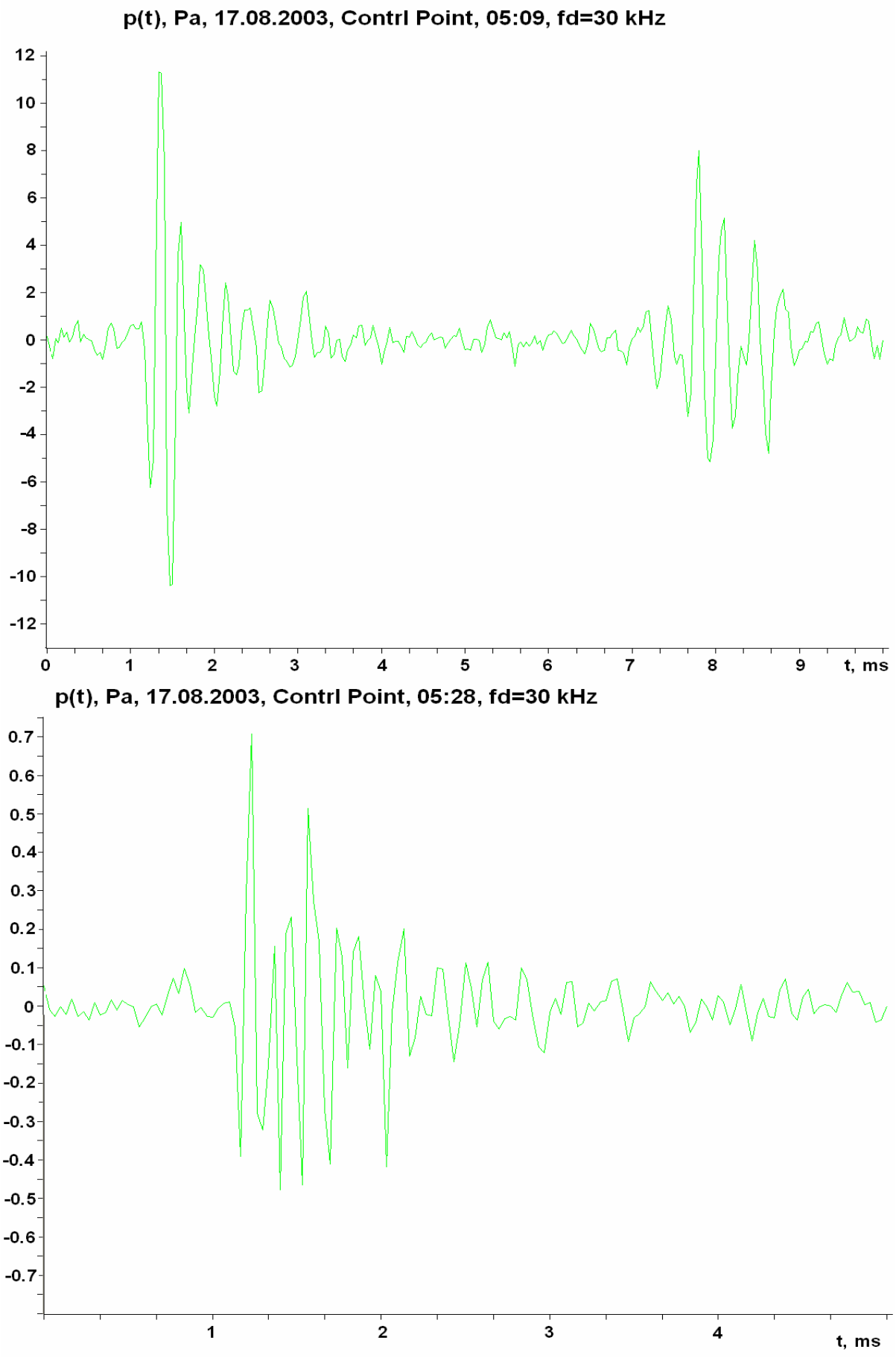

Figure 5.10 - Further biogenic impulses recorded on the HF channel (30 kHz sample rate) of the control station - 17 August 2003.

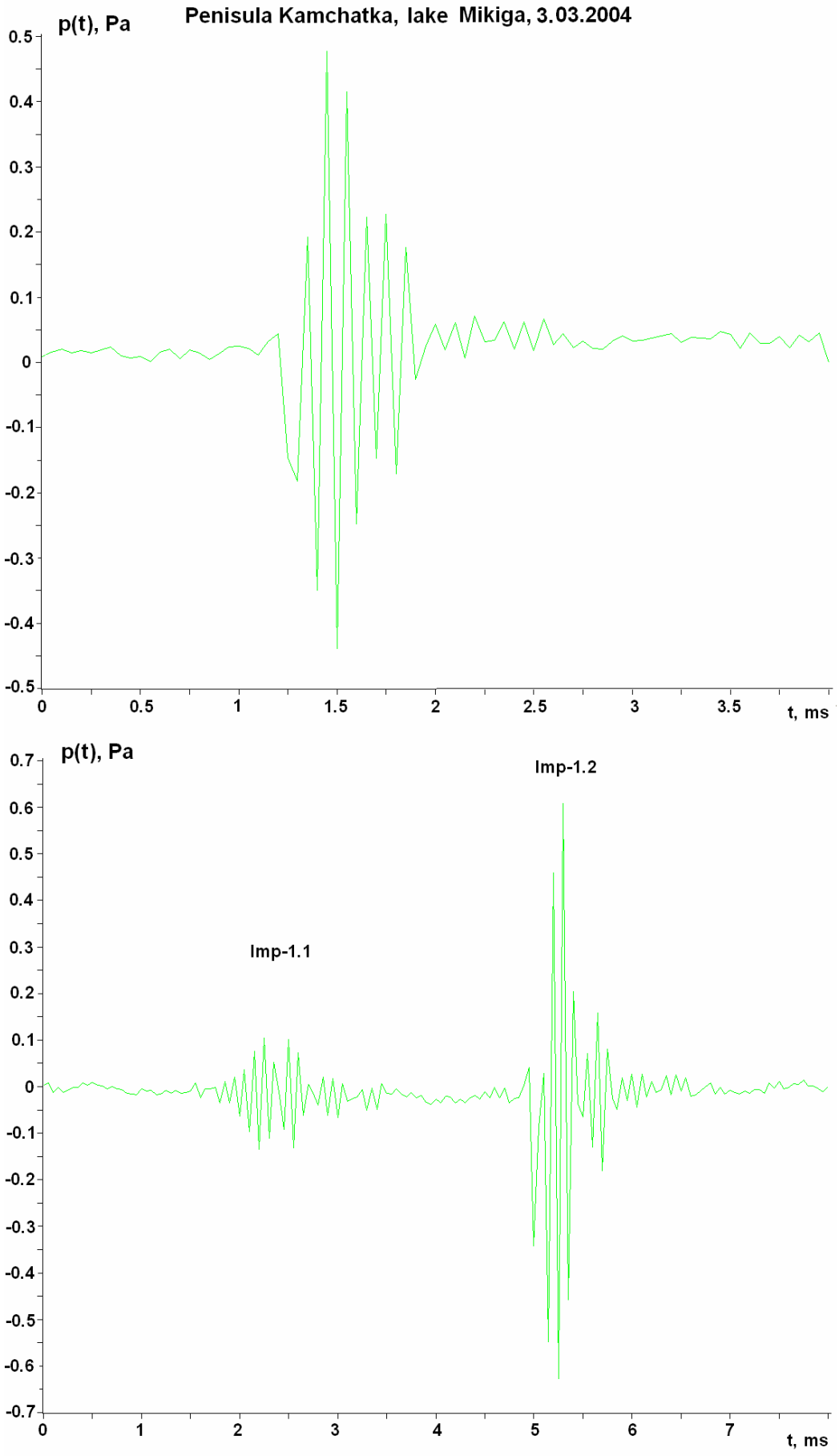

Figure 5.11 - Impulses generated by natural seismicity - Lake Mikizha, Kamchatka - 3 March 2004.

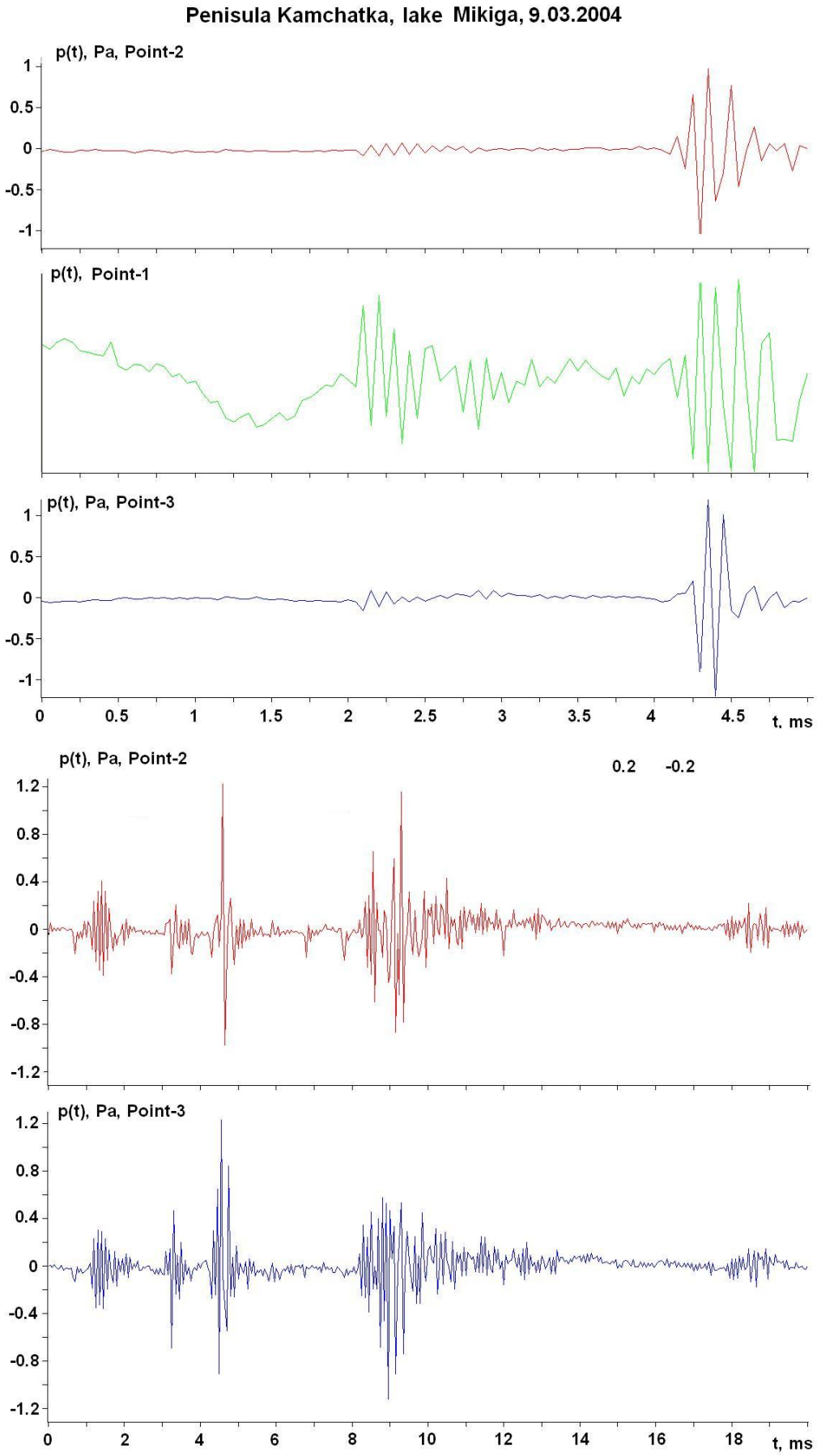

Figure 5.12 - Impulses generated by natural seismicity - recorded on three channels to determine orientation - Lake Mikizha, Kamchatka - 9 March 2004.

6 Results and Conclusions

1. The new Autonomous Underwater Acoustic Recorders designed and developed at POI performed well; they recorded high fidelity data for frequencies from 1-15,000 Hz. Synchronous measurements of broadband noise both at the source and receivers allow an accurate estimation of the TL between the source and the sonobuoy.
2. Six AUARs were built by POI and used to record ambient and anthropogenic acoustic levels on the NE Sakhalin shelf. One AUAR was lost. The hydrophysical parameters for the area were also measured using a hydrologic sonde.
3. Spectral analysis of the acoustic noise generated by wind and surface waves shows a good correlation between the data from the NE Sakhalin shelf and that of other scientists including the correlation between noise and sea state proposed by Knudsen. The noise field in the frequency band from 200-800 Hz generated by an approaching cyclone shows the clear interference structure that results from waveguide propagation on the shelf. Analysis also indicated that at shallow (10 m) water depths the noise produced by wind and surface waves is much lower than at deep (20 m) water depths. The highest ambient noise level recorded was in the frequency band from 200-1000 Hz. During a storm the ambient noise level reached 71 dB re 1 μPa/Hz, and for calm weather 48 dB re 1 μPa/Hz[34].
4. Three experiments characterized sound propagation and TL on the NE Sakhalin shelf:
   A. An autonomous tonal transducer (CW-320) was deployed for three days[35] near the Chayvo drill site to study variations in the intensity of a 320 Hz tonal signal due to spatial and temporal fluctuations in the sound velocity field. Tonal signals were propagated along and across the shelf and recorded by three AUARs thus generating three acoustic profiles. For spatial and temporal fluctuations of the sound velocity field due to internal waves propagating along the pycnocline intensity variations reach a peak on the profile oriented parallel to the shore. These intensity fluctuations correlate with Tidal Internal Waves and short wavelength internal waves propagating across the shelf. For a 6 km long acoustic profile, the intensity variations reached 14 dB with a period of ≈40 minutes, 16 dB with a period of ≈12 hours and 12 dB with a period of ≈24 hours.

[34] These values were recorded at the control station.
[35] 6 to 9 September 2003.

B. Two TL experiments were conducted using HF and LF transducers deployed at 8 m from the *Nevelskoy*. The signals were generated at the proposed location of the PA-B platform and received at the PA-B-1 and PA-B-2 monitor stations located on the 20 m and 10 m contours within the inshore feeding area. The signals were also received at the Odoptu-N location.

The frequency dependent TL estimated from these experiments shows the following characteristics[36]:

- TL is at a minimum between 100-200 Hz. TL is approximately -60 dB for PA-B-2 (20 m) and PA-B-1 (10 m) and -85 dB for Odoptu-N (10 m);
- For frequencies below 80 Hz the TL increases sharply at PA-B-1 and Odoptu-N relative to PA-B-2 due to the impact of the shallowing bottom. At 30 Hz the TL values are -68 dB (PA-B-2), -95 dB (PA-B-1) and -117 dB (Odoptu-N);
- At frequencies below 20 Hz sound propagates preferentially in the bottom and the TL decreases. At 15 Hz the TL between PA-B and PA-B-1 is -78 dB and is -67 dB to PA-B-2;
- For frequencies between 9 and 11 kHz the TL decreases sharply, reaching -66 dB to PA-B-1 and -62 dB to PA-B-2; and
- Sound propagating from PA-B to Odoptu-N has greater transmission losses at higher frequencies due to absorption and scattering by surface waves, at 8 kHz the TL is -115 dB.

Theoretical results from numerical experiments along the profile from PA-B to PA-B-1 for a model waveguide with a liquid sediment layer and elastic basement correlated well with the experimental data. Numerical modeling showed that for frequencies below 30 Hz only the zero mode (surface wave) propagates, and this mode attenuates greatly with increased frequency. The group velocity of the zero mode is 1700-1900 m/s. At higher frequencies the zero mode velocity falls to 1400-1470 m/s and the first mode appears. The first mode has a range dependent attenuation coefficient that is 2-3 times lower than the zero mode at 40-45 Hz; however, due to the shallowing of the waveguide the first mode can die off before reaching PA-B-1.

[36] See Figure 3.6.

C. Two TL experiments were conducted using HF and LF transducers deployed at 8 m from the *Nevelskoy*. The signals were generated at the proposed location of the Orlan platform (P-Orlan) and received at the Chayvo-1 and Chayvo-2 acoustic stations as well as the Orlan monitor station. Propagation experiments were conducted along the following profiles: P-Orlan to Chayvo-2 (flat bottom, 2.5 km), P-Orlan to Chayvo-1 (shallowing wedge, 7.9 km) and P-Orlan to Orlan (deepening wedge, 14.2 km).

The frequency dependent TL estimated from these experiments shows the following characteristics:

- TL for sound propagating from P-Orlan to Chayvo-1 (11 m) and Orlan (30 m) are approximately equal at almost all frequencies between 20-10000 Hz even though the profile to Orlan is almost twice as long as the profile to Chayvo-1.
- The Orlan monitor station is located on the closest 95% kernel probability contour of the offshore gray whale feeding area. The TL for sound propagating from the proposed location of the Orlan platform to this station is:
  - For frequencies lower than 100 Hz TL < -80 dB.
  - For frequencies between 150 and 300 Hz TL ≈ -60 dB.
  - For frequencies between 1.5 and 10 Hz TL < -70 dB.
- TL for sound propagating along a profile from PA-B to Odoptu-N profile (shallowing wedge, 28 km) is approximately equal to the TL for a profile from PA-B to Orlan (flat waveguide, 63.4 km).

Numerical experiments were conducted for a model waveguide with a bathymetric profile corresponding to that from Chayvo-1 to Orlan (~21 km). These theoretical experiments showed that for sound generated by a source on the bottom near the shore (at 1 m) the TL is lower:

- For frequencies between 10 and 30 Hz TL ≈ -100 dB.
- For frequencies between 60 and 100 Hz TL < -110 dB.
- For a frequency of 200 Hz TL = -130 dB.

5. The Chayvo well site was used as an analog to the proposed Odoptu well site[37] conditions, any noise propagating from the Chayvo well site was monitored for a variety of drilling activities. Drilling operations being conducted at the Chayvo well site were analyzed to determine if noise generated by these land based drilling operations would couple into the water and propagate seawards from the well site. A number of typical operations were evaluated, these included drilling, casing, tripping and general topside drilling operations (Figure 4.1).

   None of the sonograms *G(f,t)* or spectra *G(f)* analyzed show any evidence of an increase in the anthropogenic acoustic level received at the Chayvo-1, Chayvo-2 or Chayvo-3 acoustic stations or the Orlan monitor station due to activities at the Chayvo well site. No correlation could be found between drilling operations at the Chayvo well site and the level of the acoustic field monitored offshore.
6. A seismic survey was being acquired in the Lunskoye license area during the time of the 2003 expedition. Impulses from this survey were recorded at the Lunskoye monitor station at the southern 95% kernel probability contour of the offshore gray whale feeding area. The amplitude of the impulses recorded at this station during seismic acquisition at Lunskoye reached ~10 Pa (141 dB_{peak} re 1 μPa[38], 135 dB_{rms} re 1 μPa), significantly below the level known to cause a disturbance to 10% of feeding gray whales (163-164 dB_{rms} re 1 μPa).
7. Temporal analysis of acoustic signals recorded at a variety of locations on the NE Sakhalin shelf showed that:
   - At night, impulses, probably generated by marine animals, were observed at all the monitored locations (including the control station, which was a significant distance from any anthropogenic activity).
   - The main characteristics of these signals are a combination of high ($\approx$1.2-1.5 kHz) and low (3-70 Hz) frequency impulses. The amplitude of the high-frequency impulses reached 12 Pa (142 dB re 1 μPa/Hz).
   - Acoustic impulses were recorded with maximum energy at 8 kHz.

[37] The Odoptu field will be developed using deviated wells drilled from well pads on the coast (Figure 1.2). There has been some concern that the noise from this development may propagate to the inshore feeding area, disturbing the gray whales that feed there.

[38] A few of the highest amplitude peaks were clipped, however this will not materially change the rms estimate.

8. An experiment at Lake Mikizha (Kamchatka peninsula) conducted in March 2004 showed that acoustic impulses with a frequency of 4 kHz can be generated by the formation of cascaded fractures due to the rapid release of stress prior to an earthquake. The amplitude of these impulses can reach 12 Pa (142 dB re 1 μPa/Hz).
9. Impulses were observed at Chayvo-1 and Chayvo-3 that differed significantly from those recorded on other parts of the NE Sakhalin shelf. Their key characteristics are that they form a packet of 3-5 pulses of greater than 10 second duration, have a frequency of ≈7 Hz and an amplitude of 9 Pa (139 dB re 1 μPa/Hz).

7 Future plans

The development of digital AUARs by POI has significantly increased the dynamic range and bandwidth of the acoustic data recorded in 2002. Using the digital 2-channel AUAR with a 16-bit ADT (96 dB), a 60 Gb hard drive, and hydrophones calibrated from 1 Hz to 10 kHz allowed accurate acoustic measurements to be made from 1 to 15,000 Hz. These self-contained recorders allowed synchronous acoustic measurements to be made across the NE Sakhalin shelf.

Eight new AUARs will be assembled in 2004, building on the experience gained from the 2003 field expedition, bringing the total number of AUARs to 13. Some changes will be made to the AUARs fabricated in 2004:

- The container shape will be changed to allow easier deployment and retrieval.
- A broader band hydrophone with a refined gain will be used.
- The gain will be changed to minimize the instrument noise at low input amplitudes.
- The flash memory capacity will be increased to 1 GB to reduce the dead time.
- The hard-drive capacity will be increased to 80 GB to increase the recording time.
- The AUAR will be able to operate continuously for at least 15 days.
- A programmable standby mode will be incorporated to optimize power usage.

A new mid-frequency transducer and complex broadband signal generator will allow improved TL estimation at frequencies from 15-15000 Hz. A low-frequency resonant seismic electromagnetic transducer will be developed, and if tests on the shelf of the Japanese Sea are successful it will be used to study sound propagation from the coast at Odoptu.

Detailed hydrologic profiling using the sonde and vessel sonar will be conducted to allow the impact of variations in the hydrologic field on sound propagation to be investigated and to improve the accuracy of numerical modeling. Additionally, three distributed temperature sensors will be deployed from the vessel to measure the spatial and temporal parameters of the internal waves. These are the main source of spatial fluctuations in the sound velocity field and impact acoustic propagation on a shelf with a developed seasonal pycnocline.

The acoustic studies conducted in the Molikpaq and Chayvo areas in 2002 and 2003 confirmed that synchronous signals recorded by multiple recorders could be used for effective TL experiments. In 2004 comprehensive TL studies will investigate sound propagation from the planned construction/development areas to the inshore and offshore gray whale feeding areas.

Any acoustic measurements undertaken in a high current regime such as the NE Sakhalin shelf can be affected by flow noise due to the interaction of the water flow with the stationary hydrophone. This can bias low frequency (<25 Hz) acoustic measurements and make studies of low frequency transmission loss difficult. The 2003 data was contaminated with this flow noise. Prior to the 2004 field expedition POI will investigate recording and analysis methods to reduce the effect of this noise on TL measurements.

The amount of data collected during the 2004 field expedition is expected to be significant. POI is creating software to archive, analyze and plot this large volume of field data.

8 Acknowledgements

The authors would like to thank the V.I. Il`icev Pacific Oceanological Institute, FEB Academy of Sciences of Russia (POI), (Тихоокеанский океанологический институт им. В.И. Ильичева ДВО РАН), for permission to conduct this work.

The authors would also like to acknowledge the following personnel from POI, who while they did not contribute to the report, contributed significantly to the success of the program in the field. Scientists: Sc. S.V. Borisov (Борисов С.В.), A.V. Gritsenko (Гриценко А.В.).

The authors also wish to thank the crew of the *Nevelskoy* for their hospitality and assistance while conducting acoustic measurements in the vicinity of PA-B and Chayvo.

Finally the authors would like to thank Dr. Sc. G.I. Dolgih (Долгих Г. И.)(POI), Dr. Richard T. Houck, Dr. H. Rodger Melton (ExxonMobil Upstream Research Co.) and Dr. Charles I. Malme (LGL) for reviewing this report.

Our special thanks go to the investment companies, their employees and consultants, without whom the present work could not have been conducted. These include:
LGL Ltd. - Dr. S.R. Johnson, S.K. Meier and Dr. S.B. Yazvenko.
Exxon Neftegas Ltd. - M. Esengalieva, N. Chernigovskaya, M.R. Jenkerson, C.R. Martin and H.R. Melton
Sakhalin Energy Investment Company Ltd. - A. Yarmolchuk

9 Authors

From the V.I. Il`icev Pacific Oceanological Institute, Far East Branch, Academy of Sciences of Russia:
Sc. M.V. Kruglov (Круглов М.В.)
Dr. Sc. A.N. Rutenko (Рутенко А.Н.)

10 Bibliography

1. Bondar, L.F., Gritsenko A.V., Zakharov V.A., Kovzel` D.G. and Rutenko A.N. (1993). Digital radio telemetry system for the collection and results of its application in studies of sea reverberation characteristics // Acoustical Physics, Vol.39, no.2, pp.118-122.
2. Borisov, S.V., Gritsenko A.V., Jenkerson M.R., Rutenko A.N., and Hodzevich A.V. (2002) Evaluating and Monitoring Acoustic Transmission from the Odoptu 3D seismic Survey 5 August - 9 September, 2001; Sakhalin, Russian Federation // Pacific Oceanological Institute (FEB RAS) report for Exxon Neftegas Ltd.
3. Borisov, S.V., Gritsenko A.V., Rutenko A.N., and Hodzevich A.V. (2003) Results of Acoustic Studies Within and Adjacent to the Piltun-Astokh License Area 1 to 6 August, 2001 and 17 to 24 September, 2001; Sakhalin, Russian Federation // Pacific Oceanological Institute (FEB RAS) report for Exxon Neftegas Ltd. & Sakhalin Energy Investment Company.
4. Borisov, S.V., Gritsenko A.V., Kruglov M.V., Korotchenko R.A., and Rutenko A.N. (2003) Results of Acoustic Studies between Molikpaq and Piltun and Near Chayvo Bay 12 September to 23 September, 2002; Sakhalin, Russian Federation // Pacific Oceanological Institute (FEB RAS) report for Exxon Neftegas Ltd. & Sakhalin Energy Investment Company.
5. Borisov, S.V., Gritsenko A.V., and Rutenko A.N. (2004) Acoustic Studies on the North East Sakhalin Shelf, Volume 1: Equipment, Methodology and Data; 15 August to 20 September, 2003; Sakhalin, Russian Federation // Pacific Oceanological Institute (FEB RAS) report for Exxon Neftegas Ltd. and Sakhalin Energy Investment Co.
6. Furduev, A.V. (1998) Underwater noise of spatially inhomogeneous wind above the sea // Ocean acoustics. M.: GEOS, pp. 124-130.
7. Knudsen V.O., Alford R.S. and Emling J.W. (1948) Underwater ambient noise // J. Mar. Res. Vol. 7. № 3, pp. 410-429.
8. Kruglov, M.V., and Rutenko A.N. (2003) Transmission Loss Studies on the North-East Sakhalin Shelf 2001 and 2002; Sakhalin, Russian Federation // Pacific Oceanological Institute (FEB RAS) report for Exxon Neftegas Ltd. and Sakhalin Energy Investment Co.
9. Kuptsov, et al. (2003) Character change in natural seismic emissions related to early stages in the development of seismic events // Seismoacoustics of transition zones. Vladivostok Far Eastern University, pp. 108-109.

10. Kuryanov, B.F. (1998) Ocean low-frequency noise conception development for 50 years // Ocean acoustics. M.: GEOS, pp. 116-124.
11. Miller, J.F. and Wolf S.N. (1980) Modal acoustic transmission loss (MOATL): A transmission loss computer program using a normal mode model of acoustic field in the ocean // Naval research laboratory, Washington.
12. Perrone, A.J. (1969) Deep-ocean ambient noise spectra in the Northwest Atlantic // J. Acoust. Soc. Amer. Vol. 46, №3, pp. 762-770.
13. Rice, G. (1982) Earthquake source mechanics // M.: Mir. 217p.
14. Richardson, W.J., Greene C.R., Malme C.I. and Thomson D.H. (1995). Marine mammals and noise. Academic Press Limited. 576 p.
15. Rutenko, A.N. (2003) Effect of internal waves on the intensity and interference structure of the sound field in shelf zone // Acoustic Physics Vol. 49. № 4, pp. 449-454.
16. Sobolevsky, E.I., et.al. (Соболевский Е.И. и др.) (2000) Report for Sakhalin Energy Investment Company (Отчет для «Сахалин Энерджи Инвестмент Компани Лтд.»).
17. Zhou, J.X., Zhang X.Z., Rogers P.H. (1991) Resonant interaction of sound wave with internal solitons in the coastal zone // J. Acoust. Soc. Amer. Vol. 90. № 4, pp. 2042-2054.

Appendix A - Description of data used for the TL studies

Station		Date		Time		Time	AUAR	Location		H	Gain		Sens.	Comments
Name	#	Start	End	Start	End		#	Latitude	Longitude	(m)	LF	HF	(mV/Pa)	
Orlan	2	15-Aug	20-Aug	9:00	18:15	129.25	№ 1	52°21.624	143°35.154	33	4	80	49.8	On 16 August from 07:10 to 09:30 an acoustic signal was radiated from the PA-B location (52°55.604; 143°29.536, depth - 28 m)
Piltun	3	15-Aug	21-Aug	15:00	5:15	134.25	№ 3	52°49.335	143°24.857	20	4	80	50.8	
PA-B-1	4	15-Aug	20-Aug	15:00	20:40	125.66	№ 4	52°54.027	143°20.633	11.5	4	80	52.8	
PA-B-2	5	15-Aug		15:09		LOST	№ 5	52°54.797	143°23.489	21	4	80	51.8	
Odoptu-N	7	15-Aug	21-Aug	16:00	6:10	134.17	№ 2	53°09.077	143°17.449	10.5	4	80	51.6	
Control	8	15-Aug	19-Aug	16:00	5:10	85.17	№ 6	53°25.979	143°11.495	20	8	80	51.5	
Control	8	2-Sep	4-Sep	18:00	13:30	43.50	№ 4	53°25.940	143°10.876	20	8	80	52.8	On 6 September from 07:20 to 09:04 a broadband acoustic signal was radiated from the ORLAN location (52°24.703; 143°23.573, depth - 13 m) From 09:50 on 6 September to 20:00 on 9 September a 320 Hz CW signal was radiated from 52°22.747; 143°23.510, depth - 16 m Seismic exploration at Lunskoye
Odoptu-S	6	4-Sep	10-Sep	19:03	0:30	125.45	№ 3	53 03.729	143 18.362	11	8	80	50.8	
PA-B-1	4	4-Sep	10-Sep	18:55	14:10	139.25	№ 2	52°54.02	143°20.058	10	8	80	51.6	
Chayvo-1	9	6-Sep	11-Sep	1:00	15:00	134.00	№ 1	52°27.829	143°18.977	11	8	80	49.8	
Chayvo-2	10	6-Sep	11-Sep	1:00	15:10	134.17	№ 4	52°25.885	143°24.599	17	8	80	52.8	
Orlan	2	6-Sep	9-Sep	1:00	14:40	133.67	№ 6	52°21.591	143°34.999	32	8	80	51.5	
Lunskoye	1	9-Sep	13-Sep	21:00	7:00	82.00	№ 6	52°00.140	143°38.227	46	8	80	51.5	
Chayvo-3	11	17-Sep	19-Sep	1:00	13:50	60.50	№ 4	52°26.838	143°20.590	17	8	80	52.8	TL experiments were conducted from the PA-B location (52°55.598; 143°30.083) on 17 September from 06:30 to 09:20 (depth - 30 m) and from 22:30 on the 18 September to 02:26 on the 19 September (depth - 31 m)
Chayvo-1	9	17-Sep	19-Sep	1:00	13:50	60.50	№ 3	52°27.786	143°18.665	10.5	8	80	50.8	
PA-B-2	5	16-Sep	18-Sep	23:00	9:40	34.67	№ 2	52°54.884	143°23.361	22	8	80	51.6	
PA-B-1	4	16-Sep	19-Sep	23:00	19:10	68.17	№ 6	52°54.212	143°20.712	12	8	80	51.5	
Odoptu-S	6	18-Sep		18:00		FAIL	№ 2	53°03.651	143°18.307	10	8	80	51.6	
Odoptu-N	7	18-Sep	20-Sep	18:10	8:30	38.34	№ 1	53°08.919	143°17.457	11.5	8	80	49.8	